NASA CR-152047

(NASA-CR-152047) USER'S MANUAL: SUBSONIC/SUPERSONIC ADVANCED PANEL PILOT CODE Technical Report, May 1977 - Feb. 1978 (Boeing Military Airplane Development) 127 p HC A07/MF A01 CSCL 01A G3/02

N78-30047

Unclas 29593

User's Manual
Subsonic/Supersonic Advanced Panel Pilot Code

Jack Moran, Edward N.Tinoco,
and
Forrester T.Johnson

February 1978

Boeing Military Airplane Development
P.O. Box 3707
Seattle Washington 98124

for
Ames Research Center
National Aeronautics and Space Administration

NASA CR-152047

ERRATA

July, 1978

1. Pages i, 1, 24, and 25
   The SCOPE operating system is SCOPE 2.1.3 not 3.4.4

2. Page 4, Equation 1 should read:

$$B^2 \frac{\partial^2 \phi}{\partial x_c^2} + \frac{\partial^2 \phi}{\partial y_c^2} + \frac{\partial^2 \phi}{\partial z_c^2} = 0$$

3. Page 7, line 18 should be corrected to read:
   .....however, a rectangular grid could not....

4. Page 10 lines 3 and 4 should read:
   ....consist of 5 rows and 4 columns, while the lower one has 5 columns and 4 rows.

   lines 12 and 13, "increasive" should read "increasing"

5. Page 11, Figure 1.6
   Interchange "Row" and "Column".

6. Page 12, line 7 should read:
   ....points of the coarser....

   line 18 should read:
   ....which are not corner control points....

7. Page 18, equation 2 should read:

$$CU\,(\overline{w}_u \cdot \overline{n}) + \overline{TU} \cdot \overline{v}_u + DU\,\phi_u$$
$$+\ CL\,(\overline{w}_\ell \cdot \overline{n}) + \overline{TL} \cdot \overline{v}_\ell + DL\,\phi_\ell = BET \qquad (2)$$

   line 11 should read:
   ...while $\overline{w}$ is the....

8. Page 19, line 13 should read:

$$\sigma = (\overline{w}_u - \overline{w}_\ell) \cdot \overline{n}$$

9. Page 20, line 2 should read:
   ....all panels lie within the Mach cone ....

10. Page 31, lines 8, 10, and 12
    "I-1" should read "I=1"

11. Page 32, line 6 should be corrected to read:
point L are (ZM(1,L), ZM(2,L), ZM(3,L))

12. Page 35, line 13 should read
....If NROPT=1, the user ....

line 17 should read:
....Thus, if NACASE ≥1,....

13. Page 36, line 8 should be corrected to read:
SUBROUTINE CCOF (CU, CL, TU, TL, DU, DL, NCT, NBIN)

line 11 should be corrected to read:
SUBROUTINE CBET (BET, NBIN)

line 15 should be corrected to read:
....BETA (8),....

delete lines 25 and 26:
and the other quantities have been described previously.

14. Page 39, common block in Figure 2.2 should be identical to common block on Fig. 2.10

15. Page 43, line 24 should read:
....that wake networks only....

16. Page 50, Comment: It was not necessary to reset the composite boundary conditions for the wake networks. The edge matching procedure will override these boundary conditions for the wake networks and apply the correct conditions.

17. Page 54, the description of NLOPT=9 should read:
Difference between upper and lower surface perturbation potential...

18. Page 55, the velocity parameters "v" are vector quantities "$\bar{v}$"

19. Page 58, line 1 should be corrected to read:
.....the side abut nothing.....

line 3 should be corrected to read:
....apply to network corner control points.)

line 9 add the following sentence:
The edge matching indicator is further explained in the program source code.

20. Page 60 Isentropic pressure coefficient equation should read:

$$C_p = -\frac{2}{\gamma M_\infty^2} \left\{\left[1 + \frac{\gamma+1}{2} M_\infty^2 (2u + u^2 + v^2 + w^2)\right]^{\frac{\gamma}{\gamma-1}} - 1\right\} \quad \text{(Isentropic)}$$

21. Page 111 Equation on line 17 should read

$$\sum_{i=1}^{9} w_i(\sigma_i - \sigma_o - \sigma_x X_i - \sigma_y Y_i)^2$$

22. Page 113 under the heading "Panel", 3 should read 5

23. Page 116 line 1 should read:
....Along BF, these quadratics....

line 21 should read:
.... edge being weighted 10^4 more....

User's Notes:

1. User's would be well advised to check the fidelity of the panel representation of the actual configuration. Unit normal vectors calculated from a flat panel representation do not necessarily converge to the correct value for the actual curved surface as the number of panels is increased. The program's interpretation can be checked by plotting NX vs X from the control point data illustrated in Figure 3.4.

2. The discussion on page 12 on adjacent networks of differing paneling densities should be correct. The user is warned though that extensive check out of the technique has not been done.

3. Recent experience in supersonic analysis indicates that the angle of attack and sideslip should be aligned with the compressibility axis for best results contrary to the discussion on page 31.

1 Report No	2 Government Accession No	3 Recipient's Catalog No
NASA CR-152047		

4 Title and Subtitle	5 Report Date
User's Manual-Subsonic/Supersonic Advanced Panel Pilot Code	February, 1978
	6 Performing Organization Code
7 Author(s)	8 Performing Organization Report No
Jack Moran, Edward N. Tinoco, and Forrester T. Johnson	
	10 Work Unit No
9 Performing Organization Name and Address	11 Contract or Grant No
Boeing Military Airplane Development P. O. Box 3707 Seattle, Washington 98124	A - 36078B
	13 Type of Report and Period Covered
12 Sponsoring Agency Name and Address	Contractor Report May 1977 - Feb 1978
National Aeronautics and Space Administration Washington, D. C. 20546	14 Sponsoring Agency Code

15 Supplementary Notes

Technical Monitor
Larry L. Erickson
NASA Ames Research Center

16 Abstract

The purpose of this report is to present sufficient instructions for running the subsonic/supersonic advanced panel pilot code developed under contract NAS2-7729, "Development of a FLEXSTAB Computer Program" pertaining to Advanced Aerodynamics Technology (TASK III, Category 2 - Supersonic Steady Flow). This software was developed as a vehicle for numerical experimentation and it should not be construed to represent a finished "production" program. The pilot code is based on a higher order panel method using linearly varying source and quadratically varying doublet distributions for computing both linearized supersonic and subsonic flow over arbitrary wings and bodies.

This User's Manual contains complete input and output descriptions. A brief description of the method is given as well as practical instructions for proper configurations modeling. Computed results are also included to demonstrate some of the capabilities of the pilot code.

The computer program is written in Fortran IV for the SCOPE 3.4.4 operations system of the Ames CDC 7600 computer. The program uses overlay structure and thirteen disk files, and it requires approximately 132000 (Octal) central memory words.

17 Key Words (Suggested by Author(s))	18 Distribution Statement
Panel Aerodynamics Configuration analysis Pressure distribution Subsonic/Supersonic Flow Computer Program	Unclassified - Unlimited

19 Security Classif (of this report)	20 Security Classif (of this page)	21 No of Pages	22 Price*
Unclassified	Unclassified	119	

*For sale by the National Technical Information Service, Springfield, Virginia 22151

Table of Contents

Table of Contents (continued)

List of Figures

List of Figures (Continued)

List of Figures (Continued)

List of Tables

0.0 Summary

The purpose of this report is to present sufficient instructions for running the advanced panel pilot code developed under contract NAS2-7729, "Development of a FLEXSTAB Computer Program" pertaining to Advanced Aerodynamics Technology (TASK III, Category 2 - Supersonic Steady Flow). This software was developed as a vehicle for numerical experimentation and it should not be construed to represent a finished "production" program. The code is based on a higher order panel method using linearly varying source and quadratically varying doublet distributions for computing both linearized supersonic and subsonic flow over arbitrary wings and bodies.

This User's Manual contains complete input and output descriptions. A brief description of the method is given as well as practical instructions for proper configurations modeling. Computed results are also included to demonstrate some of the capabilities of the pilot code. Results to date have shown very reasonable comparisons between the advanced panel pilot code and other theories and experimental data. Recent studies at The Boeing Company have indicated that configurations as complicated as a supercruiser fighter delivering a standoff weapon as shown in Figure 0.1 are within the capabilities of the pilot code.

The computer program is written in FORTRAN IV for the SCOPE 3.4.4 operating system of the NASA-Ames CDC 7600 computer. The program uses overlay structure and thirteen disk files, and it requires approximately 132000 (Octal) central memory words.

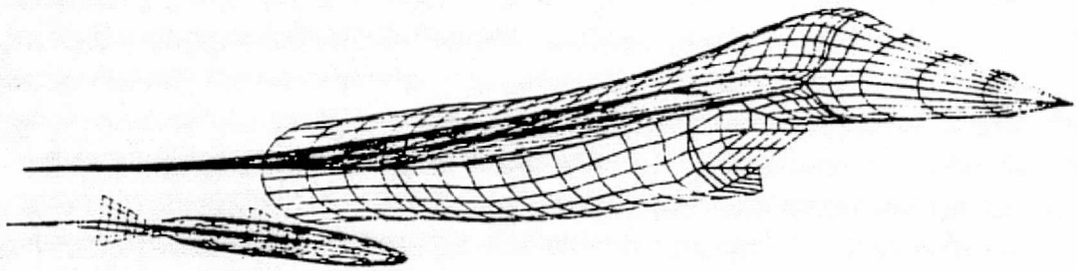

Figure 0.1 Supercruiser Delivering a Standoff Weapon

1.0 General Description

The advanced panel pilot code is intended to solve a variety of boundary value problems in steady subsonic or supersonic inviscid flow. The typical situation is the analysis of the flow past a prescribed configuration. The body surfaces are specified and the flow properties sought in a body-fixed (x,y,z) systen, called the global coordinate system. The flow far upstream of the body is characterized by its Mach number M_∞ and angles of attack and yaw, α and β respectively.

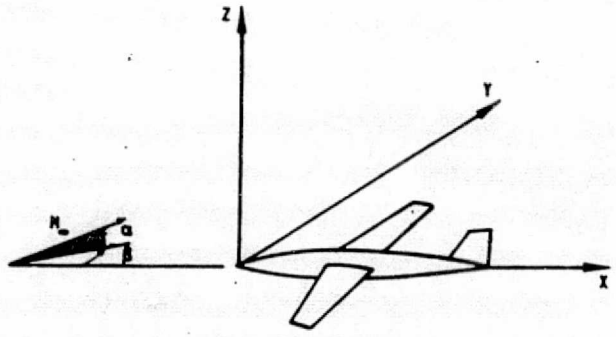

Figure 1.1 Global Coordinate System

The resultant flow is considered to be a small perturbation of a uniform flow. The direction of this uniform flow relative to the (x,y,z) system is given by angles α_c and β_c . Compressibility axes (x_c, y_c, z_c) are defined so that the x - axis is aligned with the undisturbed flow. Thus, the (x, y, z) system is produced by rotating the (x_c, y_c, z_c) system through β_c about the z axis, and then through α_c about the new y_c axis.

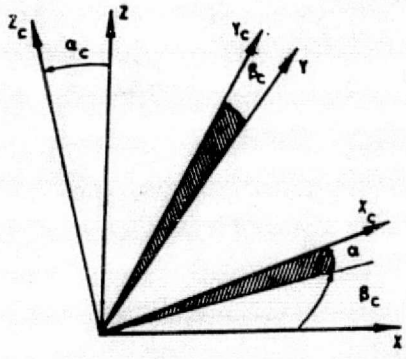

Figure 1.2 Compressibility Axis

It is generally advisable to take the undisturbed flow direction to be that of the free-stream; i.e., to set $\alpha = \alpha_c$ and $\beta = \beta_c$. However, if the same configuration is to be analyzed at a fixed Mach number for a range of α and β , computing time can be considerably reduced by fixing α_c and β_c somewhere in the middle of the ranges of α and β of interest, and to regard the differences $\alpha - \alpha_c$ and $\beta - \beta_c$ as contributions to the perturbation flow. Results presented in Section 4.2 show this can be satisfactory as long as $\alpha - \alpha_c$ and $\beta - \beta_c$ are less than one or two degrees for supersonic solutions. Criteria for subsonic solutions have not yet been established but previous experience indicates differences as great as 10 degrees may be acceptable.

If terms quadratic in the differences between the local velocity, pressure, and density and their values in the freestream are neglected, the flow is irrotational, with a perturbation velocity potential which satisfies, see ref. 1,

$$B^2 \frac{\partial^2 \phi}{\partial x_c^2} + \frac{\partial^2 \phi}{\partial y_c^2} + \frac{\partial^2 \phi}{\partial z_c} = 0 \qquad (1)$$

where

$$B^2 = 1 - M_\infty^2$$

The velocity is related to ϕ by

$$\overline{V} = \overline{V}_\infty + \left(\frac{\partial \phi}{\partial x_c}, \frac{\partial \phi}{\partial y_c}, \frac{\partial \phi}{\partial z_c} \right)$$

in compressibility coordinates and

$$\overline{V} = \overline{V}_\infty + \left(\frac{\partial \phi}{\partial x}, \frac{\partial \phi}{\partial y}, \frac{\partial \phi}{\partial z} \right)$$

in the global coordinates.

On any solid surface, the basic boundary condition is that the total mass flux vector $\rho\overline{V}/\rho_\infty$ be parallel to the surface. To a first approximation, the perturbation mass flux vector is given by

$$\overline{w} = \left(B^2 \frac{\partial\phi}{\partial x}, \frac{\partial\phi}{\partial y}, \frac{\partial\phi}{\partial z}\right)$$

in compressibility coordinates. Thus the fundamental boundary condition is that

$$(\overline{w} + \overline{V}_\infty) \cdot \overline{n} = 0$$

on all solid surfaces (and any other stream surfaces), where $\overline{n}$ is the unit normal to the surface, directed into the flow.

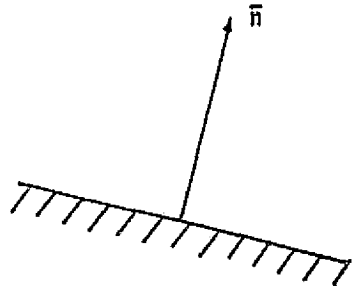

Figure 1.3 Direction of Unit Normal Vector

The method on which the advanced panel code is based is to represent the potential as a superposition of fundamental solutions of the partial differential equation (1). These fundamental solutions are sources and doublets whose locations are prescribed but whose strength must be determined so as to meet the boundary conditions. Specifically, they are distributed continuously (or nearly so) over all the wetted surfaces of the configuration under study, over whatever vortex sheets are shed from trailing edges, and, in special cases, over other surfaces as well, such as inlet faces, exhausts, etc.

The surfaces are approximated as a continuous network of quadrilateral "panels" whose vertices are basic input to the program. The panels are not necessarily planar, but are divided into plane triangular subpanels. On each subpanel, the source strength is approximated as linear in local planar coordinates, while the doublet strength is taken to be quadratic. The parameters of these linear and quadratic functions are put in terms of certain fundamental unknowns which include the source and doublet strengths at the center of each panel. These unknowns are then determined by simultaneous solution of the algebraic system which results by stipulating that the boundary conditions be satisfied at a sufficient number of control points. Once this is accomplished, the potential and velocity fields are known. The pressure field can then be calculated from an appropriate pressure-velocity relationship, and forces and moments calculated by integration.

1.1 PANELING

In all but the simplest cases, it is useful to divide the configuration to be analyzed into a number of networks. These are the surfaces whose shape is the basic input to the program. For flow past a cone, a single network will suffice. It is simply the outer surface of the cone. Similarly, only a single network need be used to represent an isolated quadrilateral a wing of zero thickness. (However, in both cases additional networks are required to model wakes.)

Usually the networks collectively describe the outer (wetted) surfaces of the configuration under study and its wakes. However, it is also possible to use networks which are not exposed to the fluid. For example, one way to model the flow past thin wings is to distribute sources on their upper and lower surfaces, and vortices or doublets over the mean (camber) surface within the wing. Also, to examine the flow at points off the body, one may put a network through those points without disturbing the flow simply by specifying zero jumps across the network in the potential and in the normal component of mass flux.

1.1.1 Specification of a Single Network Surface.

Every network surface is specified by giving the coordinates of an array of grid points which is basically quadrilateral. That is, the array consists of NM "rows" of grid points which each contain NN points, where NN is the number of "columns" of grid points. Often, as in the cases of flow past a cone or past a delta wing, a triangular array would be more convenient. This is easily accomplished by letting a single physical grid point belong to several rows or columns, as is illustrated in Fig. 1.4 for the paneling of a triangular wing surface. Here we show three alternative arrangements of grid points, which are the intersections of the grid lines shown. In the case of paneling "A", if we decide (arbitrarily) to label the lines parallel to BC as the "columns" of the network and the rays which meet at A the "rows", we have rows of 5 columns each, and point A belongs to all 7 rows. In paneling "B" point B belongs to 5 columns and in "C", point C belongs to 7 rows.

While the generally quadrilateral organization of grid points is sufficiently general for most purposes, some care must be taken. For example, however, a rectangular could not be used on a circular domain. However, it is easy to find a grid which is acceptable, as shown in Fig. 1.5.

Naturally, not every arrangement of points is equally effective. If the triangles shown in Fig. 1.4 represent the surface of an arrow wing, for example, it would be desirable to locate the confluence of rows or columns at the forward vertex of the wing, since the conicity of the flow yields significant variations of the flow parameters in that neighborhood. See Section 4.3 for the results of using various panelings to analyze a thin delta wing.

The difference between a row and a column cannot be detected until the grid points are given numerical labels for purposes of identification. Grid points in the same column are always labelled consecutively, while

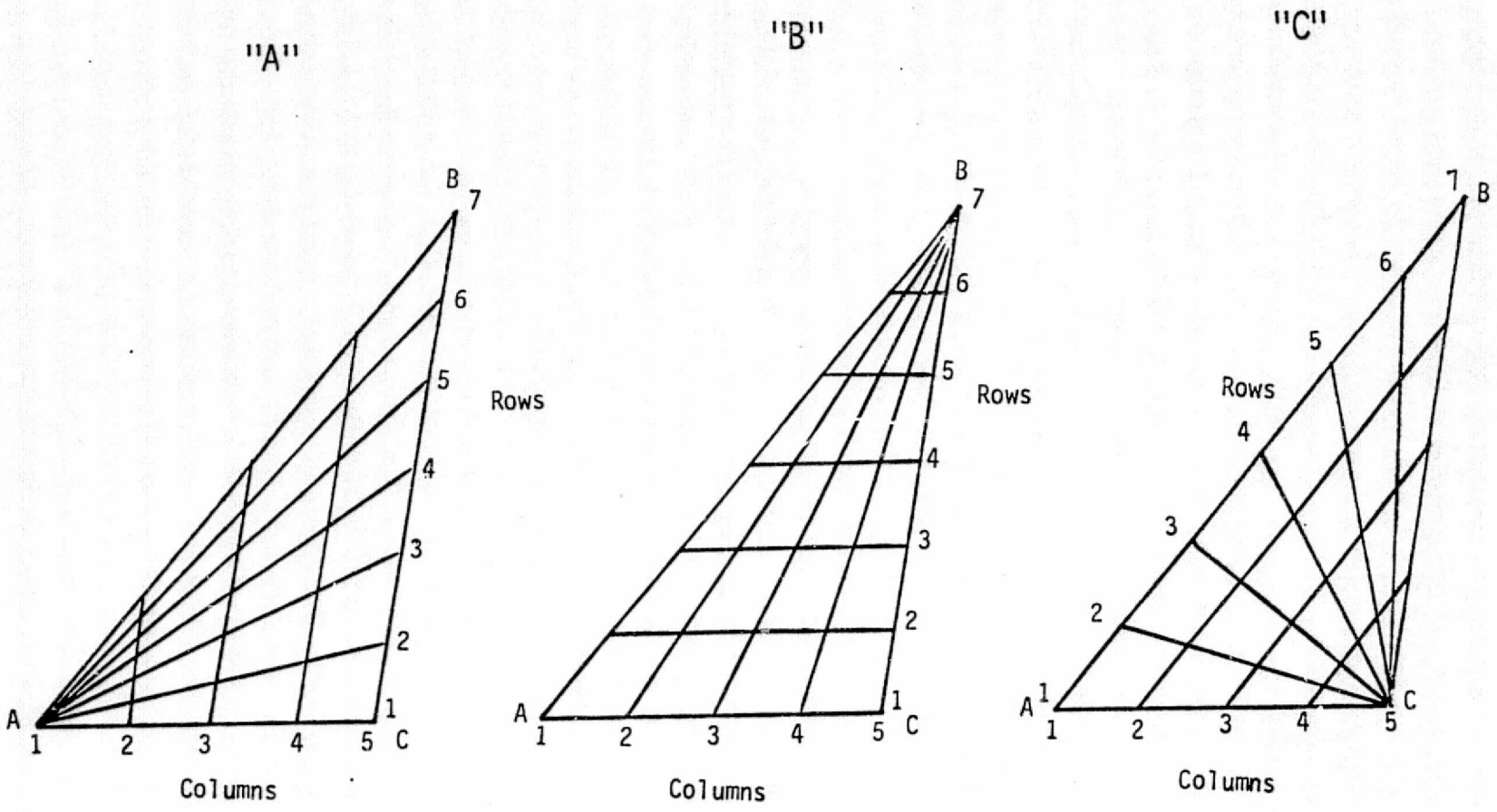

Figure 1.4 Aiternative Paneling of an Arrow Wing

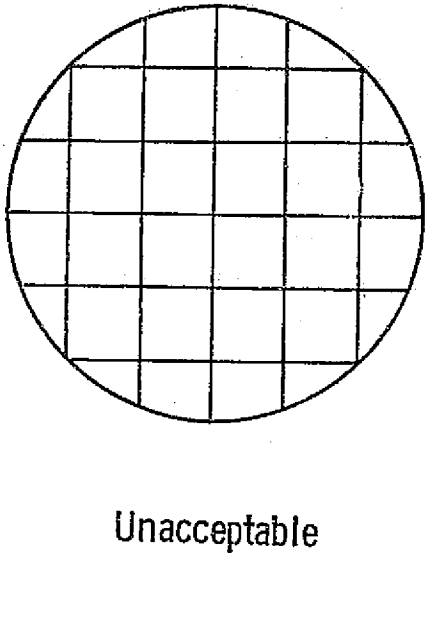

Unacceptable

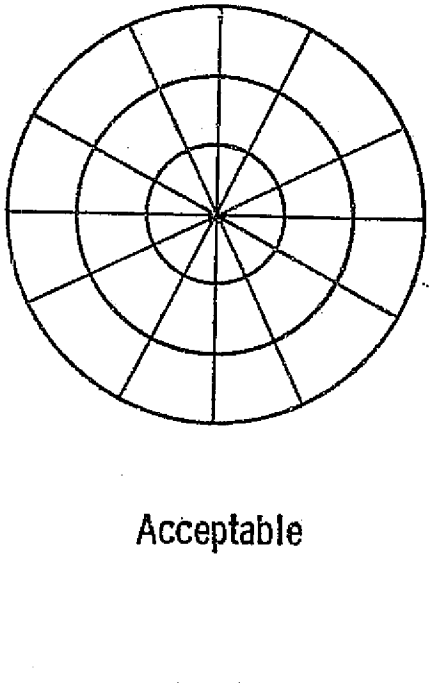

Acceptable

Figure 1.5 Alternate Panelings of a Circle

the grid point labels of adjacent points in the same row differ by the number of columns. Thus, given the grid point labels shown in Fig. 1.6, the network on top would be said to consist of 4 rows and 5 columns, while the lower one has 4 columns and 5 rows.

An important point to note is that the labeling of points within the network is used to distinguish the "upper" surface of the network from its "lower" surface. When the network is part of the surface of a solid body, the upper surface is often chosen to be the side exposed to the flow, while the lower surface is within the body.

The sence of a network maybe defined by the vectors N and M. The vector N corresponds to a column of grid points directed in the direction of increasive grid point labler, while the vector M corresponds to a row of grid points directed in the direction of increasive grid point labels. Then the vector N x M is directed out of the surface, or into the flow when the network bounds the flow as mentioned earlier. Thus, for either labeling or grid points shown in Fig. 1.6, the "upper" surface of the network is under the printed side of the page.

1.1.2 Notes on Multi-Network Problems.

Two points need to be kept in mind in dealing with more than one network. One is simply a matter of bookkeeping. All grid points on a configuration must be uniquely labeled; points on different networks must have different numbers. Further, grid points which are common to more than one network must have different labels when regarded as grid points belonging to the different networks.

The second point is that it is necessary to use exactly the same grid points for two adjacent networks with similar grid density on their juncture, unless one or both networks is free of doublets. The program will run if this requirement is ignored, but the doublet strength will then be discontinuous at the network boundary, which is usually disastrous

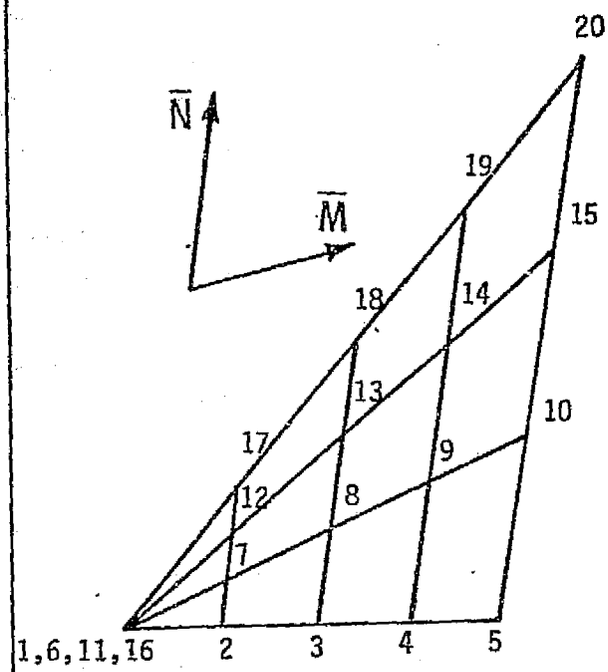

Row	Points	Columns	Points
1	1 - 5	1	1,6,11,16
2	6 -10	2	2,7,12,17
3	11 - 15	3	3,8,13,18
4	16 - 20	4	4,9,14,19
		5	5,10,15,20

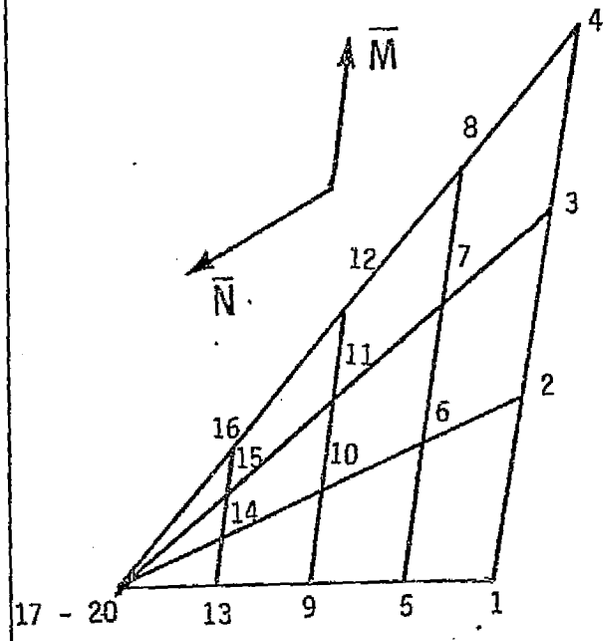

Row	Points	Column	Points
1	1 - 4	1	1,5,9,12,17
2	5 - 8	2	2,6,10,14,18
3	9 - 12	3	3,7,11,15,19
4	13 - 16	4	4,8,12,18,20
5	17 - 20		

Figure 1.6 Labelling of Rows, Columns and Grid Points

in supersonic flow even if the resultant effective vortex system is weak.

It is permissible for two adjacent doublet networks to have different grid densities so long as the grid points of one network are identical to a subset of the grid points of the other at their juncture. Moreover, the grid points of the finer network must lie precisely (within the accuracy of the machine for a supersonic solution) on the rectilinear curve (straight line segments) joining the grid points of the courses networks. Examples illustrating this point are shown in Fig. 1.7. Small mis-matches are allowed for subsonic solutions.

A related point is that abutting doublet networks must abut along complete edges, i.e., their network corner gird points must concide. For example, at a wing-body juncture, the body surface must be split into six separate networks at axial lines and at cross-sections which pass through the points at which the wing's leading and trailing edges meet the body. That is, of the arrangement of networks shown in Fig. 1.8, the upper one is correct but the lower is not. In the lower one, the two wing networks (its upper and lower surfaces) meet the body at points which are not control points for the body surface panels; therefore, continuity of doublet strength cannot be enforced at those points. In the upper arrangement, the wing networks meet the body at points which are corner points of four body-surface networks, and which therefore are control points.

1.1.3 Surface Fitting.

The four grid points on two adjacent rows and two adjacent columns determine a quadrilateral, which need not be planar.

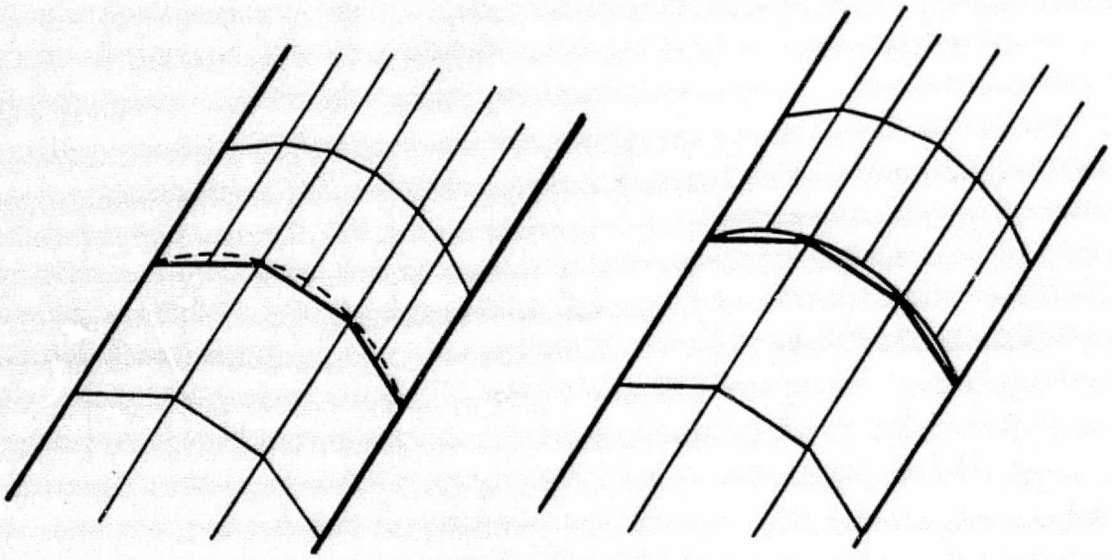

Acceptable

Not Acceptable *

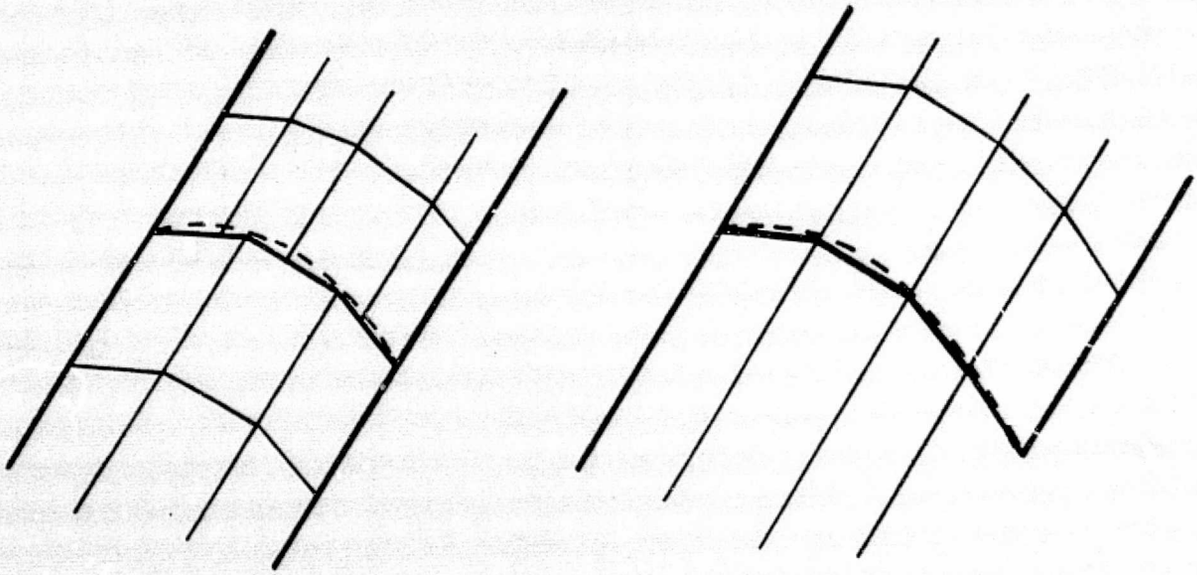

Not Acceptable *

Not Acceptable

*Acceptable for subsonic solutions only

Figure 1.7 Adjacent Networks with Different Paneling Densities

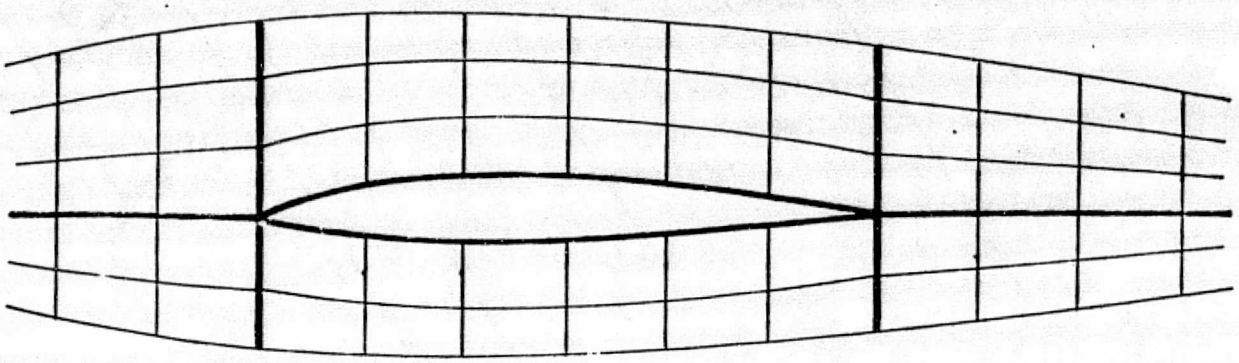

Correct

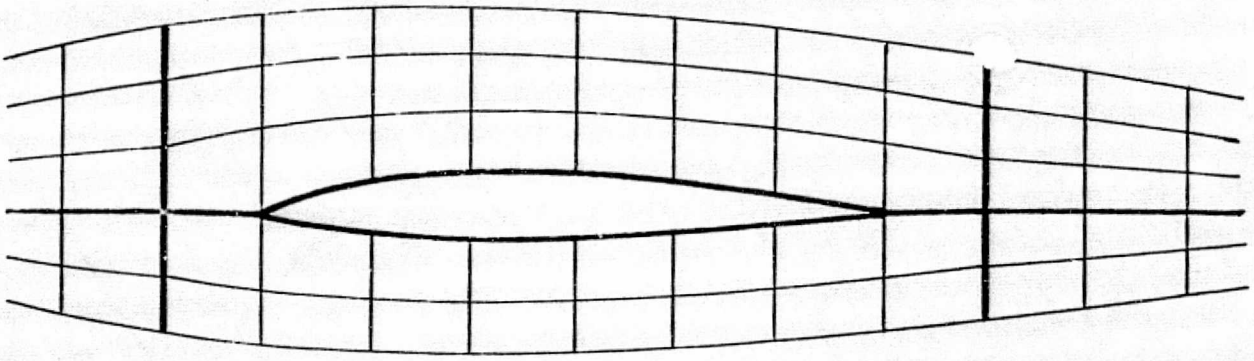

Incorrect

Figure 1.8 Splitting of Body Surface into Networks at Wing-body Juncture

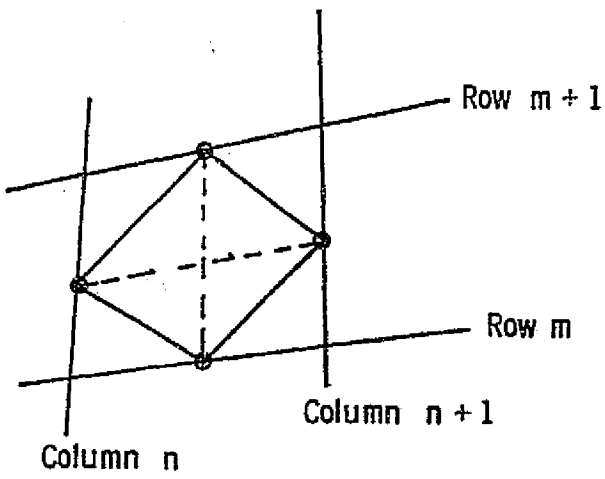

Figure 1.9 Subpanel Geometry

However, the midpoints of the sides of this quadrilateral (shown as 0's in Fig. 1.9) determine another quadrilateral, which is planar (in fact, it is a parallelogram). Therefore, each set of four adjacent grid points (i.e., points like the dots in Fig. 1.9 which lie on two adjacent rows and two adjacent columns) is used to generate an approximating surface which consists of four triangles and one parallelogram, the corners of the parallelogram being the midpoints of the lines joining the four grid points. For computational convenience, the parallelogram is further subdivided into four triangles as shown by the dotted lines in Fig. 1.9. Since they all lie in the same plane, this subdivision is without geometrical significance. However, as is described in Appendix A, different doublet distributions are used on the four triangles within the parallogram.

The nonplanar surface generated by the four adjacent grid points is termed a panel. As described above, each panel consists of eight triangular (and hence planar) subpanels, four of which comprise a parallelogram.

1.2 SINGULARITY DISTRIBUTION

Generally, every panel of every network is covered with a continuous distribution of sources and doublets. The source distribution is linear in the two coordinates which describe position on the panel, while the doublet distribution is quadratic. As described in Appendix A, the

parameters which describe the variations of both the source and doublet strengths on the panels are related to certain basic unknowns, namely

- o the source strength at the center* of every panel;
- o the doublet strength at the center of every panel;
- o the doublet strength at the midpoint of every panel edge which lies on the boundary of the network;

  and

- o the doublet strength at every corner of the network.

This is accomplished in such a way that the doublet strength is continuous between subpanels and between panels. However, neither the source strength nor the derivative of the doublet strength normal to the edge is exactly continuous between panels.

Naturally, the number of equations used to determine the singularity strength must match the number of unknowns. These are generated by imposing appropriate boundary conditions at selected "control points". Specifically, two boundary conditions are imposed at every panel center, one at the midpoint of every panel edge which lies on the network boundary, and one at every network corner point**, Fig. 1-10.

The number of control points on a quadrilateral network (as shown in the upper part of Fig. 1.10) is (NM + 1) x (NN + 1), where NM is the number of rows and NN the number of columns of the network. When one

* By "center" of a panel, we mean just the average position of its four corner points. If the panel has only three distinct corner points, the grid point which is input twice is counted twice as heavily as the other two.

**To avoid singularities in the perturbation velocities due to discontinuities in the value or slope of the singularity distributions at panel or subpanel boundaries, control points are actually displaced slightly from the geometric center of the panel (which is the vertex of subpanels) and from the network edge.

J15-047

ORIGINAL PAGE IS
OF POOR QUALITY

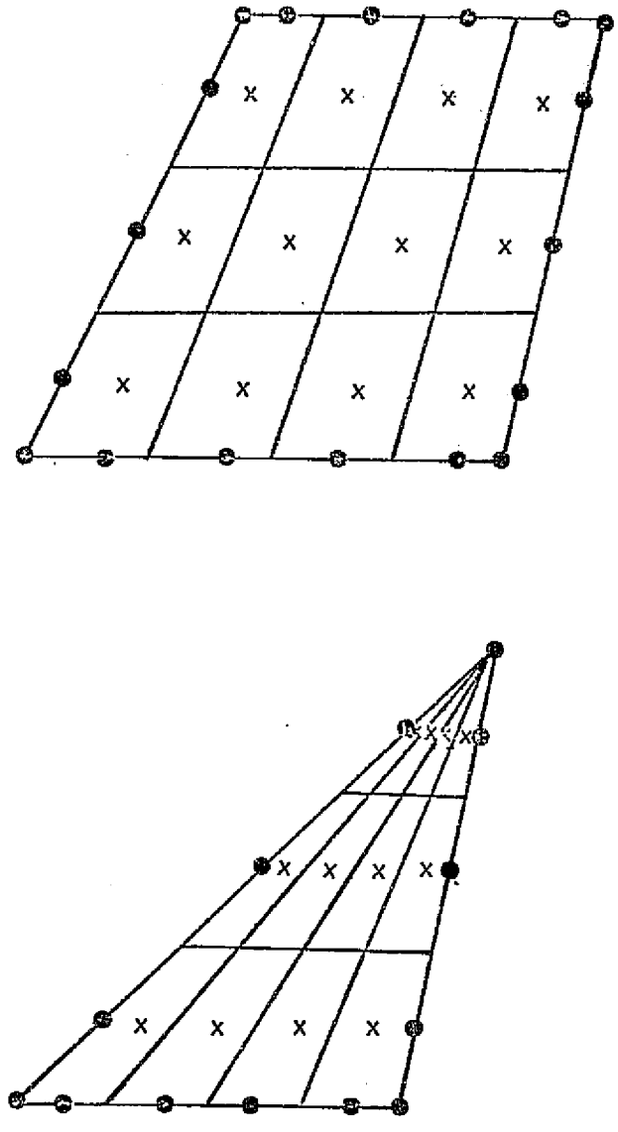

● One Boundary Condition Required

× Two Boundary Conditions Required

Figure 1.10 Location of Control Points

D1 4100 7740 ORIG.2/71

edge of the network collapses to a point as in the lower part of Fig. 1.10, this number is reduced automatically.

What we are describing here is the usual case in which the network is to be covered with both sources and doublets. The user has the option of suppressing either singularity type, as will be described immediately. Other options are available for the treatment of wakes.

1.3 BOUNDARY CONDITIONS

The general form of the boundary condition imposed at a control point is:

$$\begin{aligned} &CU\ (\overline{w}_u \cdot \overline{n}) + \overline{TU} \cdot \overline{v}_u + DU\ \phi_n \\ +\ &CL\ (\overline{w}_\ell \cdot \overline{n}) + \overline{TL} \cdot \overline{v}_\ell + DL\ \phi_\ell = BET \end{aligned}$$

Here CU, $\overline{TU}$, DU, CL, $\overline{TL}$, DL and BET are to be specified, while $\overline{w}$ is the perturbation mass flux vector, $\overline{v}$ the perturbation velocity vector, and ϕ the perturbation potential. The subscripts u and l distinguish upper and lower surfaces of the network, respectively, and $\vec{n}$ is the unit normal directed from the lower to the upper surface of the network (i.e., in the N×M direction). $\overline{TU}$ and $\overline{TL}$ are tangetial vectors. While the code contains both design and analysis type networks, only the use of analysis networks is discussed herein.

At every panel-center control point, two boundary conditions of Eq. (2) must be specified, unless the network is specified as source- or doublet-free in which case only one condition like Eq. (2) is required. For control points on the edge or corner of a network, only one boundary condition like Eq. (2) is imposed, unless the network is doublet-free, in which case none are required.

1.3.1 Boundary Conditions on Closed Impermeable Surfaces

Under rather loose conditions, the potential at any point in the flow may be represented by distributing sources and doublets over the surfaces which bound the flow. The contributions of the sources and doublets may be split in various ways more or less according to the taste of the analyst. Some analyses are based almost entirely on source distributions, while others rely solely on doublets. However, Morino et al (ref. 2) showed that numerical problems in determining the singularity strengths were reduced if they were, in effect, rendered unique by stipulating that the perturbation potential vanish inside the body. So doing has the following effects:

1. The source strength

$$\sigma = (\overline{w_u} - w_\ell) \cdot \overline{n}$$

becomes identical to the normal component of the perturbation mass flux on the outer surface of the body, $\overline{w}_u \cdot \overline{n}$ which, if the surface is impenetrable, is simply the negative of the normal component of the freestream velocity. In other words, the source strength is known from the condition of impenetrability to be

$$\sigma = - \overline{V}_\infty \cdot \overline{n}$$

2. The doublet strength reduces to the perturbation potential on the outer surface, ϕ_u . Hence the perturbation velocity on the body surface can be computed by simply differentiating the doublet strength.

In the pilot code, Morino-type boundary conditions are imposed by setting $(\overline{w}_u - \overline{w}_\ell) \cdot \overline{n} = -\overline{V}_\infty \cdot \overline{n}$ at all panel-center control points, and $\phi_\ell = 0$ at both panel-center and network-edge control points.

In supersonic flow these boundary conditions may only be applied on subinclined networks (i.e., all panels lie with the Mach cone from their respective leading edges). Superinclined boundary conditions are discussed later in Section 1.3.3.

1.3.2 Wake Boundary Conditions.

All doublet or composite networks must be followed downstream by another doublet or composite network or by a wake type network. This is necessary even for supersonic trailing edges to insure correct edge matching. A pure doublet wake network may be one of two types (designated "type 18" or "type 20"). Fig. 1-11 illustrates the use of these two network types. A wake network of type 18 is used behind a wing, with the boundary condition $\overline{w} \cdot \overline{n} = - \overline{V}_\infty \cdot \overline{n}$ specified on the leading edge, and no other boundary conditions being imposed. (This network type has only leading edge control points; there are no other control points.) The doublet strength on a type 18 network varies in the spanwise direction, but is constant in the streamwise direction. This enables the kutta condition to be satisfied. A type 18 network is also used behind the body in insure that the flow leaves the surface tangetially.

A wake network of type 20 is used behind a curved body, and is a surface of constant doublet strength. The boundary conditions imposed are the same as before $\overline{w} \cdot \overline{n} = - \overline{V}_\infty \cdot \overline{n}$ but this condition is applied at the origin of the M-N coordinate system only, on the leading edge control point. Again there are no other control points. Often the leading edge of such a network will be collapsed to a point, this point being the intersection of the wing trailing edge and the body. In both types of wake networks, the distinction between rows and columns is no longer arbitrary. The M vector must always point in the down stream direction as shown in Fig. 1.11. A type 20 network must not attach along a supersonic edge-o.k., if wake network attaches at a point.

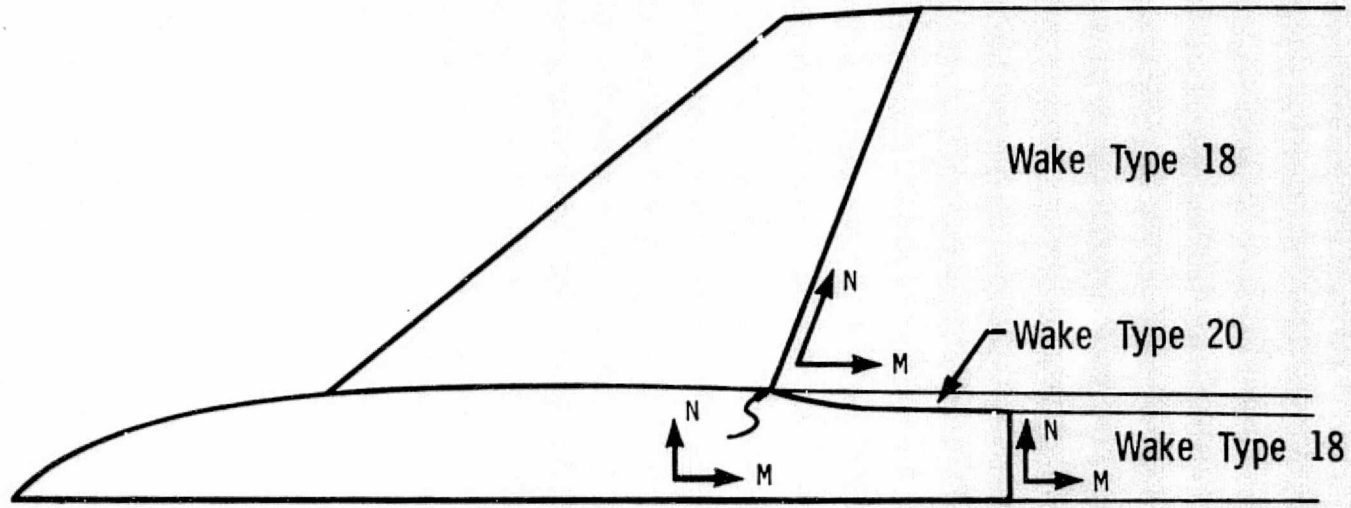

Figure 1.11 Wake Paneling

1.3.3 Superinclined Boundary Conditions - Supersonic Flow Only.

In the analysis of the complete aircraft configurations in supersonic flow, one has to take account of the flow into the inlets of the jet engines. Where primary interest is in the pressure distribution on the exterior surfaces, the nacelle may be effectively closed by using a network of superinclined panels (panels inclined ahead of the Mach cone from their respective leading edges) to cover the inlet. Boundary conditions can be applied only to the downstream side of any superinclined network. In subroutine INPUT a superinclined network is designated as a composite network in the same way as for subinclined networks, see Fig. 1.10. With the downstream side denoted by the subscript 1, the boundary conditions

$$\overline{w}_\ell \cdot \overline{n} = 0$$

and

$$\phi_\ell = 0$$

are applied, the former at panel center control points and the later at both panel-center and network edge control points. These boundary conditions produce free stream flow downstream of the network. Again, note that superinclined boundary conditions are only applied in supersonic flow.

1.4 FORCES AND MOMENTS

Forces and moments on each network are calculated in the following manner. Let S be a portion of a physical surface. The force coefficient vector C_F on S is defined as

$$\overline{C}_F = \frac{1}{S_R} \iint_S C_p \overline{n}\, ds$$

where S is a specified condiguration reference area and $\bar{n}$ is the unit normal to the surface S (in the direction N x M).

A pressure coefficient can be defined for each side of S since there is always flow on both sides of S (although the flow on one side may be of no physical interest, e.g. inside a thick wing). The side of S on which the normal $\bar{n}$ points outward is called the upper surface and the other side of S is called the lower surface. Hence, both an upper and lower surface force coefficient can be defined. If the flow on both sides of S is physically significant (e.g., on a thin wing) then the total force coefficient for S must be considered as the sum of the upper and lower surface force coefficients. An upper surface, lower surface, and "sum" force coefficient are computed for each network. Moreover, these coefficients are accumulated separately over all (non-wake) type networks. The accumulated values are useful only when the physically significant force coefficient happens to be upper surface, lower surface, or "sum" for all networks of a given configuration. For example, the total force coefficient for a body and thin wing combination would have to be computed by hand by adding the upper surface body force coefficient to the "sum" wing force coefficient.

The moment coefficient C_M at a point R_R about an axis $\bar{t}_R$ is defined by

$$\bar{C}_M = \frac{1}{S_R T_R} \bar{t}_R \cdot \iint_S (\bar{R} - \bar{R}_R) \times \bar{n} C_p \, ds$$

where T_R is a configuration reference length for the axis $\bar{t}_R$. Moment coefficients are calculated for $\bar{t}_R$ equal to each of the three coordinate axis. An upper surface, lower surface, and "sum" value is computed for each of these coefficients and these are to be interpreted in the same manner as described for the force coefficients.

1.5 PROGRAM DESCRIPTION

The computer program is written in FORTRAN IV for the SCOPE 3.4.4 operating system of the Ames CDC 7600 computer. The program uses overlay structure and thirteen disk files (including input and output files), and it requires approximately 132000 (Octal) central memory words. This program has been designed with the primary objective of verifying new concepts and numerical experimentation.

The computer program consists of one main overlay, eleven primary overlays, and two use libraries. The program flowchart shown in Figure 1.12 illustrates the overall functions the program performs.

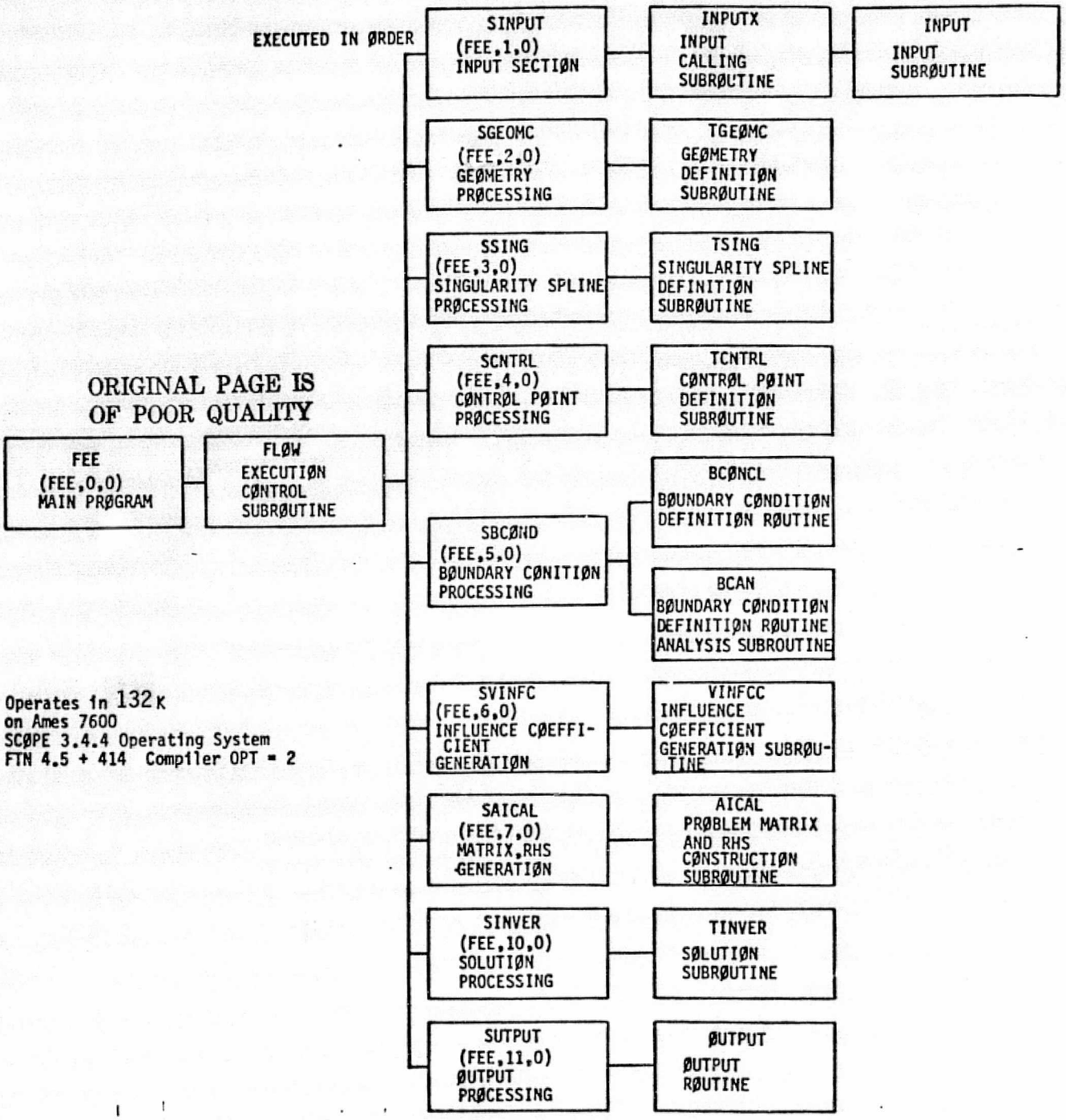

Operates in 132K
on Ames 7600
SCØPE 3.4.4 Operating System
FTN 4.5 + 414 Compiler OPT = 2

1.12 Program Flow Chart

2.0 Input Data Description

All input quantities are fed into the program in the subroutine called INPUT. A variety of INPUT routines were used during the course of the Category 2 work. It was found that in the majority of cases it was more efficient to use FORTRAN coded input than data card input. This is because about 90% of the test configurations were regular in shape and corner point data could be easily generated with code. On those occasions when externally generated corner point data was employed simple read statements were inserted at appropriate places in the code.

As is summarized in Fig. 2-1: the input sequence is divided into four basic sections:

1. The General Specifications section defines the basic parameters that control the amount of printout, defines the number of solutions, defines the reference parameters, etc.
2. The Flow Conditions seciton defines the combinations of angle of attack and sideslip to be analyzed.
3. The Network Geometry Specificaitons define the network geometry. This can be generated in the INPUT subroutine by the appropriate FORTRAN statements or generated externally to the program and read in on cards.
4. The Boundary Condition Specifications section tends to be the most complex. Boundary conditions for each panel center and panel edge control point are specified in this section as well as the specification of network edge matching conditions.

These sections will now be described in detail. An alphabetized glossary of the input variables is given in Table 2.1.

2.1 GENERAL SPECIFICATIONS

Variables related to the basic problem specification which must be supplied in INPUT include:

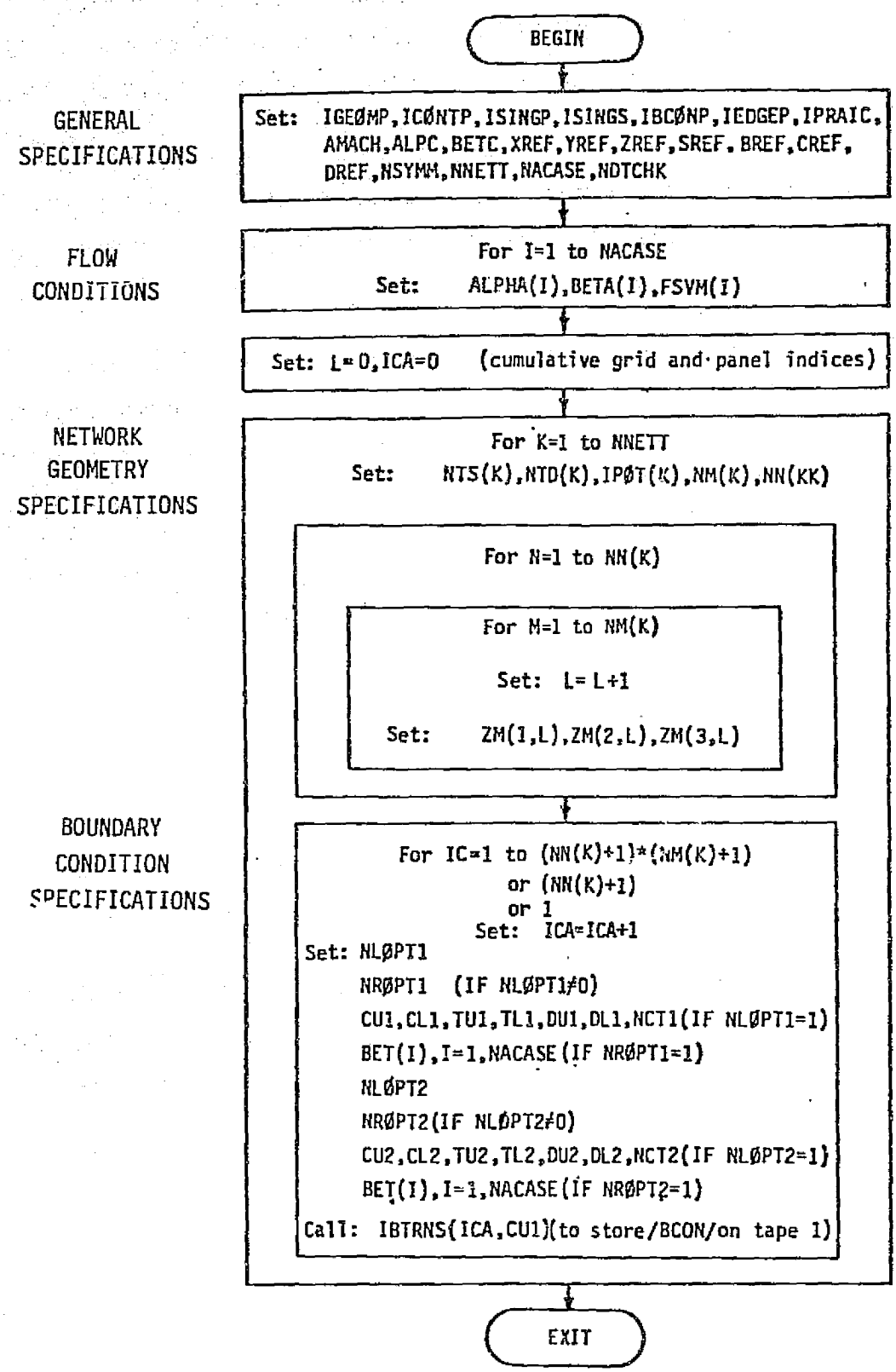

Figure 2.1 Input Data Sequence

AMACH	= Mach number of flow far upstream (M_∞)
ALPC, BETC	= Angles defining orientation of compressibility axes α_c, β_c relative to body-fixed axes.
NACASE	= Number of different combinations of α and β to be studied for the same configuration, α_c, β_c, and M_∞ (must not exceed 8).
NSYMM	= 0 if the flow is not symmetrical about the x-z plane.
	= 1 if the flow is symmetrical about the x-z plane.
	= 2 if the flow is symmetrical about the x-z and x-y plane.
NNETT	= Number of networks (must not exceed 50).
SREF	= Reference area for dimensionless force and moment coefficients.
(XREF, YREF, ZREF)	= Components of point about which moment coefficients are computed.
(BREF, CREF, DREF)	= Reference lengths for computation of (x,y,z) components of dimensionless moment coefficient.

The pilot code presently has the following size limitations:

$1 \leq$ NNETT ≤ 50

$1 \leq$ NACASE ≤ 8

In picking NNETT, the necessity for wake networks should not be forgotten; see Section 1.3.2.

There are default options for most of the above-listed parameters; see Table 2.1. In particular, note that, unless otherwise stated, the reference lengths for the moment computation are each 1.0, and the moments are taken about e origin. These default options are often satisfactory. The amount of output may be controlled by variables set in INPUT. See Section 3 for a description of the output.

IGEOMP	= 1 if geometry diagnostic data (in addition to mesh point data) are desired*
ISINGP	= 1 if singularity spline data are desired*
ICONTP	= 1 if control point and edge downwash data are desired
IBCONP	= 1 of boundary condition defining parameters are desired
IEDGEP	= 1 if edge matching diagnostic data are desired
ISINGS	= 1 if singularity strength data are desired
IPRAIC	= L if influence coefficient diagnostic data is desired for the Lth control point
NDTCHK	= 1 for program stop immediately before commencement of influence coefficient calculations. This can be used as a data check before committing the program to full execution.

The default value of these variables is 1, so that the corresponding data are output unless they are set equal to 0 (except for IPRAIC, whose default value is 0).

*Usually these data are not required.

2.2 FLOW CONDITIONS

As many as eight combinations of angle of attack, sideslip, and free-stream velocity magnitude may be specified in a single run. Results may be suspect if the specified angles of attack and sideslip differ from the compressibility axis angles by more than one or two degrees in supersonic flow.

ALPHA (I)	= Angle of attack at upstream infinity relative to body-fixed axes (I-1, ..., NACASE)
BETA (I)	= Sideslip angle at upstream infinity relative to body-fixed axes (I-1, ..., NACASE)
FSVM (I)	= Freestream velocity magnitude-Default value 1.0 (I-1, ..., NACASE)

2.3 NETWORK GEOMETRY SPECIFICATIONS

The panel corner point geometry may be generated within the INPUT subroutine by appropriate FORTRAN code or the geometry may be generated by some external paneling programs and read in on cards. Sometimes, especially when the network geometry is given as the punched-card output of some pre-processor program, the grid points are ordered in such a way as to make the outward normal point in the wrong direction. When this is the case, a subroutine MNSWCH may be called to make column into rows and vice versa:

```
CALL MNSWCH(ZM(I,L), NM(K), NN(K))
```

Here K is the identifier of the network whose rows and columns are to be switched, and L is the label of the first grid point in that network. MNSWCH also interchanges the row and column numbers NM(K) and NN(K) in the process.

The input variables defining the networks are:

NM(K) = Number of rows in Kth network (must be $\geq$ 2)

NN(K) = Number of columns in Kth network (must be $\geq$ 2)

ZM(I,L) = Ith coordinate of Lth grid point (I=1,2,3)
That is, the global coordinates of the grid point L are (ZM(L,L), ZM(2,L), AM(3,L))

Also, the pilot code is currently limited to a total of 1500 grid points, 1500 control points and 1000 panels, which may be distributed at will among the different networks.

In setting up neighboring networks, the points raised in Section 1.1.2 must be kept in mind.

2.4 BOUNDARY CONDITIONS

One or two boundary conditions must be imposed at every control point, depending on the type of network and the location of the control point. First, the type of network must be specified, as follows:

NTS(K) = 0 if the Kth network is source-free
= 1 if sources are distributed on the Kth network as described in Section 1.2

NTD(K) = 0 if the Kth network is doublet-free
= 12 if doublets are distributed on the Kth network as described in Section 1.2.
= 18 for a "type 18" wake network (see Section 1.3.2)
= 20 for a "type 20" wake network (see Section 1.3.2)

Both NTS and NTD must be specified for each network (K=1, ..., NNETT). If either parameter is zero, or if NTD = 18 or 20, one and only one boundary condition must be set at every panel center control point. Otherwise, two

conditions are required at every panel-center control point. If NTD≠0 one and only one boundary condition is required at each network-edge control point, as shown in Fig. 1.10.

The general form of the boundary condition, Equation (2) in Section 1.3, requires the specification of parameters CU, $\overline{TU}$, DU, CL, $\overline{TL}$, DL, and BET. This is accomplished by setting up a DO-loop in subroutine INPUT which assigns to every control point values of the following five parameters:

ICA	= A counter to distinguish one control point from another.
NLOPT1, NLOPT2	= Parameters governing left sides for the two boundary conditions at the control point (if only one boundary condition is to be applied, one of these parameters is set equal to zero.
NROPT1, NROPT2	= Parameters governing corresponding right sides of the two boundary conditions.

That is, the left and right side of Equation (2) are controlled by setting values of two parameters, NLOPT and NROPT. This is done twice for each control point, the suffixes 1 and 2 being used to distinguish the two boundary conditions.

The implications of particular choices of NLOPT and NROPT and NROPT are summarized in Tables 2.2 and 2.3, respectively. Options NLOPT = 2,3,4 and 5 are used when normal mass-flux boundary conditions are to be applied, while NLOPT = 11, 12, 13 and 14 are useful for normal velocity boundary conditions. With any of these eight choices of NLOPT, the standard boundary condition of impermeability requires NROPT = 3 to select the right side of the boundary condition. NLOPT = 0 is used for a null boundary condition when only one is required. Thus, the Morino-type boundary conditions discussed in Section 1.3.1 require:

NLOPT1 = 5
NROPT1 = 3
NLOPT2 = 7
NROPT2 = 2

at all panel-center control points, and

NLOPT1 = 0
NROPT1 = arbitrary
NLOPT2 = 7
NROPT2 = 2

at all network-edge control points. For the wake networks discussed in Section 1.3.2, we set

NLOPT1 = 0
NROPT1 = arbitrary
NLOPT2 = 2
NROPT2 = 3

at all control points (which are all on the network leading edge).

For the superinclined networks of Section 1.3.3,

NLOPT1 = 3
NROPT1 = 2
NLOPT2 = 7
NROPT2 = 2

at panel-center control points. At network-edge control points,

NLOPT1 = 0
NROPT1 = arbitrary
NLOPT2 = 7
NROPT2 = 2

While the above alternatives cover the most likely possibilities, the user may need to use other forms of the boundary condition (2). By setting NLOPT = 1, the coefficients of the left side may be set in subroutine INPUT. In so doing, one must also set the value of a parameter NCT for the control point in question:

If NLOPT = 1, set

NCT = 1 if DU = DL = $\overline{TU}$ = $\overline{TL}$ = 0 (i.e., if the boundary condition will involve only the normal component of perturbation mass flux)

= 4 if CU = CL = $\overline{TU}$ = $\overline{TL}$ = 0 (i.e., if the boundary condition will involve only the perturbation potential)

= 2 otherwise

Setting NLOPT1 = 1 requires the user to specify, in INPUT, the values of NCT1, CU1 and CL1 (unless NCT1 = 4), DU1 and DL1 and (unless NCT1 = 1), and $\overline{TU}$ and $\overline{TL1}$ (only if NCT1 = 2). Setting NLOPT2 = 1 requires, instead, the specification of NCT2, CU2 and CL2, etc.

Similarly, the right side of Equation (2) can be set according to the user's special needs in INPUT by setting NROPT = 1. If NORPT1 = 1, the user specifies BET1, while if NROPT2 = 1, it is BET2 that must be supplied in INPUT. To allow for the possibility that BET depends on the angles of attack and/or side-slip, or on the magnitude of the freestream velocity, BET1 and BET2 are vectors of length 8. Thus, if NACASE 1, the user must set BET1(I) or BET2(I) for I = 1,..., NACASE.

If the coefficients of the boundary condition (2) depend on the location of the control point, it will not be possible to set them in INPUT, since the locations of the control points are not set until after subroutine IBTRNS (see below) is called. In such cases, and possibly others, the user must supply subroutines (CCOF and/or CBET. These will be called by the program at time boundary conditions are being applied.

Subroutine CCOF will have as arguments the parameters of the left side of equation (2), CU, CL, DU, DL, $\overline{TU}$, $\overline{TL}$ as well as the indicator NBIN. The parameters $\overline{TU}$ and $\overline{TL}$ must be dimensioned variables, with dimension 3. Similarly CBET has arguments BET and NBIN where BET is a dimensioned

variable with dimension 8. Data on the control point location can be communicated through COMMON block /CNTRQ/. Should BET depend on the freestream flow conditions, they can be furnished CBET through COMMØN block /ACASE/. The structure of these blocks is given below. If both boundary conditions at a control point must be specified using CCOF and/or CBET they can be distinguished by the indicator NBIN=1 or 2.

If NLOPT = 10, user supplies

```
    SUBROUTINE CCOF (CU, CL, TU, TL, DU, DL, NCT)
    DIMENSION TU(3),TL(3)
```

If NROPT = 5, user supplies

```
    SUBROUTINE CBET (BET)
    DIMENSION BET (8)
```

If either or both cases, the following common blocks may be userful:

```
    COMMON/CNTRQ/ZC(3), ZNC(3), ZDC,IPC,ICC,JZC,JCN,KC
    COMMON/ACASE/ALPHA(8), BETA(8, FSVM(8)) FSV(3,10),IACASE, NACASE
    COMMON/BCOND/DUM (18), NCT,NLOPT, NROPT
```

Here

ZC(I)	= Ith coordinate of control point whose boundary condition is being set
ZNC(I)	= Ith coordinate of outward surface normal at control
KC	= Network of control point
FSVM(I)	= Magnitude of freestream velocity in Ith case
FSV(I,J)	= Ith component of freestream velocity in Jth case and the other quantities have been described previously.

and the other quantities have been defined previously.

If Morino-type boundary conditions are applied, the user gains one additional option, namely the method to be used for computing the flow velocity on the network surface. Generally, this can be done by summing the velocity fields due to the source and doublet distributions over all the networks. However, as noted in Section 1.3.1, use of Morino-type boundary conditions in theory makes the velocity on a particular panel identical with the gradient of the doublet strength on that panel. One can thus avoid calculation of the velocity influence coefficients, and so save substantial CPU and IO time, or compute the surface flow velocities both from a sum over the entire system or networks and from the doublet-strength gradient, so as to gain a measure of the adequacy of the paneling The controlling parameter is IPOT(K), K being the network label.

IPOT(K)

= 2 if the velocities and pressures at control points on the upper surface of the Kth network are to be computed from the gradient of the local doublet strength.

= 1 if they are to be computed both from the doublet strength gradient and by integrating over the entire system of singularities

= 0 all velocities and pressures on the Kth network are to be computed only by integrating over the entire system of singularities

= -1 if the velocities and pressures at control points on the lower surface of the Kth network are to be computed both by differenting the local doublet strength and integrating over the networks.

= -2 if the lower surface velocities and pressures are to be computed by differentiating the local doublet strength.

Options IPOT(K) = -1 and -2 would be used if it were the lower surface of the network which is wetted, and the potential on its upper surface set equal to zero (i.e., if NLOPT1 = 5, NROPT1 = 6, NLOPT2 = 6, NROPT2 = 2). If IPOT(K) = $\pm$ 1, the forces and moments due to the upper or lower surface pressure distribution is calculated from the pressures corresponding to the doublet-strength gradient velocity field.

Once the boundary conditions are set at a particular control point, they are filed by calling subroutine IBTRNS (ICA, CUI). As illustrated in Fig. 2.1, this is done on a networks-by-network basis with ICA being a cumulative control point counter.

For non-wake networks, the control point index (IC in Fig. 2.1) ranges from 1 to (NN(K) + 1) * (NM(K) + 1). For type 18 wake networks, it goes from 1 to (NN(K) + 1), while for type 20 networks IC goes from 1 to 1.

2.5 EXAMPLES

An example of subroutine INPUT is given in Fig. 2.2.

This example was used to generate the data reported in Section 4.6 below. It could be adapted to any case for which the network geometries were available on punched cards in the following format:

1. The first card gives the number of networks.
2. For each network, the first card gives the numbers of rows and columns. For each column, succeeding cards give the global coordinates (x, y, z) of the grid points in order of increasing grid-point labels, two points to a card (the format for all cards is 6F10.6). This is done for each column in succession, so that the points are read in the order illustrated in Fig. 1.6. The example does assume Morino-type boundary conditions on all networks. Since the boundary-condition specification tends to be the most complex part of INPUT to the program, we give a number of examples below to illustrate what must be done in different situations.

```
      SUBROUTINE INPUT
C
C  THE COMMON BLOCKS WHICH FOLLOW MUST ALWAYS BE PART OF
C  THIS SUBROUTINE, VERBATIM
C
      COMMON/ACASE/ALPHA(10),BETA( 8 ),FSVM( 8 ),FSV(3, 8 ),IACASE,NACASE
      COMMON/BCON/CU1,CL1,TU1(3),TL1(3),DU1,DL1,BET1( 8 ),NCT1,NLOPT1,
     +  NROPT1,CU2,CL2,TU2(3),TL2(3),DU2,DL2,BET2( 8 ),NCT2,NLOPT2,NROPT2
      COMMON/CASE/ICASE,NCASE
      COMMON/COMPRS/AMACH,BETAMS,BETAM,SBETAM,ABETMS,ALPC,BETC,
     +  COMPD93),AROTC(9),AROTCI(9)
      COMMON/DATCHK/INDTCHK
      COMMON/INDEX/NTS(50),NTD(50),NM(50),NN(50),NZ(50),NP(50),NSS(50),
     +  NSD(50),NC(50),NBC(50),NZA(51),NPA(51),NSSA(51),NSDA(51),
     +  NCA(51),NBCA(51),IPOT(50),NNETT,NZMPT,NPANT,NSNGT,NSNGU,NSNGK,
     +  NCTRT,NBCOT
      COMMON/MSPNTS/ZM(3,1500)
      COMMON/PRNT/IGEOMP,ISINGP,ICONTP,IBCONP,IEDGEP,ISINGS,IPRAIC
      COMMON/SYMM/NSYMM
C
C  THE FOLLOWING COMMON BLOCKS ARE OFTEN USEFUL
C
C  IN /NCONS/, PI=3.14...,PI2=PI*2,PI4I=PI/4
C
C  /SKRCH1/ PROVIDES SPACE FOR WHATEVER PREPROCESSING OF GRID POINT
C  DATA MAY BE REQUIRED
C     COMMON/NCONS/PI,PI2,PI4I
C     COMMON/SKRCH1/DUMMY(22500)
C
C  SET TERMINATION LIMIT
C
      NDTCHK = 0
C
C  SET OUTPUT CONTROLS
C     ISINGP=0  $  IGEOMP=0
      ICONTP=1  $  IBCONP=1  $  IEDGEP=1  $  ISINGS=1  $  IPRAIC=1
C
C  SET BASIC FLOW PARAMETERS
C
      AMACH=2.05
      ALPC=2.  $  BETC=0.
      NACASE=1
      DO 100 IACASE=1,NACASE
      ALPHA(IACASE)=2.  $  BETA(IACASE)=0.
  100 CONTINUE
      NSYMM=1
C
C  SET UP GRID POINTS
C
C  HERE THEY ARE READ IN IN STANDARD FORM USED IN THE
C  230 GRID GENERATION PROGRAM
C
C
C
C     FIRST READ IN NUMBER OF NETWORKS
C
      READ (5,1000) ANET
 1000 FORMAT(6F10.6)
      NNETT=ANET
      L=0
      DO 210 K=1,NNETT
C
C     FOR EACH NETWORK, READ IN NUMBERS OF ROWS AND COLUMNS
C
      READ (5,1000) A,B
      M=A  $  N=B  $  NM(K)=M  $  NN(K)=N  $  NPOINT=N*M
      DO 200 J=1,N
C
C     FOR EACH COLUMN, READ IN COORDINATES OF EACH GRID POINT
C
      IL=(J-1)*M+L+1  $  IU=J*M+L
      READ (5,1000) ((ZM(IC,I),IC=1,3),I=IL,IU)
  200 CONTINUE
  210 L=NPOINT+L
C
C  SET UP BOUNDARY CONDITIONS
C
C  HERE THEY ARE PHI=0 ON LOWER SURFACE AT ALL CONTROL POINTS AND
C  SOURCE STRENGTH CANCELLING FREESTREAM AT ALL SOURCE CONTROL POINTS
C
      ICA=0
      DO 340 K=1,NNETT
      NTS(K)=1  $  NTD(K)=12  $  IPOT(K)=1
      NMP1=NM(K)+1  $  NNP1=NN(K)+1
      DO 330 N=1,NNP1
      DO 320 M=1,NMP1
      NLOPT1=5  $  NROPT1=3  $  NLOPT2=7  $  NROPT2=2
      IF ((M.EQ.1).OR.(M.EQ.NMP1).OR.(N.EQ.1).OR.(N.EQ.NNP1)) NLOPT1=0
C
  310 ICA=ICA+1
      CALL IBTRNS(ICA,CU1)
  320 CONTINUE
  330 CONTINUE
  340 CONTINUE
C
C  THIS COMPLETES THE INPUT PHASE.  NOW DIRECT THE PROGRAM TO CARRY OUT
C  THE CALCULATIONS AND OUTPUT THE DESIRED RESULTS
C
      RETURN
      END
```

ORIGINAL PAGE IS
OF POOR QUALITY

Figure 2.2 Sample Input Subroutine

2.5.1 Example 1: Morino-Type Boundary Conditions.

The boundary-conditions section of the INPUT subroutine shown in Fig. 2.2 assigns Morino-type boundary conditions to control points which are ordered column by column, just as are the grid points. As can be seen from Fig. 2.3, for a network with NM rows and NN columns of grip points, there are NM + 1 rows and NN + 1 columns of control points. In the first and last rows and columns, only one boundary condition is required ($\phi_\ell = 0$), while both boundary conditions are required at all other control points. This is reflected in the IF-statement of the programming illustrated in Fig. 2.2.

For networks in which one edge collapses to a point, see Fig. 2.4, the number of control points is less than (NM + 1) · (NN + 1). However, the programming listed in Fig. 2.2 will still be usable. The program recognizes the apparent redundancy in control points, and automatically stores the appropriate data for the tip control point just once.

2.5.2 Example 2: Source Panel Network.

The network consists only of sources, whose strength is to be specified equal to Q, a constant. It is still necessary to cycle the DO-loop thru the potential edge control points, so that the only changes from Example 1 are that:

```
NLOPT1 = 5
NROPT1 = 1
NLOPT2 = 0
NROPT2 = 0
```

and, before calling IBTRNS, one sets BET1 = Q.

2.5.3 Example 3: Doublet Panel Network.

The network consists only of doublets, whose strength is to be specified, and there is no adjacent network (such a network was specified to generate a disturbance in the checkout of the superinclined network). Some care must be taken in this specification. The doublet strength must vanish on any free network edge; otherwise a line vortex will be generated there,

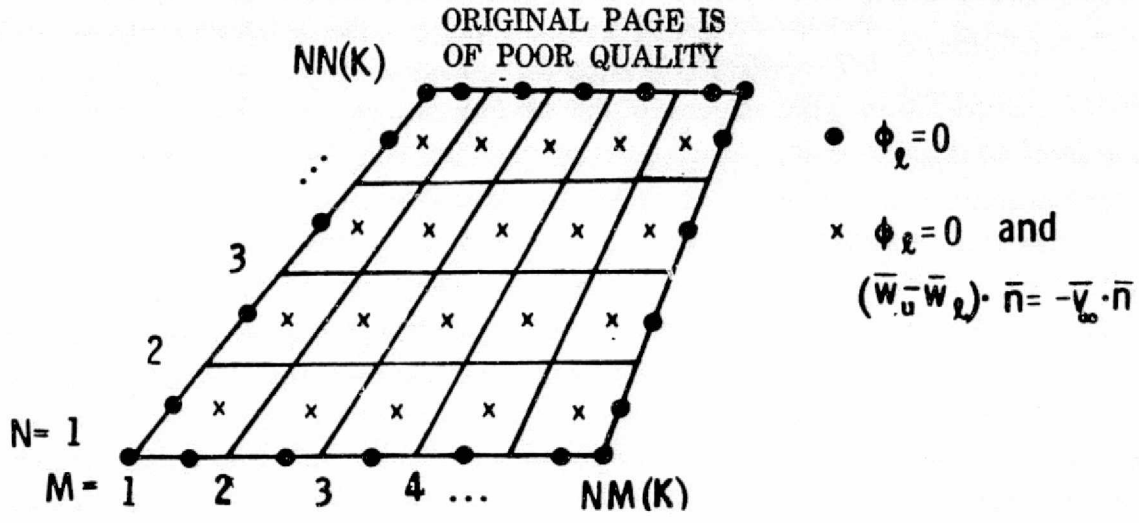

Figure 2.3 Control Points for Example 1: Quadrilateral Network

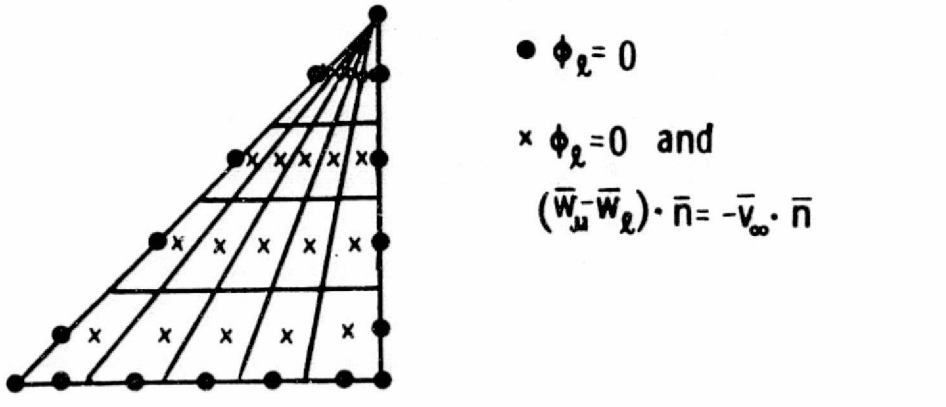

Figure 2.4 Control Points for Example 1: Triangular Network

and the analysis specifically deletes line-vortex contributions to the velocity field (for numerical convenience). This is an example in which the right side of the boundary condition will depend on the control point location, and so a case where we must set NROPT = 5 and supply a subroutine CBET.

Changes required in the DO-loop of Example 1 are as follows:

```
    DO 330 N = 1, NNP1
    DO 320 M = 1, NMP1
    NLOPT1 = 9
    NROPT1 = 5
    NLOPT2 = 0
    NROPT2 = 0
    ICA = ICA + 1
    CALL IBTRNS (ICA, CU1)
320 CONTINUE
330 CONTINUE
```

Here is an example of the subroutine CBET which must be supplied:

```
    SUBROUTINE CBET (BET)
    DIMENSION BET (8)
    COMMON/CNTRQ/ZC(3), ZNC(3), DUM, IDUM(4), KC
    COMMON/DOUBLET/SIZE(2)
    DEL = SIZE (1) ** 2
    Y = ZC (2)
    Z = ZC(3)
    BET = 9./16. * (1. - (Y/DEL) ** 2) * (1. - (Z/DEL) ** 2)/DEL
    ** 2
    RETURN
    END
```

Note the communication of some miscellaneous data (the vector SIZE (2)) to CBET through yet another common block.

2.5.4 Example 5: Multi-Network Wing Body Configuration.

Our final example, the piece de resistance, is a wing-body problem. The configuration is shown in Fig. 2.5. As noted in Section 1.2.3, it is essential to make the points at which the leading and trailing edges of the wing meet the body at corner points of the singularity network. Thus, it is necessary to split the body surface into 6 networks, and the wing surface into two, as indicated in Fig. 2.6. Since this configuration is being to modeled for supersonic flow, it is not necessary to close off the base of the body to form a closed surface. In subsonic flow this would be necessary. The wing fillet, which is part of the body networks, gave us considerable trouble in insuring a perfect match between the grid points on the edges of the neighboring networks. Our solution is depicted in Fig. 2.7.

It is necessary to model both the body's and the wing's wake. Because of the fillet, we required a "type 18" network to trail from the wing itself and a "type 20" to fill the gap between the wing's wake and the body. Two "type 18" networks were used to model the body's trailing wake. The complete system of networks is shown in Fig. 2.8 with the directions of the M and N vectors for each network given in the 3-views of Fig. 2.9.

We are now ready to set up the boundary conditions. On the four wake networks (9, 10, 11, 12), the boundary condition is that the total mass flux be parallel to the surface. This is accomplished by setting NLOPT1 = 0, NROPT1 = 0, NLOPT2 = 2, NROPT2 = 3 for each control point on the wake network. Recall from Section 1.3.2 that networks only have control points at their leading edge. The configuration networks form a closed impermeable boundary so we wish the source strength to cancel the normal component of the freestream mass flux, and the doublet distribution to make the perturbation potential inside the configuration vanish. This is accomplished by setting NLOPT1 = 5, NROPT1 = 3, NLOPT2 = 7 and NROPT2 = 2 at all panel-control points ($(\overline{W}_u - \overline{W}_\ell) \cdot \overline{n} = \overline{V}_\infty \cdot \overline{n}$ and $\phi_\ell = 0$) and setting NLOPT1 = 0, NLOPT2 = 7 and NROPT2 = 2 at all panel edge control points ($\phi_\ell = 0$).

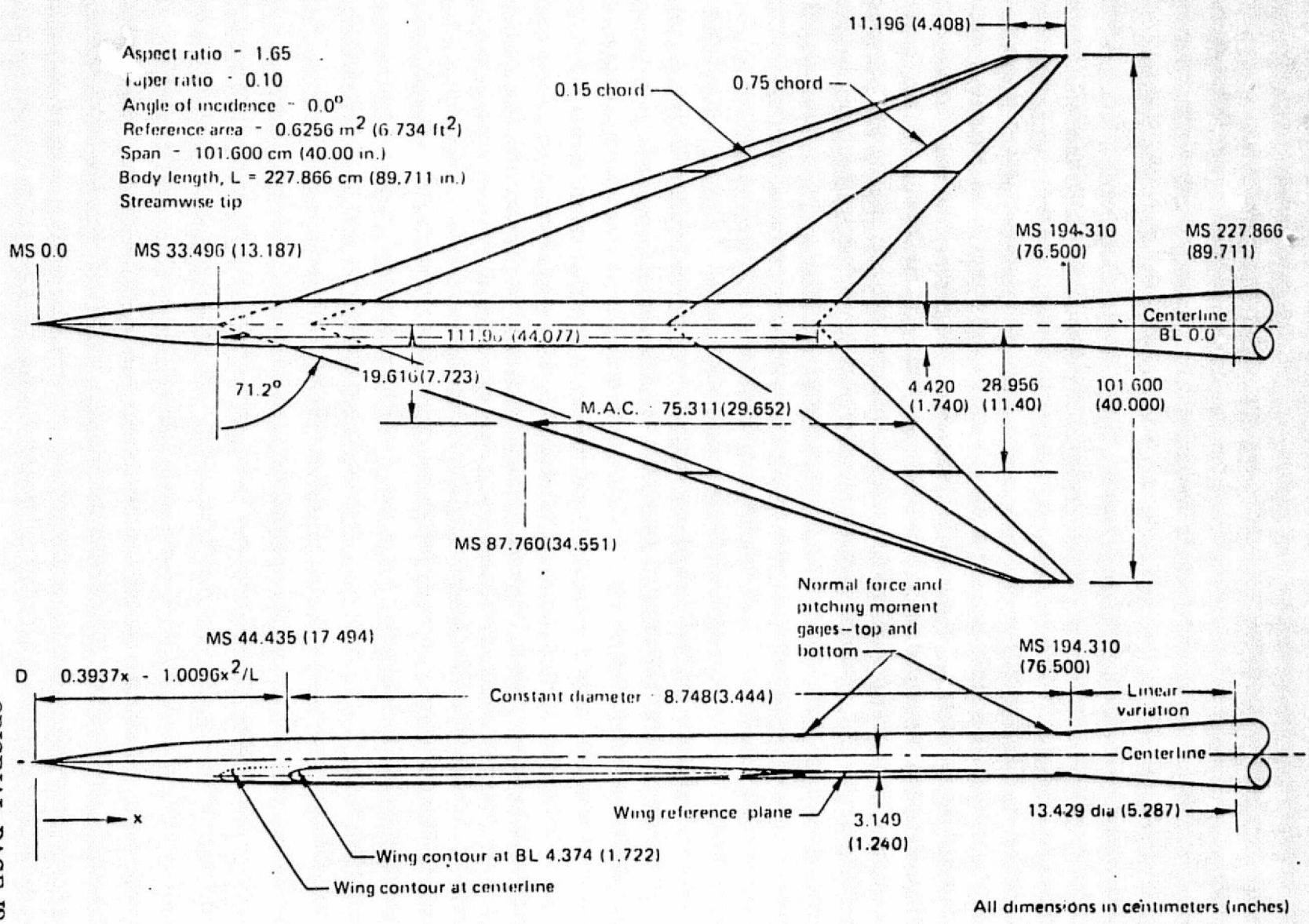

FIGURE 2.5 Arrow - Wing Body: General Arrangement

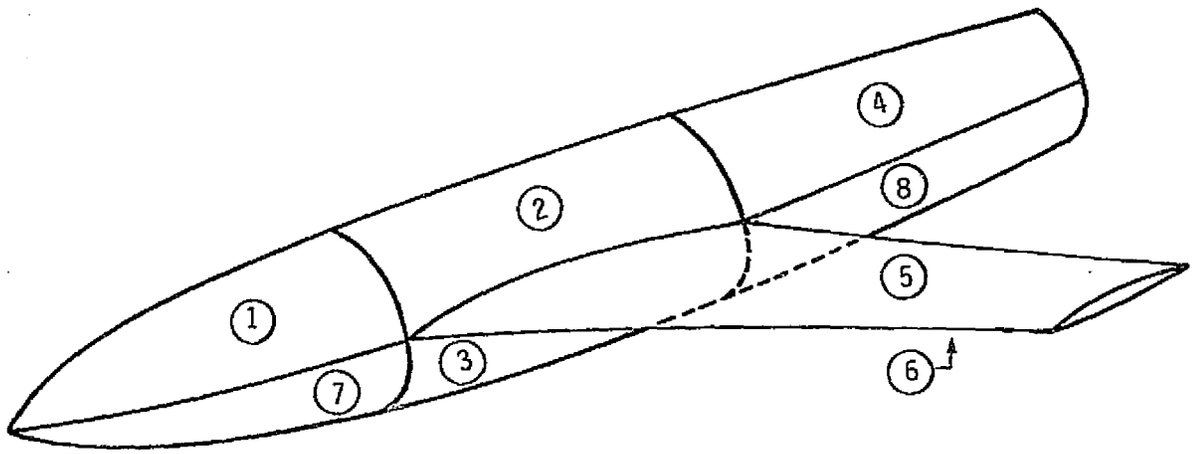

Figure 2.6 Wing-body Networks

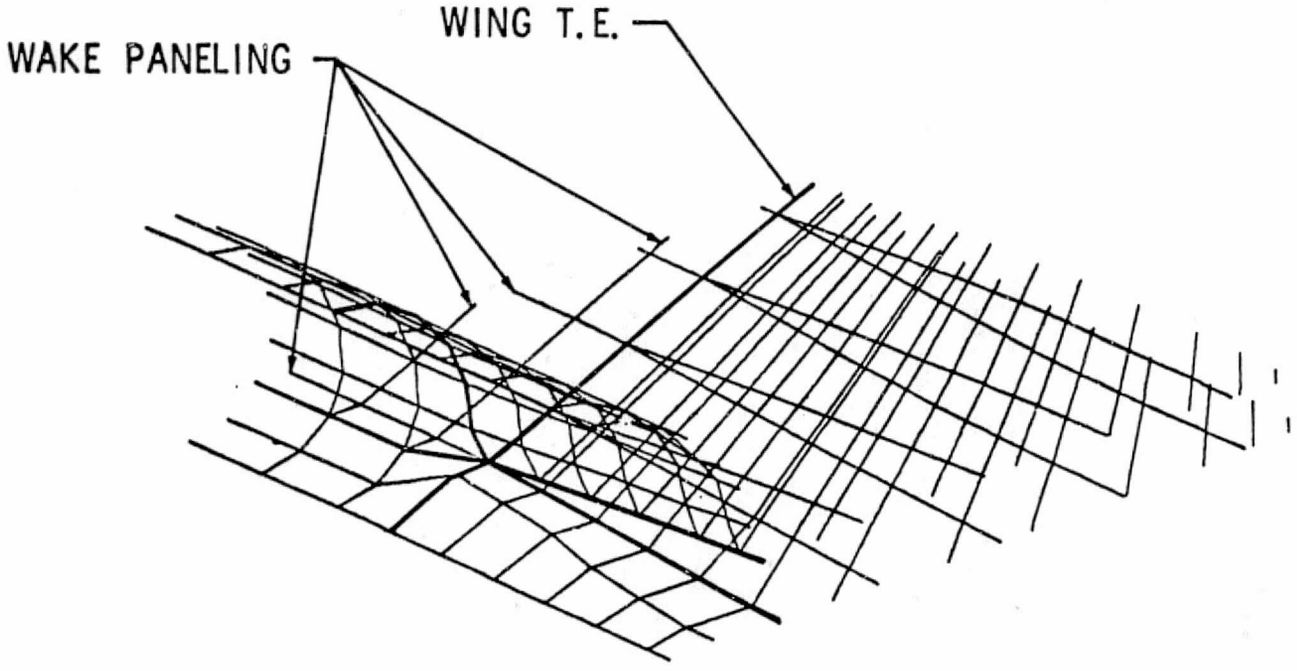

FIGURE 2.7 WING - BODY INTERSECTION DETAIL - T.E.

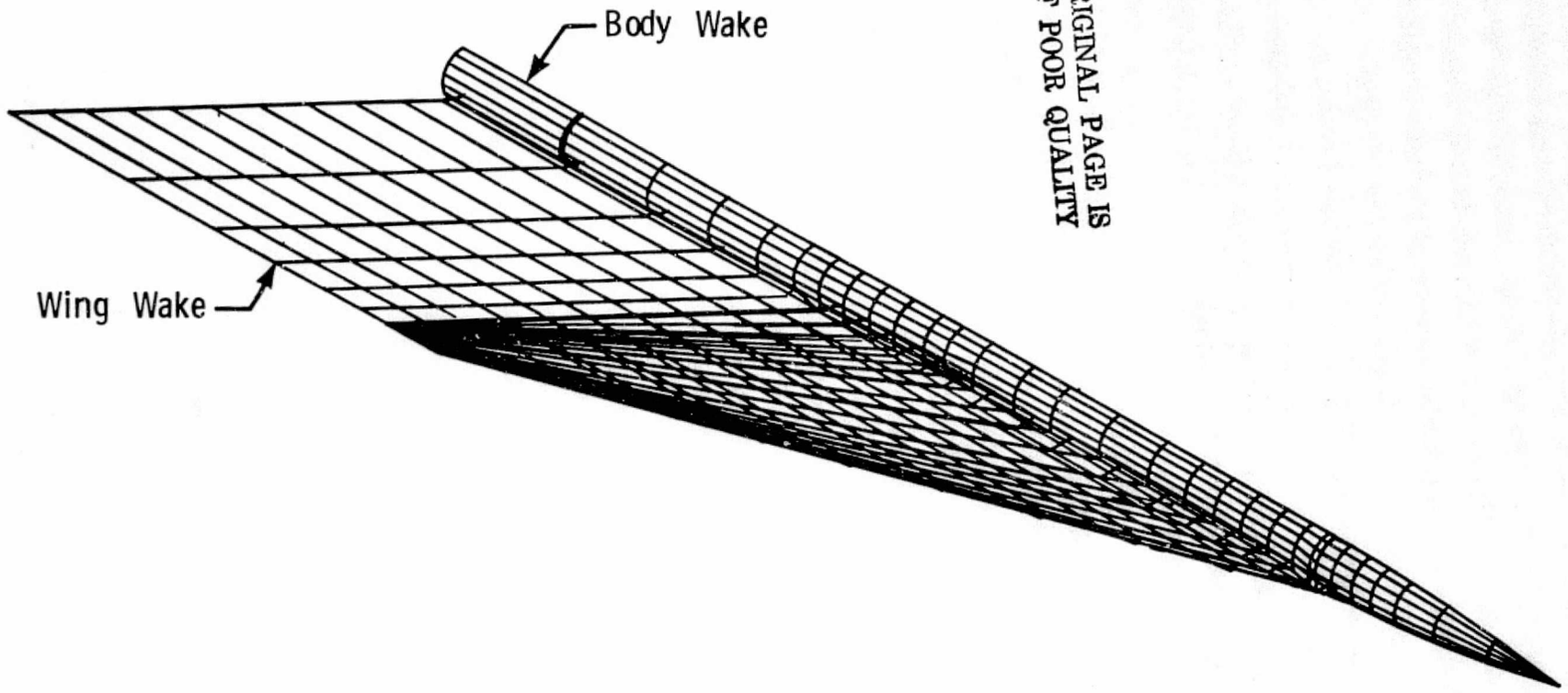

FIGURE 2.8 ARROW WING / BODY PANELING

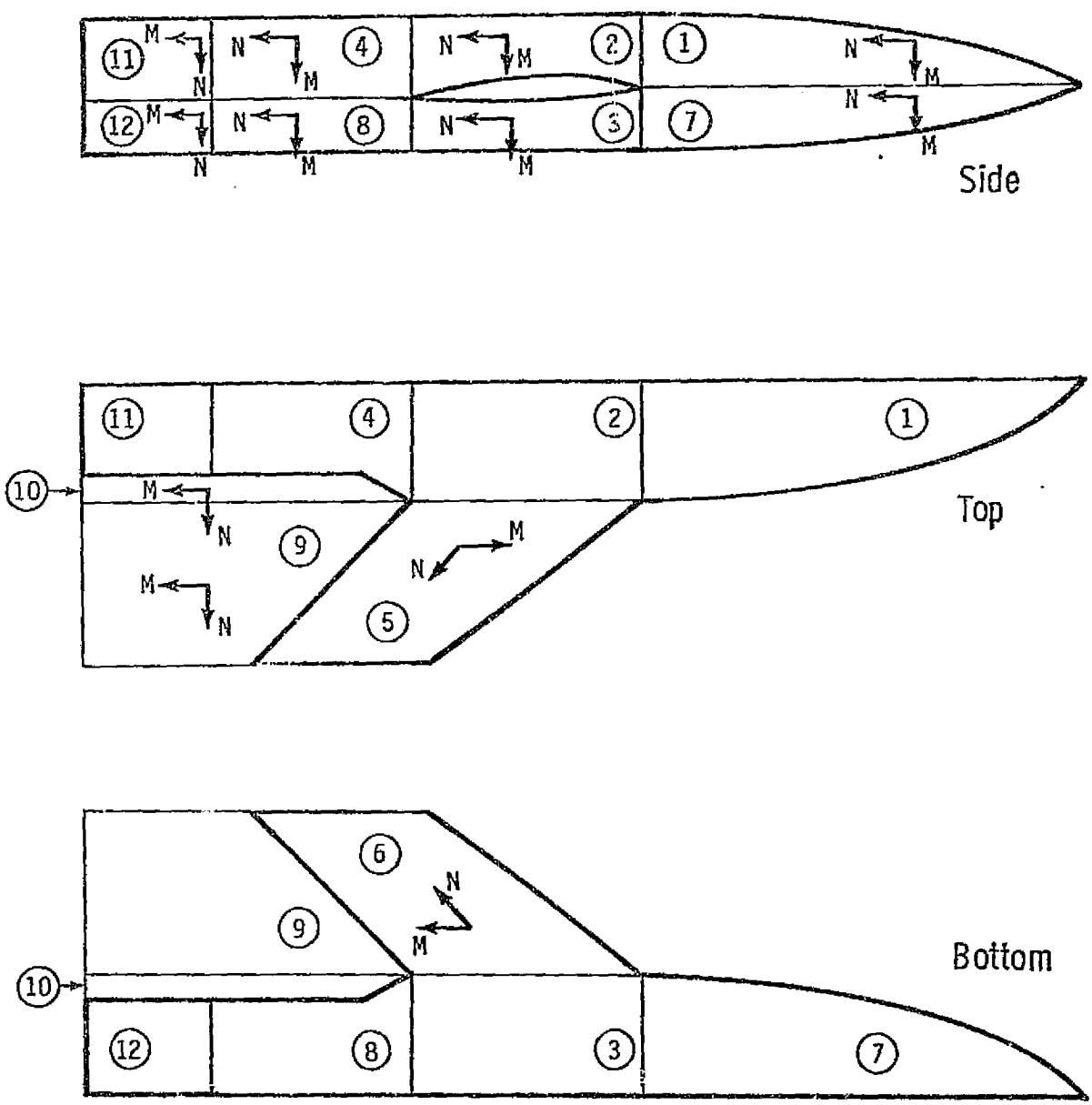

Figure 2.9 Directions of $\vec{M}$ and $\vec{N}$ Vectors on Wing-Body Networks

The subroutine INPUT used for this configuration is illustrated in Fig. 2-10. In order to reduce computing costs, IPOT(K) = 2. This instructs the program to compute only the potential influence coefficients deleting the velocity influence coefficient calculations. With this option the velocities and pressures of control points are calculated by differentiating the local doublet strergth.

The paneling coordinates have been generated external to the pilot code. Geometry coordinates are read in by network in 6F10.0 format.

Networks numbered 10 or greater were inadvertently generated with the wrong NxM sense. A call to subroutine MNSWCH reverses the order of the input array.

Networks 1 to 8 are designated composite source-doublet networks; networks 9 and greater are designated wake type 18 networks, except for network 10 which is a type 20. Morino-type boundary conditions are specified for the configuration surface networks (1-8). Once the boundary conditions have been specified for all networks, a call to subroutine IBTRNS stores the data on a random access file using ICA as an index.

```
      SUBROUTINE INPUT

      COMMON/ACASE/ALPHA (8),BETA(8),FSUM(8),FSU(3,8),IACASE, NACASF
      COMMON/BCON/CU1,CL1,TU1(3),TL1(3),DU1,DL1,BET1(8),NCT1,NLOPT1,
      CNROPT1,CU2,CL2,TU2(3), TL2(3),DU2,DL2,BET2(8),NCT2,NLOPT2,NROPT2
      COMMON/CASE/ICASE,NCASE
      COMMON/COMPRS/AMACH,BETAMS,BETAM,SBETAM,ABETMS,ALPC,BETC,
      CCOMPD(3),AROTC(9),AROTCI(9),CZINU(3,3)
      COMMON/DATCHK/NDTCHK

      COMMON/INDEX/NTS(50),NTD(50),NM(50),NN(50),NZ(50),NP(50),NSS(50),
      CNSD(50),NC(50)NBC(50),NZA(51), NPA(51),NSSA(51),NSDA(51),NCA(51),
      CNBCA(51),IPOT(50),NNETT,NZMPT,NPANT,NSNGT,NSNGU,NSNGK,NCTRT,NBCOT
      COMMON/MSPNTS/ZM(3,1500)
      COMMON/NCONS/PI,PI2,PI4I
      COMMON/PRNT/IGEOMP,ISINGP,ICONTP,IEDGEP, ISINGS, IPRAIC
      COMMON /SYMM/NSYMM

C
C SET OUTPUT CONTROLS
C
      ISINGP=0
      IGEOMP=0

C
C SET-TERMINATION LIMIT
C
      NDTCHK=0
C
C SET BASIC FLOW PARAMETERS
C
      AMACH=1.7
      NSYMM=1
      NACASE=1
      ALPHA(1)=2.0
      ALPC=2.0
      BETC=0
C
C SET UP NETWORK GEOMETRY
C
C     FIRST READ IN NUMBER OF NETWORKS
C
      READ(5,100) ANET
      NNETT=ANET
      L=0
      ICA=0

C
C     NZA NEED NOT BE SET IN INPUT, BUT IS USED HERE ONLY TO
C     FACILITATE SUBSEQUENT CALL OF MNSWCH
C
      NZA(1)=0
      DO 3000 K=1,NNETT
C
C SET SINGULARITY TYPE
C
C
C     COMPOSITE SOURCE - DOUBLET NETWORKS
C
      NTS(K)=1
      NTD(K)=12
C
C     NETWORKS 9 or GREATER ARE WAKE NETWORKS
C
      IF(K.GE.9) NTS(K)=0
      IF(K.GE.9) NTD(K)=18
      IF(K.EQ.10) NTD(K)=20
C
C SET INDICATOR FOR COMPUTING POTENTIAL INFLUENCE COEFFICIENTS
C     ONLY TO REDUCE CPU AND IO COSTS
C
      IPOT(K)=2
C
C     FOR EACH NETWORK, READ IN NUMBERS OF ROWS AND COLUMNS
C
      READ(5,100)A,B
  100 FORMAT (6F10.0)
  105 M=A
      N=B
      NN(K)=N
      NM(k)=M
C
C     READ NETWORK GEOMETRY
C
      DO 20 J=1,N
      READ(5,100)((ZM(JJ,I+L),JJ=1,3),I=1,M)
      L=L+M
   20 CONTINUE
      NZAP1=NZA(k)+1
C
C     N X M ORDER OF NETWORKS 10 OR GREATER IS INCORRECT
C     CALL SUBROUTINE MNSWCH TO REVERSE ORDER
C
      IF(K.GE.10) CALL MNSWCH(ZM(1,NZAP1),NM(K),NN(K))

C
C     NZ NEED NOT BE SET IN INPUT, BUT IS CALCULATED HERE ONLY
C     TO FACILITATE SUBSEQUENT CALLS OF MNSWCH
C
      NZ(K)=NM(K)*NN(K)
      NMP1=NM(K)+1
      NNP1=NN(K)+1

C
C SET BOUNDARY CONDITIONS
C
      DO 150 N=1,NNP1
      DO 140 M=1,NMP1
C
C     WAKE NETWORKS REQUIRE BOUNDARY CONDITIONS ONLY FOR LEADING EDGE
C
      IF((NTD(K).EQ.18).AND.(M.GT.1)) GO TO 150
      IF((NTD(K).EQ.20).AND.(M.GT.1)) TO TO 3000

C
C     COMPOSITE PANEL MASS FLUX BOUNDARY CONDITIONS
C
      NLOPT1=5
      NROPT1=3
      NLOPT2=7
      NROPT2=2
C
C     ONLY ONE BOUNDARY CONDITION SHOULD BE ENTERED FOR EDGE CONTROL POINTS
C
      IF((M.EQ.1).OR.(M.EQ.NMP1).OR.(N.EQ.1).OR.(N.EQ.NNP1))NLOPT1=0
  130 ICA=ICA+1
C
C     IBTRNS SETS UP BOUNDARY CONDITION DATA ON A RANDOM
C     FILE USING ICA AS AN INDEX
C
      CALL IBTRNS(ICA,CU1)
  140 CONTINUE
  150 CONTINUE
 3000 NZA(K+1)=NZA(K)+NZ(K)
      RETURN
      END
```

Figure 2.10 INPUT Subroutine for Arrow-Wing Body

TABLE 2-1 SUMMARY OF INPUT QUANTITIES

QUANTITY	DEFINITION	DEFAULT VALUE	COMMON BLOCK
ALPC	Compressibility direction angle (of attack) in degrees	0.	/CØMPRS/
ALPHA (I)	Ith angle of attack in degrees	0.	/ACASE/
AMACH	Mach Number	0.	/CØMPRS
BETA (I)	Ith angle of yaw in degrees	0.	/ACASE/
BETC	Compressibility direction angle (of yaw) in degrees	0.	/CØMPRS/
BET1(I)	Ith right hand side of first boundary condition (see BET of equation(2))	0.	/BCØN/
BET2(I)	Ith right hand side of second boundary condition (See BET of equation (2))	0.	/BCØN/
BREF	x-axis value of T_R (SECTION 1.4)	1.	/FMCØF/
CL1	Value of CL for first boundary condition (See equation (2))	0.	/BCØN/
CL2	Value of CL for second boundary condition (See equation (2))	0.	BCØN/
CREF	y-axis value of T_R (SECTION 1.4)	1.	/FMCØF/
CU1	Value of CU for first boundary condition (See equation (2))	0.	/BCØN/
CU2	Value of CU for second boundary condition (See equation (2))	0.	/BCØN/
DL1	Value of DL for first boundary condition (See equation (2))	0.	/BCØN/
DL2	Value of DL for second boundary condition (See equation (2))	0.	/BCØN/
DREF	z-axis value of T_R (SECTION 1.4)	1.	/FMCØF/
DU1	Value of DU for first boundary condition (See equation (2))	0.	/BCØN/
DU2	Value of DU for second boundary condition (See equation (2))	0.	/BCØN/
FSVM(I)	Ith Freestrea velocity magnitude	1.	/ACASE/
IBCØNP	=1 for printout of boundary condition diagnostic data	1	/PRNT/
ICØNTP	=1 for printout of control point diagnostic data	1	/PRNT/

TABLE 2-1 SUMMARY OF INPUT QUANTITIES
(CONT'D)

QUANTITY	DEFINITION	DEFAULT VALUE	COMMON BLOCK
IEDGEP	=1 for printout of edge matching diagnostic data	1	/PRNT/
IGEØMP	=1 for printout of geometry diagnostic data	1	/PRNT/
IPØT(K)	= 0 for computation of resultant velocities at network control points using velocity influence coefficients ±1 for added computation of resultant velocities at network control points using doublet strength gradient ±2 for computation of resultant velocities from doublet strength gradient (+ for upper surface velocities with lower surface perturbation stagnation and - for the opposite) = L for printout of influence coefficient diagnostic data for L^{th} control point	0	/INDEX/
IPRAIC	=1 for printout of influence coefficient diagnostic data	1	/PRNT/
ISINGP	=1 for printout of singularity spline diagnostic data	1	/PRNT/
ISINGS	=1 for printout of resultant values of singularity strength and gradient at panel corners, center and edge midpoints	1	/PRNT/
NACASE	Number of simultaneous solutions (freestream vectors)	1	/ACASE/
NCT1	= 1 first boundary condition concerns normal mass flux only 2 first boundary condition is arbitrary 4 first boundary condition concerns potential only	2	/BCØN/
NCT2	Same as NCT1 but for second boundary condition	2	/BCØN/
NDTCHK	= 0 program run to completion 1 program stop immediately before influence coefficient calculation	0	/DATCHK/
NLØPT1	First boundary condition left hand side option	0	/BCØN/
NLØPT2	Second boundary condition left hand side option	0	/BCØN/
NRØPT1	First boundary condition right hand side option	0	/BCØN/
NRØPT2	Second boundry condition right hand side option	0	/BCØN/

TABLE 2-1 SUMMARY OF INPUT QUANTITIES
(CONT.)

QUANTITY	DEFINITION	DEFAULT VALUE	COMMON BLOCK
NM(K)	Number of grid point rows in Kth network	-	/INDEX/
NN(K)	Number of grid point columns in Kth network	-	/INDEX/
NNETT	Total number of networks	-	/INDEX/
NSYMM*	= 0 for no planes of flow symmetry 1 for x-z plane of flow symmetry with $y \geq 0$ half of configuration input 2 for x-z and x-y planes of flow symmetry with $y \geq 0$ and $z \geq 0$ quarter of configuration input	0	/SYMM/
NTS(K)	Source type of Kth network	-	/INDEX/
NTD(K)	Doublet type of Kth network	-	/INDEX/
SREF	Configuration reference area (SECTION 1.4)	1.	/FMCØF/
XREF	x-component of R_R (SECTION 1.4)	0.	/FMCØF/
YREF	y-component of R_R (SECTION 1.4)	0.	/FMCØF/
ZM(I,L)	Ith component of Lth grid point (L is a cumulative index for all grid points in the total configuration)	-	/MSPNTS/
ZREF	z-component of R_R (SECTION 1.4)	0.	/FMCOF/

*If NSYMN = 1 or 2 is selected, the force and moment coefficients will be computed from the pressures acting on half, and a quarter of the configuration, respectively.

Table 2.2

Effect of Various Choices for NLOPT on Left Side of Boundary Condition (2)

NLOPT	Left Side of Equation	Significance
0	---	Boundary condition is ignored (used when none or one boundary condition is to be applied to a control point
1	Arbitrary	Parameters of boundary condition are set in INPUT
2	$\bar{w}_u \cdot \bar{n}$	Normal component of perturbation mass flux on upper surface
3	$\bar{w}_\ell \cdot \bar{n}$	Normal component of perturbation mass flux on lower surface
4	$\frac{1}{2}(\bar{w}_u + \bar{w}_\ell) \cdot \bar{n}$	Average of upper and lower surface normal perturbation mass flux
5	$(\bar{w}_u - \bar{w}_\ell) \cdot \bar{n}$	Difference between upper and lower-surface normal mass flux (source strength
6	ϕ_u	Upper-surface perturbation potential
7	ϕ_ℓ	Lower-surface perturbation potentials
8	$\frac{1}{2}(\phi_u + \phi_\ell)$	Average of upper and lower-surface perturbation potentials
9	$\phi_u - \phi_\ell$	Difference between upper and lower surface potential (doublet strength)
10	Arbitrary	Parameters of boundary conditions reset in subroutine CC0F
11	$\bar{v}_u$	Upper-surface perturbation velocity

Table 2.2 (Cont.)

Effect of Various Choices for NLOPT on
Left side of Boundary Condition (2)

NLOPT	Left Side of Equation	Significance
12	v_ℓ	Lower-surface perturbation velocity
13	$\frac{1}{2}(v_u + v_\ell)$	Average of upper and lower-surface perturbation velocities
14	$(v_u - v_\ell)$	Difference between upper- and lower-surface perturbation velocities

Table 2.3

Effect of Various Choices for NROPT on Right Side of Boundary Condition (2)

NROPT	BET (Right Side of Equation (2))	Significance
1	Arbitrary	BET will be specified in INPUT
2	0	
3	$-\overline{V}_\infty \cdot \overline{n}$	If NLOPT=2, equation (2) says total mass flux is parallel to surface. If NLOPT=5, equation (2) specifies source strength so as to cancel freestream mass flux
4	$-\overline{V}_C \cdot (x/\beta^2, y, z)$ $\overline{V}_C$ =freestream velocity in terms of components along compressibility axes)	If NLOPT=7 and NTS=0 (no sources) it can be shown that equation (2) implies no flow thru surface
5	Arbitrary	BET will be specified in CBET.
6	$\overline{V}_\infty \cdot \overline{n}$	Same as 3 but for surface with lower side exposed to flow

3.0 Output Data Description

In this section we describe the organization of the output. The nomenclature employed in the output is summarized completely in Table 3-1.

3.1 GEOMETRY (MESH POINT) DATA

The program always lists the coordinates of all grid points, along with their unique labels, row number, column number, and network number. Specifying the network geometry is perhaps the trickiest part of setting up INPUT. The geometry data are always worth examination to see if any mistakes have been made, particularly in assigning grid points to rows and columns. These data are illustrated in Fig. 3.1. This is followed immediately by an identification of whatever subpanels are "superinclined"; i.e., whose normals are inclined to the compressibility reference axis by more than the Mach angle. Except in special cases, such as representative of inlets, superinclination of a panel indicates that the small-disturbance assumptions underlying the analysis are being violated. Moreover, the answer will be invalid if boundary conditions at the control point(s) on the panel assume subinclination. In addition, the program will identify subpanels that are close to being superinclined (probably violating small disturbance assumption and print the value of the dot product of the subpanel normal with the subpanel conormal.

The listing of the actual corner points is followed by a printout of which sides of which doublet networks the program believes abut. This data is shown in Fig. 3.2 and is particularly useful in helping the user to determine whether the input grid points satisfy the second point of Section 1.1.2. The data is grouped according to abutments (i.e., groups of coincident network sides). Network sides are numbered counter clockwise from 1 to 4 with the first side corresponding to the first row of grid points and the fourth side corresponding to the first column of grid points (see Fig. 3.3). Of particular interest are abutments involving only one side whose control points are characterized as forcing doublet

strength to vanish. This implies that the side abute nothing - which may possibly be contrary to the user's wish. (The characterization of control points does not apply to network control points.)

3.2 CONTROL POINT DATA

Unless the user specifies ICONTP ≠ 1, the program next lists, for each potential* control point, its label (what is called ICA in the INPUT), network number, panel number, subpanel number, coordinates, the components of the unit normal vector to the subpanel on which it is situated, and an edge matching indicator. The unit normal should be directed from lower to upper surface of the network. This is worth checking. If it is misdirected, a call to MNSWCH may be necessary; see Section 2.3. Excessive variation from one control point to the next of the components of n often indicates that the panel size is too large. These data are illustrated in Fig. 3-4.

3.3 BOUNDARY CONDITION DEFINING PARAMETERS

Unless the user specified IBCONP ≠ 1, the program outputs, for every control point, the parameters CU, CL, $\overline{TU}$, $\overline{TL}$, DU, DL, NCT and BET for the boundary condition(s) imposed at that point. Also included are the control point label ICA and the values of NLOPT and NROPT. Especially in multi-network problems, for which the setting of boundary conditions on network edges can be tricky, these data are often worth a look. These data are illustrated in Fig. 3-5.

3.4 PROBLEM AND NETWORK INDICES

These data, illustrated in Fig. 3-6, are always generated. They give the basic statistics on the problem size, both totally and network by network. Current limits are:

*Data are also output for the midpoints of panel edges which lie on the boundaries even of source-only networks; these points are not otherwise treated as control points.

Total number of grid points (NZMPT) $\leq$ 1500
Total number of control points (NCTRT) $\leq$ 1500
Total number of panels $\leq$ 1000

3.5 EDGE DOWNWASH CONDITIONS

These may be suppressed by stipulating IEDGEP $\neq$ 1. They give the calculated matching information at control points on the edges of doublet networks. The output is intended to verify that this matching has occurred. These data are also shown in Fig. 3.6.

3.6 EQUATION SOLUTION DATA

These data, shown in Fig. 3.7 and Fig. 3.8 are always printed out. They give the order of the algebraic system governing the singularity strength, an error estimate, and pivoting information.

3.7 AERODYNAMIC INPUT DATA

Next the program always outputs the values of M, α , and β also shown in Fig. 3.8.

3.8 SINGULARITY DATA

Unless ISINGS is set $\neq$ 1, the program next prints out the source strength, the doublet strength, and the components of the gradient of the doublet strength along the row and column directions and in direction normal thereto as well as along the global coordinate axes. This is done for nine points on every panel: the four corners, the mid points of each side, and the panel center. These data, shown in Fig. 3.9, are useful in checking the continuity of the doublet strength from one network to another.

3.9 LOCAL AERODYNAMIC DATA

These data are always printed out, and usually contain the major results of the analysis. For every panel center-control point on every network, the following quantities are listed as illustrated in Fig. 3.10:

Source Strength
Doublet strength
Doublet strength gradient
Perturbation velocity potential*
Total velocity potential*
Total mass flux potential*
Perturbation mass flux vector*
Total mass flux vector*
Normal and tangential components of total
Mass flux vector*
Normal component of perturbation mass flux vector*
Pressure coefficient*

Quantities starred are listed for both the upper and lower surfaces of the network. Four different pressure formulas are used for the pressure coefficient:

$$C_p = -2u \quad \text{(Linearized)}$$

$$C_p = -2u - v^2 - w^2 \quad \text{(Slender Body)}$$

$$C_p = -2u - (1 - M_\infty^2)\, u^2 - v^2 - w^2 \quad \text{(Second Order)}$$

$$C_p = \frac{2}{\gamma M_\infty^2} \left\{ \left[1 + \frac{\gamma+1}{2} M_\infty^2 (1 - u^2 - v^2 - w^2) \right]^{\frac{\gamma}{\gamma-1}} - 1 \right\} \quad \text{(Isentropic)}$$

Here (u, v, w) is the perturbation velocity vector, referred to compressibility coordinates. Also listed are the differences in the four pressure coefficients across the network (upper surface value minus lower), the control point label, the panel label, the control point coordinates, and the components of the freestream velocity. If the INPUT parameters IPOT(K) = 1 for the Kth network velocity potentials, mass flux vectors, and pressure coefficients on the upper surface are computed (and listed) twice. The first time (line 2 or the output block), their values are based on the local gradient of the doublet strength; the second time (line 3 of the output block), on the integral over the entire singularity distribution. If IPOT(K)= -1 the same holds for lower surface quantities with the lower line being that data computed from the doublet strength gradient. For the options IPOT(K) = $\pm$ 1 there should be little difference between the redundant data. If a significant difference does occur it usually means that paneling is inadequately dense or the surface is insufficiently closed (i.e., there is too large a hole in the paneling through which the fluid is flowing) for the use of the Morino-type boundary conditions. An almost certain indicator of such inadequacies is the existence of significant non-zero normal flows (i.e., WNU or WNL as computed from the influence coefficient) on the side of the surface bounding the physical flow of interest.

These results are followed by listings, illustrated in Fig. 3.11, of the forces and moments acting on the network surface both totally and for each column of the network. The three lines of data given for each column (and for the whole network) refer to the forces and moments on the upper surface, the lower surface, and the sum of the two. The user may have to combine contributions from different networks manually rather than rely on the automatically accumulated totals. For example, if the wing of a wing-body combination has no thickness, the wing's contribution to the force involves both its upper and lower surfaces, while only the upper (outside) surface of the body makes a physically meaningful contribution.

GEOMETRY DATA

MESH POINT DATA

NUMBER	ROW	COLUMN	NET. NO.	X	Y	Z
1	1	1	1	0.0000000000	0.0000000000	0.0000000000
2	2	1	1	.0100000000	0.0000000000	0.0000000000
3	3	1	1	.0400000000	0.0000000000	0.0000000000
4	4	1	1	.0900000000	0.0000000000	0.0000000000
5	5	1	1	.1600000000	0.0000000000	0.0000000000
6	6	1	1	.2500000000	0.0000000000	0.0000000000
7	7	1	1	.3600000000	0.0000000000	0.0000000000
8	8	1	1	.4900000000	0.0000000000	0.0000000000
9	9	1	1	.6400000000	0.0000000000	0.0000000000
10	10	1	1	.8100000000	0.0000000000	0.0000000000
11	11	1	1	1.0000000000	0.0000000000	0.0000000000
12	1	2	1	.1000000000	.0577350269	0.0000000000
13	2	2	1	.1090000000	.0577350269	0.0000000000
14	3	2	1	.1360000000	.0577350269	0.0000000000
15	4	2	1	.1810000000	.0577350269	0.0000000000
16	5	2	1	.2440000000	.0577350269	0.0000000000
17	6	2	1	.3250000000	.0577350269	0.0000000000
18	7	2	1	.4240000000	.0577350269	0.0000000000
19	8	2	1	.5410000000	.0577350269	0.0000000000
20	9	2	1	.6760000000	.0577350269	0.0000000000
21	10	2	1	.8290000000	.0577350269	0.0000000000
22	11	2	1	1.0000000000	.0577350269	0.0000000000
23	1	3	1	.2000000000	.1154700538	0.0000000000
24	2	3	1	.2080000000	.1154700538	0.0000000000
25	3	3	1	.2320000000	.1154700538	0.0000000000
26	4	3	1	.2720000000	.1154700538	0.0000000000
27	5	3	1	.3280000000	.1154700538	0.0000000000
28	6	3	1	.4000000000	.1154700538	0.0000000000
29	7	3	1	.4880000000	.1154700538	0.0000000000
30	8	3	1	.5920000000	.1154700538	0.0000000000
31	9	3	1	.7120000000	.1154700538	0.0000000000
32	10	3	1	.8480000000	.1154700538	0.0000000000
33	11	3	1	1.0000000000	.1154700538	0.0000000000
34	1	4	1	.3000000000	.1732050808	0.0000000000
35	2	4	1	.3070000000	.1732050808	0.0000000000
36	3	4	1	.3280000000	.1732050808	0.0000000000
37	4	4	1	.3630000000	.1732050808	0.0000000000
38	5	4	1	.4120000000	.1732050808	0.0000000000
39	6	4	1	.4750000000	.1732050808	0.0000000000
40	7	4	1	.5520000000	.1732050808	0.0000000000

FIGURE 3.1 GEOMETRY MESH POINT DATA

ABUTMENT LIST

ABUTMENT	SIDE	NETWORK	CHARACTERIZATION
1	1	1	CONTROL POINTS (IF ANY) USE ORIGINAL BOUNDARY CONDITIONS
2	2	1	CONTROL POINTS (IF ANY) USE ORIGINAL BOUNDARY CONDITIONS
2	4	2	CONTROL POINTS PERFORM DOUBLET MATCHING
3	3	1	CONTROL POINTS PERFORM DOUBLET MATCHING
3	1	5	CONTROL POINTS (IF ANY) USE ORIGINAL BOUNDARY CONDITIONS
4	1	2	CONTROL POINTS (IF ANY) USE ORIGINAL BOUNDARY CONDITIONS
5	2	2	CONTROL POINTS (IF ANY) USE ORIGINAL BOUNDARY CONDITIONS
5	4	3	CONTROL POINTS PERFORM DOUBLET MATCHING
6	3	2	CONTROL POINTS (IF ANY) USE ORIGINAL BOUNDARY CONDITIONS
6	4	4	CONTROL POINTS PERFORM DOUBLET MATCHING
7	1	3	CONTROL POINTS (IF ANY) USE ORIGINAL BOUNDARY CONDITIONS
8	2	3	CONTROL POINTS (IF ANY) USE ORIGINAL BOUNDARY CONDITIONS
8	1	27	CONTROL POINTS PERFORM DOUBLET MATCHING
9	3	3	CONTROL POINTS PERFORM DOUBLET MATCHING
9	1	9	CONTROL POINTS (IF ANY) USE ORIGINAL BOUNDARY CONDITIONS
9	4	31	NO CONTROL POINTS
10	1	4	CONTROL POINTS (IF ANY) USE ORIGINAL BOUNDARY CONDITIONS
10	3	22	CONTROL POINTS (IF ANY) USE ORIGINAL BOUNDARY CONDITIONS
10	1	26	CONTROL POINTS PERFORM DOUBLET MATCHING
11	2	4	CONTROL POINTS FORCE DOUBLET STRENGTH TO VANISH
12	3	4	CONTROL POINTS (IF ANY) USE ORIGINAL BOUNDARY CONDITIONS
12	1	20	CONTROL POINTS PERFORM DOUBLET MATCHING
13	2	5	CONTROL POINTS (IF ANY) USE ORIGINAL BOUNDARY CONDITIONS
13	4	6	CONTROL POINTS PERFORM DOUBLET MATCHING
14	3	5	CONTROL POINTS PERFORM DOUBLET MATCHING
14	1	10	CONTROL POINTS (IF ANY) USE ORIGINAL BOUNDARY CONDITIONS

3.2 Network Abutment Data

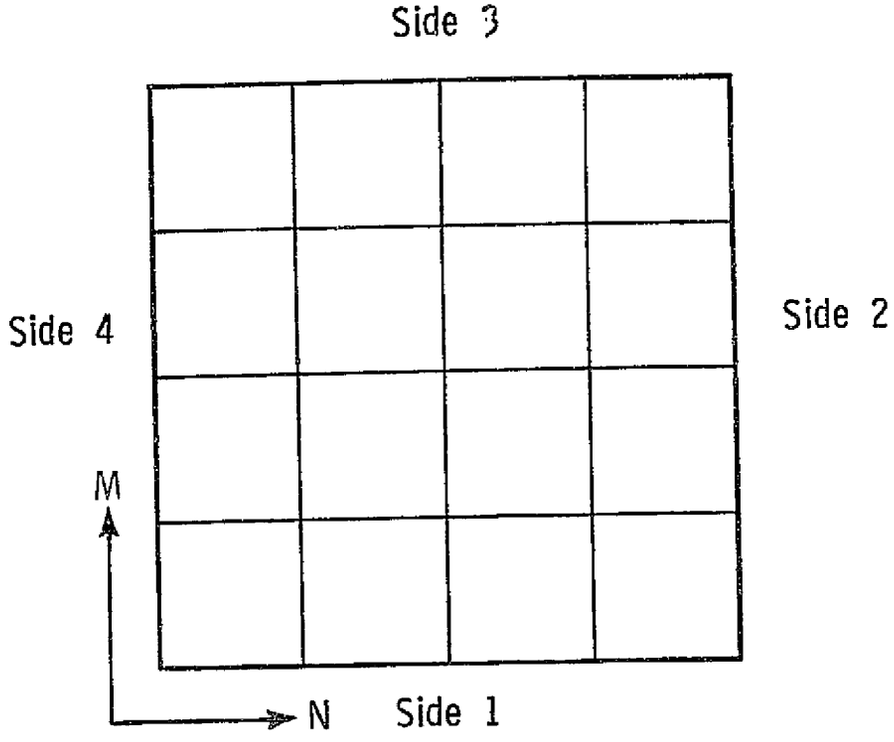

Figure 3.3 Index Convention For Network Side

CONTROL POINT DATA

CONTROL POINT LOCATIONS AND NORMALS

NC.	NET.	PAN.	SUBPAN.	X	Y	Z	NX	NY	NZ	D
1	1	1	1	.002147	.000575	0.000000	0.000000	0.000000	-1.000000	-.22224E-02
2	1	1	8	.005537	.000298	0.000000	0.000000	0.000000	-1.000000	-.61433E-03
3	1	2	8	.026734	.000908	0.000000	0.000000	0.000000	-1.000000	-.19573E-02
4	1	3	8	.068064	.001560	0.000000	0.000000	0.000000	-1.000000	-.34379E-02
5	1	4	8	.129495	.002289	0.000000	0.000000	0.000000	-1.000000	-.50447E-02
6	1	5	8	.210997	.003140	0.000000	0.000000	0.000000	-1.000000	-.67694E-02
7	1	6	8	.311500	.003608	0.000000	0.000000	0.000000	-1.000000	-.74344E-02
8	1	7	8	.430911	.003608	0.000000	0.000000	0.000000	-1.000000	-.69250E-02
9	1	8	8	.570130	.003608	0.000000	0.000000	0.000000	-1.000000	-.62717E-02
10	1	9	8	.729187	.003608	0.000000	0.000000	0.000000	-1.000000	-.55270E-02
11	1	10	8	.908161	.003608	0.000000	0.000000	0.000000	-1.000000	-.47973E-02
12	1	10	4	.994465	.005555	0.000000	0.000000	0.000000	-1.000000	-.78276E-02
13	1	1	5	.050086	.028573	0.000000	0.000000	0.000000	-1.000000	-.30683E-03
14	1	1	5	.054668	.028845	0.000000	0.000000	0.000000	-1.000000	0.
15	1	2	5	.073538	.028809	0.000000	0.000000	0.000000	-1.000000	0.
16	1	3	5	.111443	.028780	0.000000	0.000000	0.000000	-1.000000	0.
17	1	4	5	.168377	.028755	0.000000	0.000000	0.000000	-1.000000	0.
18	1	5	5	.244336	.028733	0.000000	0.000000	0.000000	-1.000000	0.
19	1	6	5	.339321	.028713	0.000000	0.000000	0.000000	-1.000000	0.
20	1	7	5	.453331	.028694	0.000000	0.000000	0.000000	-1.000000	0.
21	1	8	5	.586366	.028676	0.000000	0.000000	0.000000	-1.000000	0.
22	1	9	5	.738422	.028661	0.000000	0.000000	0.000000	-1.000000	0.
23	1	10	5	.909493	.028650	0.000000	0.000000	0.000000	-1.000000	0.
24	1	10	7	.996487	.029445	0.000000	0.000000	0.000000	-1.000000	-.35606E-02
25	1	11	5	.150077	.086339	0.000000	0.000000	0.000000	-1.000000	-.27470E-03
26	1	11	5	.154176	.086583	0.000000	0.000000	0.000000	-1.000000	0.
27	1	12	5	.171056	.086550	0.000000	0.000000	0.000000	-1.000000	0.
28	1	13	5	.204966	.086522	0.000000	0.000000	0.000000	-1.000000	0.
29	1	14	5	.255902	.086498	0.000000	0.000000	0.000000	-1.000000	0.
30	1	15	5	.323861	.086476	0.000000	0.000000	0.000000	-1.000000	0.
31	1	16	5	.408844	.086456	0.000000	0.000000	0.000000	-1.000000	0.
32	1	17	5	.510850	.086436	0.000000	0.000000	0.000000	-1.000000	0.
33	1	18	5	.629881	.086418	0.000000	0.000000	0.000000	-1.000000	0.
34	1	19	5	.765933	.086402	0.000000	0.000000	0.000000	-1.000000	0.
35	1	20	5	.919000	.086391	0.000000	0.000000	0.000000	-1.000000	0.
36	1	20	7	.956497	.087245	0.000000	0.000000	0.000000	-1.000000	-.35612E-02
37	1	21	5	.250067	.144104	0.000000	0.000000	0.000000	-1.000000	-.24253E-03
38	1	21	5	.253684	.144320	0.000000	0.000000	0.000000	-1.000000	0.
39	1	22	5	.268575	.144290	0.000000	0.000000	0.000000	-1.000000	0.
40	1	23	5	.298491	.144264	0.000000	0.000000	0.000000	-1.000000	0.

FIGURE 3.4 CONTROL POINT DATA

BOUNDARY CONDITION DEFINING PARAMETERS

JC	NLD	NRD	NCT	CU BET1	CL BET2	TUX BET3	TUY BET4	TUZ BET5	TLX BET6	TLY BET7	TLZ BET8	DU BET9	DL BET10
1	2	3	1	1.0000 .0998	0.0000	0.0000	0.0000	0.0000	0.0000	0.0000	0.0000	0.0000	0.0000
2	2	3	1	1.0000 .0998	0.0000	0.0000	0.0000	0.0000	0.0000	0.0000	0.0000	0.0000	0.0000
3	2	3	1	1.0000 .0998	0.0000	0.0000	0.0000	0.0000	0.0000	0.0000	0.0000	0.0000	0.0000
4	2	3	1	1.0000 .0998	0.0000	0.0000	0.0000	0.0000	0.0000	0.0000	0.0000	0.0000	0.0000
5	2	3	1	1.0000 .0998	0.0000	0.0000	0.0000	0.0000	0.0000	0.0000	0.0000	0.0000	0.0000
6	2	3	1	1.0000 .0998	0.0000	0.0000	0.0000	0.0000	0.0000	0.0000	0.0000	0.0000	0.0000
7	2	3	1	1.0000 .0998	0.0000	0.0000	0.0000	0.0000	0.0000	0.0000	0.0000	0.0000	0.0000
8	2	3	1	1.0000 .0998	0.0000	0.0000	0.0000	0.0000	0.0000	0.0000	0.0000	0.0000	0.0000
9	2	3	1	1.0000 .0998	0.0000	0.0000	0.0000	0.0000	0.0000	0.0000	0.0000	0.0000	0.0000
10	2	3	1	1.0000 .0998	0.0000	0.0000	0.0000	0.0000	0.0000	0.0000	0.0000	0.0000	0.0000
11	2	3	1	1.0000 .0998	0.0000	0.0000	0.0000	0.0000	0.0000	0.0000	0.0000	0.0000	0.0000
12	2	3	1	1.0000 .0998	0.0000	0.0000	0.0000	0.0000	0.0000	0.0000	0.0000	0.0000	0.0000
13	2	3	1	1.0000 .0998	0.0000	0.0000	0.0000	0.0000	0.0000	0.0000	0.0000	0.0000	0.0000
14	2	3	1	1.0000 .0998	0.0000	0.0000	0.0000	0.0000	0.0000	0.0000	0.0000	0.0000	0.0000
15	2	3	1	1.0000 .0998	0.0000	0.0000	0.0000	0.0000	0.0000	0.0000	0.0000	0.0000	0.0000
16	2	3	1	1.0000 .0998	0.0000	0.0000	0.0000	0.0000	0.0000	0.0000	0.0000	0.0000	0.0000
17	2	3	1	1.0000 .0998	0.0000	0.0000	0.0000	0.0000	0.0000	0.0000	0.0000	0.0000	0.0000
18	2	3	1	1.0000 .0998	0.0000	0.0000	0.0000	0.0000	0.0000	0.0000	0.0000	0.0000	0.0000
19	2	3	1	1.0000 .0998	0.0000	0.0000	0.0000	0.0000	0.0000	0.0000	0.0000	0.0000	0.0000
20	2	3	1	1.0000 .0998	0.0000	0.0000	0.0000	0.0000	0.0000	0.0000	0.0000	0.0000	0.0000
21	2	3	1	1.0000 .0998	0.0000	0.0000	0.0000	0.0000	0.0000	0.0000	0.0000	0.0000	0.0000
22	2	3	1	1.0000 .0998	0.0000	0.0000	0.0000	0.0000	0.0000	0.0000	0.0000	0.0000	0.0000
23	2	3	1	1.0000 .0998	0.0000	0.0000	0.0000	0.0000	0.0000	0.0000	0.0000	0.0000	0.0000

FIGURE 3.5 BOUNDARY CONDITION DEFINING PARAMETERS

PROBLEM AND NETWORK INDICES

NNETT = 1 NZMPT = 121 NPANT = 100 NSNGT = 133 NSNGU = 133 NSNGK = 0 NCTRT = 133 NBCOT = 133

NTS = 0
NTD = 12
NM = 11
NN = 11
NZ = 121
NP = 100
NSS = 0
NSD = 133
NC = 133
NBC = 133

EDGE DOWNWASH CONDITIONS

JC	IPC	IP	IS	WX	WY	WZ	ZX	ZY	ZZ	F1
1	1	1	1	0.	0.	0.	.66613381E-15	0.	0.	-.69994698E+05
13	1	1	1	.50000000E-01	.28867513E-01	0.	.50000000E-01	.28867513E-01	0.	-.65182948E+06
25	11	11	1	.15000000E+00	.86602540E-01	0.	.15000000E+00	.86602540E-01	0.	-.72806527E+06
37	21	21	1	.25000000E+00	.14433757E+00	0.	.25000000E+00	.14433757E+00	0.	-.82463348E+06
49	31	31	1	.35000000E+00	.20207259E+00	0.	.35000000E+00	.20207259E+00	0.	-.95091839E+06
61	41	41	1	.45000000E+00	.25980762E+00	0.	.45000000E+00	.25980762E+00	0.	-.11231292E+07
73	51	51	1	.55000000E+00	.31754265E+00	0.	.55000000E+00	.31754265E+00	0.	-.13718833E+07
85	61	61	1	.65000000E+00	.37527767E+00	0.	.65000000E+00	.37527767E+00	0.	-.17627893E+07
97	71	71	1	.75000000E+00	.43301270E+00	0.	.75000000E+00	.43301270E+00	0.	-.24664298E+07
109	81	81	1	.85000000E+00	.49074773E+00	0.	.85000000E+00	.49074773E+00	0.	-.41082736E+07
121	91	91	1	.95000000E+00	.54848276E+00	0.	.95000000E+00	.54848276E+00	0.	-.12317542E+08
133	91	91	1	.10000000E+01	.57735027E+00	0.	.10000000E+01	.57735027E+00	0.	-.63880113E+07

FIGURE 3.6 PROBLEM AND NETWORK INDICIES AND EDGE DOWNWASH CONDITIONS

```
***** BEGIN SOLUTION OF $A| $X| = $P| *****

                METHOD

        1. DECOMPOSE $A| = $L| $U|
        2. SOLVE $L| $Y| = $B|  FOR $Y|
        3. SOLVE $U| $X| = $Y|  FOR $X|

             FILE STORAGE USED

             $A| ON LOGICAL UNIT 10
             $B| ON LOGICAL UNIT 10
             $L| ON LOGICAL UNIT 10
             $U| ON LOGICAL UNIT 10
             $Y| ON LOGICAL UNIT 10
             $X| ON LOGICAL UNIT 10

    PIVOTING DATA ON LOGICAL UNIT 10

             IN-BLOCK PIVOTING WILL BE USED

 PROBLEM IS ORDER  133 WITH     1  RIGHT HAND SIDES

       MATRIX BLOCK STORAGE

      $A| IS STORED IN ( 2) BY ( 2)BLOCKS

      $B| IS STORED IN ( 2) BY ( 1)BLOCKS

       THE $A| MATRIX WILL BE DESTROYED
       THE $B| MATRIX WILL BE DESTROYED
       DURING SOLUTION.

*****          BEGIN DECOMPOSITION          *****

       ERROR ANALYSIS - RELATIVE ERROR IS      .35E-07
       SOLUTION WILL BE STABLE

*****      BEGIN FORWARD SUBSTITUTION       *****

*****      BEGIN BACKWARD SUBSTITUTION      *****
```

FIGURE 3.7 EQUATION SOLUTION DATA

***** P I V O T I N G I N F O R M A T I O N *****

PIVOTING FOR BLOCK ROW 1 NUMBER OF ROWS IN BLOCK = 72 POSITION OF FIRST ROW OF BLOCK WITHIN TOTAL MATRIX IS 1

FOR ROW	USING ROW	FOR ROW	USING ROW	FOR ROW	USING ROW	FOR ROW	USING ROW	FOR ROW	USING ROW	FOR ROW	USING ROW	FOR ROW	USING ROW	FOR ROW	USING ROW	FOR ROW	USING ROW	FOR ROW	USING ROW
1	1	2	2	3	3	4	4	5	5	6	6	7	7	8	8	9	9	10	10
11	11	12	12	13	13	14	14	15	15	16	16	17	17	18	18	19	19	20	20
21	21	22	22	23	35	24	24	25	25	26	26	27	27	28	28	29	29	30	30
31	31	32	32	33	33	34	34	35	36	36	23	37	37	38	38	39	39	40	40
41	41	42	42	43	43	44	44	45	45	46	46	47	47	48	48	49	49	50	50
51	51	52	52	53	53	54	54	55	55	56	56	57	57	58	58	59	59	60	60
61	61	62	62	63	63	64	64	65	65	66	66	67	67	68	68	69	69	70	70
71	71	72	72																

PIVOTING FOR BLOCK ROW 2 NUMBER OF ROWS IN BLOCK = 61 POSITION OF FIRST ROW OF BLOCK WITHIN TOTAL MATRIX IS 73

FOR ROW	USING ROW	FOR ROW	USING ROW	FOR ROW	USING ROW	FOR ROW	USING ROW	FOR ROW	USING ROW	FOR ROW	USING ROW	FOR ROW	USING ROW	FOR ROW	USING ROW	FOR ROW	USING ROW	FOR ROW	USING ROW
1	1	2	2	3	3	4	4	5	5	6	6	7	7	8	8	9	9	10	10
11	12	12	11	13	13	14	14	15	15	16	16	17	17	18	18	19	19	20	20
21	21	22	22	23	24	24	23	25	25	26	26	27	27	28	28	29	29	30	30
31	31	32	32	33	33	34	34	35	36	36	35	37	37	38	38	39	39	40	40
41	41	42	42	43	43	44	44	45	45	46	46	47	48	48	47	45	49	50	50
51	51	52	52	53	53	54	54	55	55	56	61	57	57	58	60	59	58	60	59
61	56																		

69

***** SOLUTION COMPLETE *****

ESOL COST ELAPSED CPU TIME .754

MACH NUMBER = 1.41421 ANGLE OF ATTACK = 5.73000 YAW ANGLE = 0.00000

ORIGINAL PAGE IS OF POOR QUALITY

FIGURE 3.8 EQUATION PIVOTING INFORMATION AND AERODYNAMIC INPUT DATA

NETWORK NO. = 1 SOURCE NETWORK TYPE = 0 DOUBLET NETWORK TYPE = 12

SINGULARITY GRID

IP	I	J	X	Y	Z	SO	DO	DX	DY	DZ	DM	DN	DMP	DNP
1	1	1	0.00000	0.00000	0.00000	0.00000	-.00000	-.06463	.11195	0.00000	-.06463	.00001	-.11195	-.12927
1	2	1	.00500	0.00000	0.00000	0.00000	-.00034	-.07305	.05872	0.00000	-.07305	-.03372	-.05872	-.08745
1	3	1	.01000	0.00000	0.00000	0.00000	-.00073	-.08148	.06353	0.00000	-.08148	-.03838	-.06353	-.09593
1	1	2	.05000	.02887	0.00000	0.00000	-.00000	-.43543	.75142	0.00000	-.43543	-.00139	-.75142	-.86846
1	2	2	.05475	.02887	0.00000	0.00000	-.00165	-.25885	.41390	0.00000	-.25885	-.01617	-.41390	-.48791
1	3	2	.05950	.02887	0.00000	0.00000	-.00246	-.06766	.07247	0.00000	-.06766	-.02194	-.07247	-.09669
1	1	3	.10000	.05774	0.00000	0.00000	-.00000	-.61894	1.07203	0.00000	-.61894	-.00001	-1.07203	-1.23787
1	2	3	.10450	.05774	0.00000	0.00000	-.00220	-.36060	.60533	0.00000	-.36060	-.00810	-.60533	-.70455
1	3	3	.10900	.05774	0.00000	0.00000	-.00325	-.10226	.16443	0.00000	-.10226	-.00551	-.16443	-.19356
2	1	1	.01000	0.00000	0.00000	0.00000	-.00073	-.07648	.05496	0.00000	-.07648	-.03838	-.05496	-.08601
2	2	1	.02500	0.00000	0.00000	0.00000	-.00194	-.08462	.02639	0.00000	-.08462	-.05936	-.02639	-.06583
2	3	1	.04000	0.00000	0.00000	0.00000	-.00327	-.09276	.03288	0.00000	-.09276	-.06254	-.03288	-.07599
2	1	2	.05950	.02887	0.00000	0.00000	-.00246	-.16205	.23102	0.00000	-.16205	-.02360	-.23102	-.26120
2	2	2	.07375	.02887	0.00000	0.00000	-.00454	-.12963	.15052	0.00000	-.12963	-.03465	-.15052	-.19591
2	3	2	.08800	.02887	0.00000	0.00000	-.00615	-.09721	.08011	0.00000	-.09721	-.04202	-.08011	-.11875
2	1	3	.16900	.05774	0.00000	0.00000	-.00325	-.21935	.36519	0.00000	-.21935	-.00551	-.36519	-.42597
2	2	3	.12250	.05774	0.00000	0.00000	-.00587	-.16869	.25609	0.00000	-.16869	-.01467	-.25609	-.30631
2	3	3	.13600	.05774	0.00000	0.00000	-.00780	-.11803	.16066	0.00000	-.11803	-.01835	-.16066	-.19851
3	1	1	.04000	0.00000	0.00000	0.00000	-.00327	-.06879	.02628	0.00000	-.06879	-.06254	-.02628	-.06828
3	2	1	.06500	0.00000	0.00000	0.00000	-.00552	-.09151	.01376	0.00000	-.09151	-.07046	-.01376	-.05968
3	3	1	.09000	0.00000	0.00000	0.00000	-.00784	-.09383	.01563	0.00000	-.09383	-.07086	-.01563	-.06347
3	1	2	.08800	.02887	0.00000	0.00000	-.00615	-.11311	.10687	0.00000	-.11311	-.04185	-.10687	-.14988
3	2	2	.11175	.02887	0.00000	0.00000	-.00873	-.10409	.07917	0.00000	-.10409	-.04657	-.07917	-.12205
3	3	2	.13550	.02887	0.00000	0.00000	-.01110	-.09508	.05337	0.00000	-.09508	-.05169	-.05337	-.09600
3	1	3	.13600	.05774	0.00000	0.00000	-.00780	-.13508	.18901	0.00000	-.13508	-.01835	-.18901	-.23159
3	2	3	.15850	.05774	0.00000	0.00000	-.01068	-.11770	.14494	0.00000	-.11770	-.02400	-.14494	-.18518
3	3	3	.18100	.05774	0.00000	0.00000	-.01325	-.10719	.11358	0.00000	-.10719	-.02966	-.11358	-.15533
4	1	1	.09000	0.00000	0.00000	0.00000	-.00784	-.09281	.01402	0.00000	-.09281	-.07086	-.01402	-.06156
4	2	1	.12500	0.00000	0.00000	0.00000	-.01107	-.09181	.00915	0.00000	-.09181	-.07159	-.00915	-.05820
4	3	1	.16000	0.00000	0.00000	0.00000	-.01426	-.09080	.00546	0.00000	-.09080	-.07174	-.00546	-.05593
4	1	2	.13550	.02887	0.00000	0.00000	-.01110	-.09899	.06034	0.00000	-.09899	-.05126	-.06034	-.10399
4	2	2	.16875	.02887	0.00000	0.00000	-.01434	-.09606	.04922	0.00000	-.09606	-.05307	-.04922	-.09749

FIGURE 3.9 SINGULARITY GRID DATA

NETWORK NUMBER = 1 SOURCE TYPE = 0 DOUBLET TYPE = 12 NUMBER ROWS = 10 NUMBER COLUMNS = 10

JC	IP	X	Y	Z	DD	DX	DY	DZ	SO	FSVX	FSVY	FSVZ
	PHIU	WXU	WYU	WZU	PHEU	PWXU	PWYU	PWZU	CPLINU	CPSLNU	CP2NDU	CPISNU
	PHIL	WXL	WYL	WZL	PHEL	PWXL	PWYL	PWZL	CPLINL	CPSLNL	CP2NDL	CPISNL
	WNU	WNL	WTU	WTL	PHIUI	PHILI	PWNU	PWNL	CPLIND	CPSLND	CP2NDD	CPISND
14	1	.0547	.0288	0.0000	-.0016	-.2603	.4167	0.0000	0.0000	.9950	0.0000	.0998
	.0536	1.1252	.2084	.0000	-.0008	.1302	.2084	-.0998	.2603	.2069	.2239	.2067
	.0552	.8648	-.2084	.0000	.0008	-.1302	-.2084	-.0998	-.2603	-.3137	-.2968	-.2795
	-.0000	-.0000	1.1443	.8896	-.0552	-.0536	.0998	.0998	.5207	.5207	.5207	.4883
15	2	.0735	.0288	0.0000	-.0045	-.1298	.1513	0.0000	0.0000	.9950	0.0000	.0998
	.0709	1.0599	.0756	.0000	-.0023	.0649	.0756	-.0998	.1298	.1141	.1183	.1161
	.0754	.9301	-.0756	.0000	.0023	-.0649	-.0756	-.0998	-.1298	-.1455	-.1413	-.1368
	-.0000	-.0000	1.0626	.9332	-.0754	-.0709	.0998	.0998	.2596	.2596	.2596	.2549
16	3	.1114	.0288	0.0000	-.0087	-.1041	.0791	0.0000	0.0000	.9950	0.0000	.0998
	.1065	1.0471	.0356	.0000	-.0044	.0521	.0396	-.0998	.1041	.0926	.0953	.0940
	.1152	.9429	-.0396	.0000	.0044	-.0521	-.0396	-.0998	-.1041	-.1156	-.1129	-.1115
	-.0000	-.0000	1.0478	.9458	-.1152	-.1065	.0998	.0998	.2082	.2082	.2082	.2055
17	4	.1684	.0288	0.0000	-.0143	-.0961	.0491	0.0000	0.0000	.9950	0.0000	.0998
	.1604	1.0430	.0246	.0000	-.0072	.0480	.0246	-.0998	.0961	.0855	.0878	.0867
	.1747	.9470	-.0246	.0000	.0072	-.0480	-.0246	-.0998	-.0961	-.1066	-.1043	-.1031
	-.0000	-.0000	1.0433	.9473	-.1747	-.1604	.0998	.0998	.1921	.1921	.1921	.1898
18	5	.2443	.0287	0.0000	-.0215	-.0933	.0332	0.0000	0.0000	.9950	0.0000	.0998
	.2324	1.0416	.0166	.0000	-.0107	.0466	.0166	-.0998	.0933	.0830	.0852	.0842
	.2538	.9484	-.0166	.0000	.0107	-.0466	-.0166	-.0998	-.0933	-.1035	-.1013	-.1002
	-.0000	-.0000	1.0418	.9485	-.2538	-.2324	.0998	.0998	.1865	.1865	.1865	.1844
19	6	.3393	.0287	0.0000	-.0303	-.0924	.0237	0.0000	0.0000	.9950	0.0000	.0998
	.3225	1.0412	.0118	.0000	-.0151	.0462	.0118	-.0998	.0924	.0823	.0844	.0834
	.3528	.9488	-.0118	.0000	.0151	-.0462	-.0118	-.0998	-.0924	-.1025	-.1004	-.0993
	-.0000	-.0000	1.0413	.9489	-.3528	-.3225	.0998	.0998	.1848	.1848	.1848	.1827
20	7	.4533	.0287	0.0000	-.0408	-.0921	.0177	0.0000	0.0000	.9950	0.0000	.0998
	.4307	1.0410	.0088	.0000	-.0204	.0460	.0088	-.0998	.0921	.0820	.0842	.0832
	.4714	.9490	-.0088	.0000	.0204	-.0460	-.0088	-.0998	-.0921	-.1021	-.1000	-.0989
	-.0000	-.0000	1.0411	.9490	-.4714	-.4307	.0998	.0998	.1842	.1842	.1842	.1821
21	8	.5864	.0287	0.0000	-.0530	-.0919	.0136	0.0000	0.0000	.9950	0.0000	.0998
	.5569	1.0410	.0068	.0000	-.0265	.0460	.0068	-.0998	.0919	.0819	.0840	.0830
	.6099	.9490	-.0068	.0000	.0265	-.0460	-.0068	-.0998	-.0919	-.1019	-.0998	-.0987
	-.0000	-.0000	1.0410	.9491	-.6099	-.5569	.0998	.0998	.1838	.1838	.1838	.1818
22	9	.7384	.0287	0.0000	-.0670	-.0918	.0108	0.0000	0.0000	.9950	0.0000	.0998
	.7012	1.0409	.0054	.0000	-.0335	.0459	.0054	-.0998	.0918	.0818	.0840	.0830
	.7682	.9491	-.0054	.0000	.0335	-.0459	-.0054	-.0998	-.0918	-.1018	-.0997	-.0987
	-.0000	-.0000	1.0409	.9491	-.7682	-.7012	.0998	.0998	.1837	.1837	.1837	.1816

FIGURE 3.10 LOCAL AERODYNAMIC DATA

FORCE / MOMENT DATA

TOTALS FOR COLUMN 1	AREA	FX	FY	FZ	MX	MY	MZ
	.05485	0.00000	0.00000	.00472	.00014	-.00241	0.00000
	.05485	0.00000	0.00000	.00564	.00016	-.00286	0.00000
	.05485	0.00000	0.00000	.01036	.00030	-.00527	0.00000

TOTALS FOR COLUMN 2	AREA	FX	FY	FZ	MX	MY	MZ
	.04907	0.00000	0.00000	.00460	.00040	-.00246	0.00000
	.04907	0.00000	0.00000	.00557	.00048	-.00297	0.00000
	.04907	0.00000	0.00000	.01017	.00088	-.00545	0.00000

TOTALS FOR COLUMN 10	AREA	FX	FY	FZ	MX	MY	MZ
	.00289	0.00000	0.00000	.00034	.00018	-.00033	0.00000
	.00289	0.00000	0.00000	.00131	.00071	-.00127	0.00000
	.00289	0.00000	0.00000	.00166	.00089	-.00160	0.00000

TOTALS FOR NETWORK	AREA	FX	FY	FZ	MX	MY	MZ
	.28868	0.00000	0.00000	.03220	.00712	-.02134	0.00000
	.28868	0.00000	0.00000	.04282	.01022	-.02852	0.00000
	.28868	0.00000	0.00000	.07501	.01734	-.04986	0.00000

TOTAL FOR ALL NETWORKS SO FAR	AREA	FX	FY	FZ	MX	MY	MZ
	.28868	0.00000	0.00000	.03220	.00712	-.02134	0.00000
	.28868	0.00000	0.00000	.04282	.01022	-.02852	0.00000
	.28868	0.00000	0.00000	.07501	.01734	-.04986	0.00000

OUTP COST ELAPSED CPU TIME 3.099

FIGURE 3.11 FORCE & MOMENT DATA

TABLE 3-1 DEFINITION OF OUTPUT QUANTITIES

QUANTITY	DEFINITION	WHERE PRINTED	WHEN PRINTED
	Problem and Network Indices		
NNETT	Total number of networks	FLØW	ALWAYS
NZMPT	Total number of grid points	FLØW	ALWAYS
NPANT	Total number of panels	FLØW	ALWAYS
NSNGT	Total number of singularity parameters	FLØW	ALWAYS
NSNGU	Total number of unknown singularity parameters	FLØW	ALWAYS
NSNGK	Total number of a-priori known singularity parameters	FLØW	ALWAYS
NCTRT	Total number of control points	FLØW	ALWAYS
NBCØT	Total number of boundary conditions	FLØW	ALWAYS
NTS	Network source type	FLØW	ALWAYS
NTD	Network doublet type	FLØW	ALWAYS
NM	Number of corner point rows in network	FLØW	ALWAYS
NN	Number of corner point columns in network	FLØW	ALWAYS
NZ	number of corner points in network	FLØW	ALWAYS
NP	Number of panels in network	FLØW	ALWAYS
NSS	Number of singularity parameters of network source spline	FLØW	ALWAYS
NSD	Number of singularity parameters of network doublet spline	FLØW	ALWAYS
NC	Number of control points in network	FLØW	ALWAYS
NBC	Number of non-null boundary conditions in network	FLØW	ALWAYS
	Near Field/Far Field Counters		
NFS	Number of near field source AIC calculations	FLØW	ALWAYS
NFD	Number of near field doublet AIC calculations	FLØW	ALWAYS
FFS	Number of far field source AIC calculations	FLØW	ALWAYS
FFD	Number of far field doublet AIC calculations	FLØW	ALWAYS

TABLE 3-1 DEFINITION OF OUTPUT QUANTITIES (CONT'D)

QUANTITY	DEFINITION	WHERE PRINTED	WHEN PRINTED
	Equation Solution Data		
	This data is self explanatory. The printout begins with the words "BEGIN SØLUTIØN ØF [A] [X] = [B] and ends with the "SØLUTIØN CØMPLETE"	-	ALWAYS
	Singularity Data		
S	Solution singularity parameters	ØUTPUT	ALWAYS
IP	Cumulative index of panel on which singularity distribution is evaluated	ØUTPUT	ISINGS=1
I	Local row index of evaluation point	ØUTPUT	ISINGS=1
J	Local column index of evaluation point	ØUTPUT	ISINGS=1
(X,Y,Z)	Global coordinates of evaluation point	ØUTPUT	ISINGS=1
SO	Source strength value at evaluation point	ØUTPUT	ISINGS=1
DO	Doublet strength value at evaluation point	ØUTPUT	ISINGS=1
(DX,DY,DZ)	Global coordinates of gradient of doublet strength at evaluation point	ØUTPUT	ISINGS=1
(SM,SN)	Derivative of doublet strength in (row, column) directions respectively	ØUTPUT	ISINGS=1
(SMP,SNP)	Derivative of doublet strength in directions normal to (row, column) directions respectively	ØUTPUT	ISINGS=1
	Local Aerodynamic Data		
JC	Cumulative control point index	ØUTPUT	ALWAYS
IP	Index of panel containing control point	ØUTPUT	ALWAYS
(X,Y,Z)	Global coordinates of control point	ØUTPUT	ALWAYS
DO	Doublet strength	ØUTPUT	ALWAYS
(DX,DY,DZ)	Global coordinates of doublet gradient	ØUTPUT	ALWAYS
SO	Source strength	ØUTPUT	ALWAYS
(FSVX,FSVY, FSVZ)	Freestream velocity vector in global coordinates	ØUTPUT	ALWAYS

TABLE 3-1 DEFINITION OF OUTPUT QUANTITIES (CONT'D)

QUANTITY	DEFINITION	WHERE PRINTED	WHEN PRINTED
PHIU	Upper surface total potential	ØUTPUT	ALWAYS
(WXU,WYU, WZU)	Upper surface total mass flux vector in global coordinates	ØUTPUT	ALWAYS
PHEU	Upper surface perturbation potential	ØUTPUT	ALWAYS
(PWXU,PWYU, PWZU)	Upper surface perturbation mass flux vector in global coordinates	ØUTPUT	ALWAYS
CPLINU	Upper surface linearized pressure coefficient	ØUTPUT	ALWAYS
CPSLNU	Upper surface slender body pressure coefficient	ØUTPUT	ALWAYS
CP2NDU	Upper surface second order pressure coefficient	ØUTPUT	ALWAYS
CPISNU	Upper surface isentropic pressure coefficient	ØUTPUT	ALWAYS
PHIL	Lower surface total potential	ØUTPUT	ALWAYS
(WXL,WYL, WZL)	Lower surface total mass flux vector in global coordinates	ØUTPUT	ALWAYS
PHEL	Lower surface perturbation potential	ØUTPUT	ALWAYS
(PWXL,PWYL, PWZL)	Lower surface perturbation mass flux vector in global coordinates	ØUTPUT	ALWAYS
CPLINL	Lower surface linearized pressure coefficient	ØUTPUT	ALWAYS
CPSLNL	Lower surface slender body pressure coefficient	ØUTPUT	ALWAYS
CP2NDL	Lower surface second order pressure coefficient	ØUTPUT	ALWAYS
CPISNL	Lower surface isentropic pressure coefficient	ØUTPUT	ALWAYS
WNU	Normal component of upper surface total mass flux vector	ØUTPUT	ALWAYS
WNL	Normal component of lower surface total mass flux vector	ØUTPUT	ALWAYS
WTU	Magnitude of tangential component of upper surface total mass flux vector	ØUTPUT	ALWAYS
WTL	Magnitude of tangential component of lower surface total mass flux vector	ØUTPUT	ALWAYS
PHIUI	Upper surface total mass flux potential	ØUTPUT	ALWAYS
PHILI	Lower surface total mass flux potential	ØUTPUT	ALWAYS
PWNU	Normal component of upper surface perturbation mass flux vector	ØUTPUT	ALWAYS

TABLE 3-1 DEFINITION OF OUTPUT QUANTITIES (CONT'D)

QUANTITY	DEFINITION	WHERE PRINTED	WHEN PRINTED
PWNL	Normal component of lower surface perturbation mass flux vector	ØUTPUT	ALWAYS
CPLIND	Difference between upper and lower surface linearized pressure coefficient	ØUTPUT	ALWAYS
CPSLND	Difference between upper and lower surface slender body pressure coefficient	ØUTPUT	ALWAYS
CP2NDD	Difference between upper and lower surface second order pressure coefficient	ØUTPUT	ALWAYS
CPISND	Difference between upper and lower surface isentropic pressure coefficient	ØUTPUT	ALWAYS
	Force and Moment Data		
AREA	Total area of panels	FMCAL	ALWAYS
(FX,FY,FZ)	Global coordinates of force coefficient (Upper surface, lower surface, difference)	FMCAL	ALWAYS
(MX,MY,MZ)	Moment coefficients about global principal axes (upper surface, lower surface, difference)	FMCAL	ALWAYS

4.0 Computational Results

In this section we present results obtained by applying the advanced panel pilot code to a number of different problems chosen to test its range of applicability and to obtain advice on how to use it most effectively. In most of these cases, exact solutions, or at least analytical results based on linear theory, are available for purposes of comparison. For the more complex cases comparisons have been made with experimental results.

4.1 AXISYMMETRIC FLOW PAST CIRCULAR CONES

One of the simplest cases of supersonic flow for which an exact solution is available is the flow past a cone at zero angle of attack. For this case the surface pressure is constant and depends only on the upstream Mach number M_∞ and cone angle ϕ_c. Results obtained with the panel code are compared with the exact solution in Fig. 4.1.

Both velocity and mass flux boundary conditions were tried. Requiring $(\bar{w} + \bar{V}_\infty) \cdot \bar{n} = 0$ (mass flux boundary condition) on the boundary is seen to give much better results than if $(\bar{v} + \bar{V}_\infty) \cdot \bar{n} = 0$ (velocity boundary condition) on the surface when the Mach number M_∞ and cone angle ϕ_c are relatively small; i.e., within the limits we expect for a linearized theory. However, the results deteriorate less rapidly with increasing Mach number when velocity boundary conditions are used.

The simplicity of flow past a cone make it a suitable vehicle for a study of convergence. Fig. 4.2 shows the effect of the number of meridianal panels employed on the cone surface pressure at three Mach numbers. In every case three rows of panels were used in the axial direction (very little variation of pressure was observed in that direction).

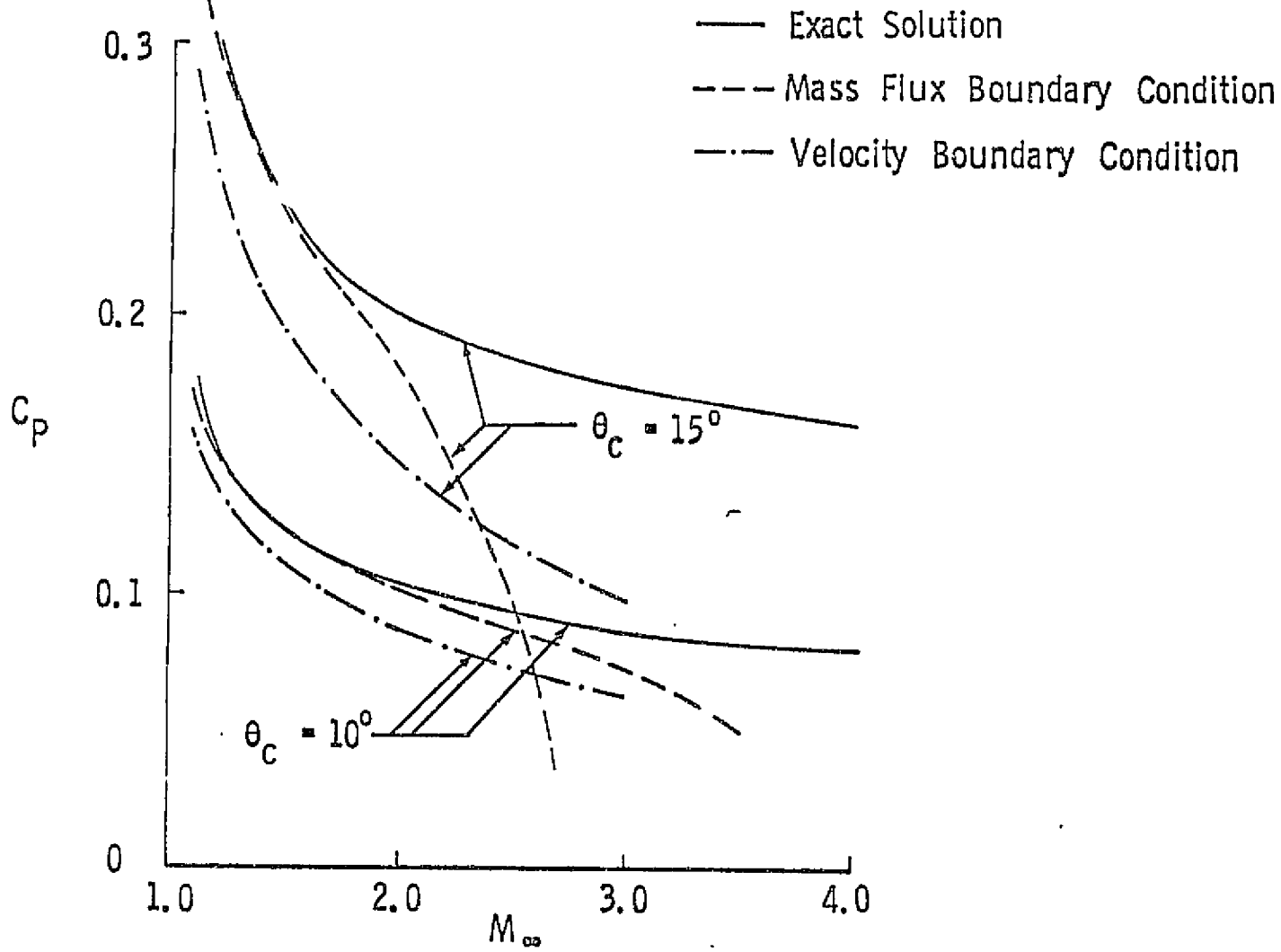

FIGURE 4.1 PRESSURE ON CONE AT 0° ANGLE OF ATTACK

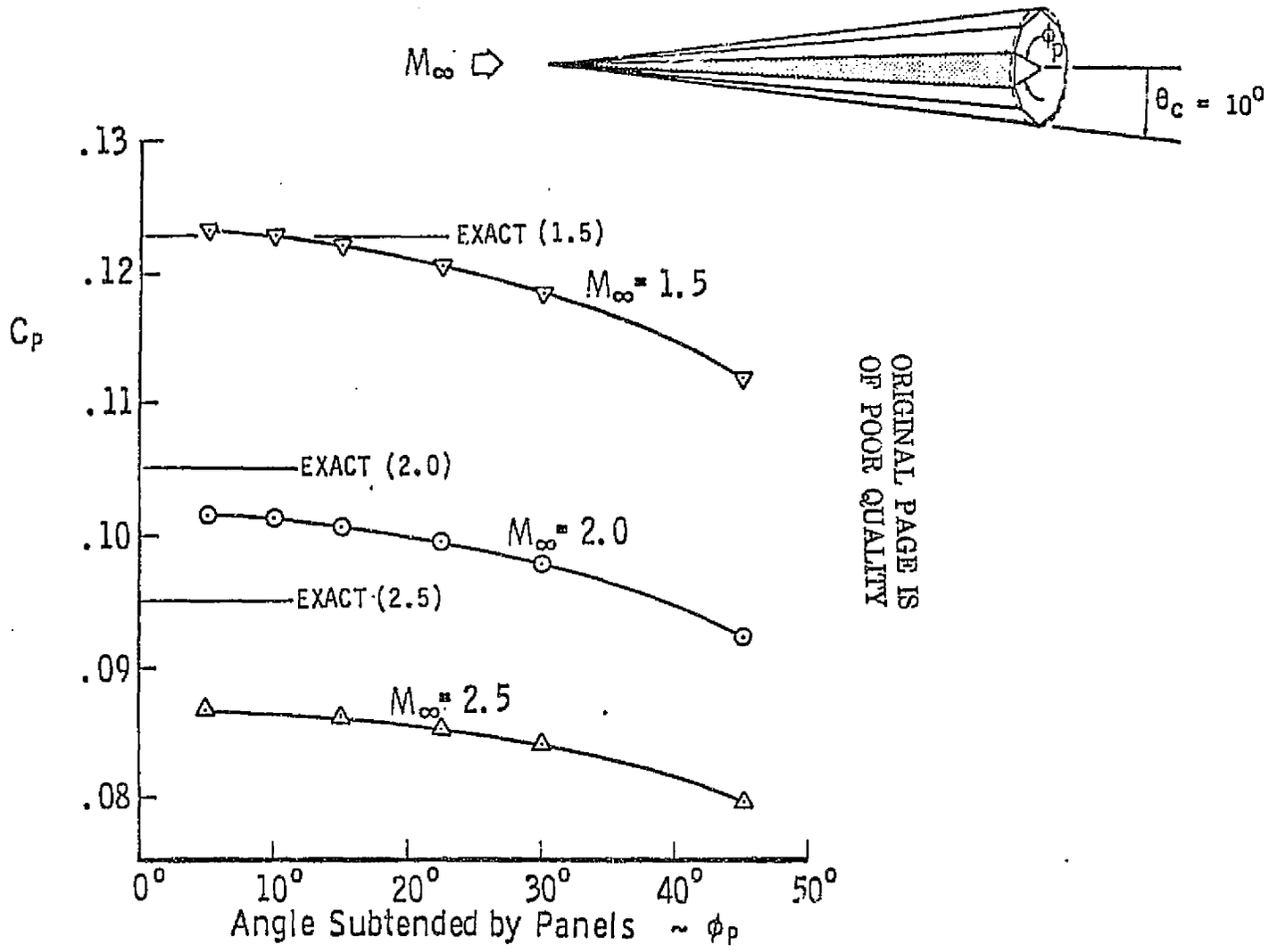

FIGURE 4.2 CONVERGENCE STUDY

It can be seen that the results are essentially converged when the angle subtended by the panels is less than 10°. This holds even when the results are converging to the incorrect answer because the Mach number and/or cone angle is too large.

Somewhat faster convergence was obtained when the grid points were selected outside the cone surface so that the panels "interpolated" rather than were inscribed by the cone, see Fig. 4.3. While such a device is not generally practical in using the panel method, we did take advantage of it in our studies related to cones. This modeling yields better results because the cross-sectional area of the "interpolated" cone better matches the actual cross-section area than does the area of an inscribed cone.

4.2 FLOW PAST CIRCULAR CONES AT ANGLE OF ATTACK

Extensive tabulations are now available of the exact solution of the flow past cones at angle of attack, Reference 3. As would be expected, the performance of the panel code deteriorates with increasing angle of attack for a given Mach number and cone angle. Fig. 4.4 thru 4.7 show the effects of the choices of compressibility axis and pressure formula for two conditions, one within the range of accuracy of the linearized theory ($M_\infty = 1.5$, $\phi_c = 10°$, $\alpha = 5°$) and one beyond it ($M_\infty = 2.0$, $\phi_c = 10°$, $\alpha = 10°$). These data clearly show the desireability of aligning the compressibility axes with the freestream direction (i.e., setting $\alpha = \alpha_c$ $\beta = \beta_c$) and indicate that either the isentropic or slender-body pressure formulas are superior to the full second-order pressure formula. See Section 3.9 for the explicit formulas.

Figs. 4.8 and 4.9 give another comparison of the use of velocity and mass flux boundary conditions. As was observed in connection with Fig. 4.1, mass flux boundary conditions give much better results when linear theory is expected to be valid, but velocity boundary conditions are less wrong outside those limits of validity.

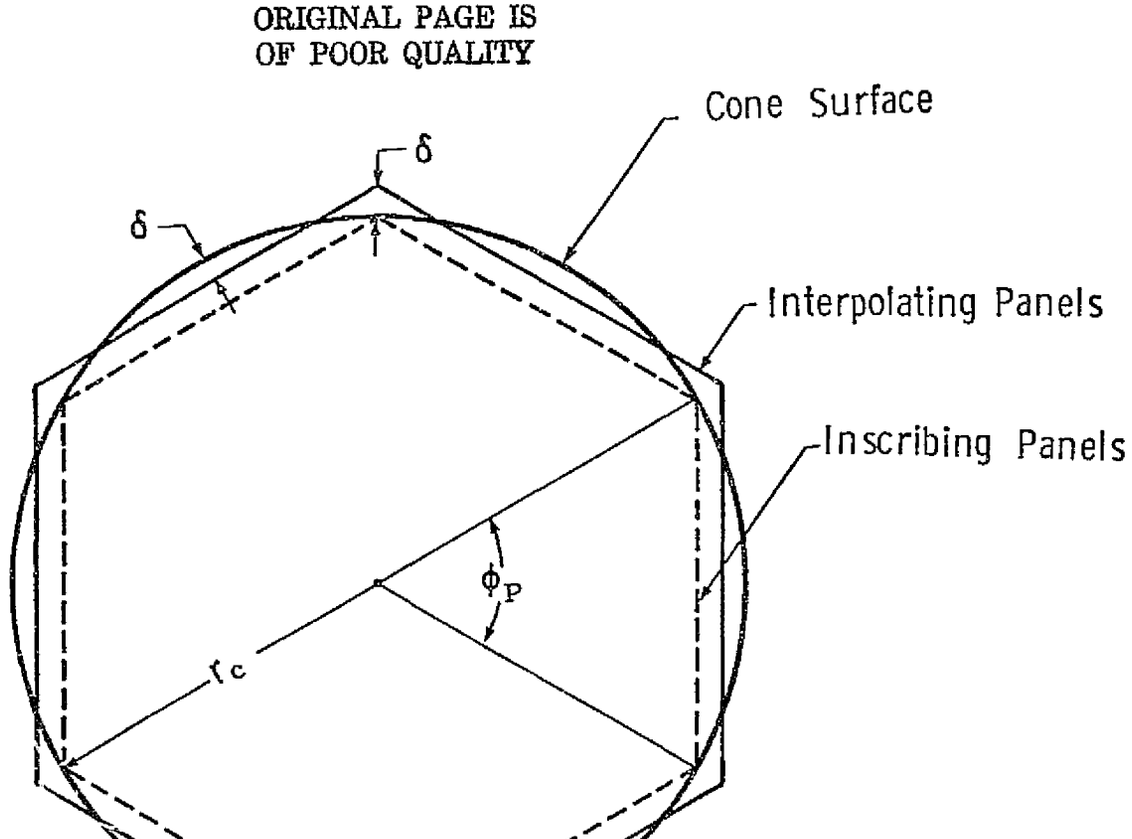

$$\frac{\delta}{r_c} = \frac{1 - \cos(\phi_P/2)}{1 + \cos(\phi_P/2)}$$

FIGURE 4.3 USE OF PANELS TO "INTERPOLATE" CONE SURFACE RATHER THAN TO INSCRIBE IT

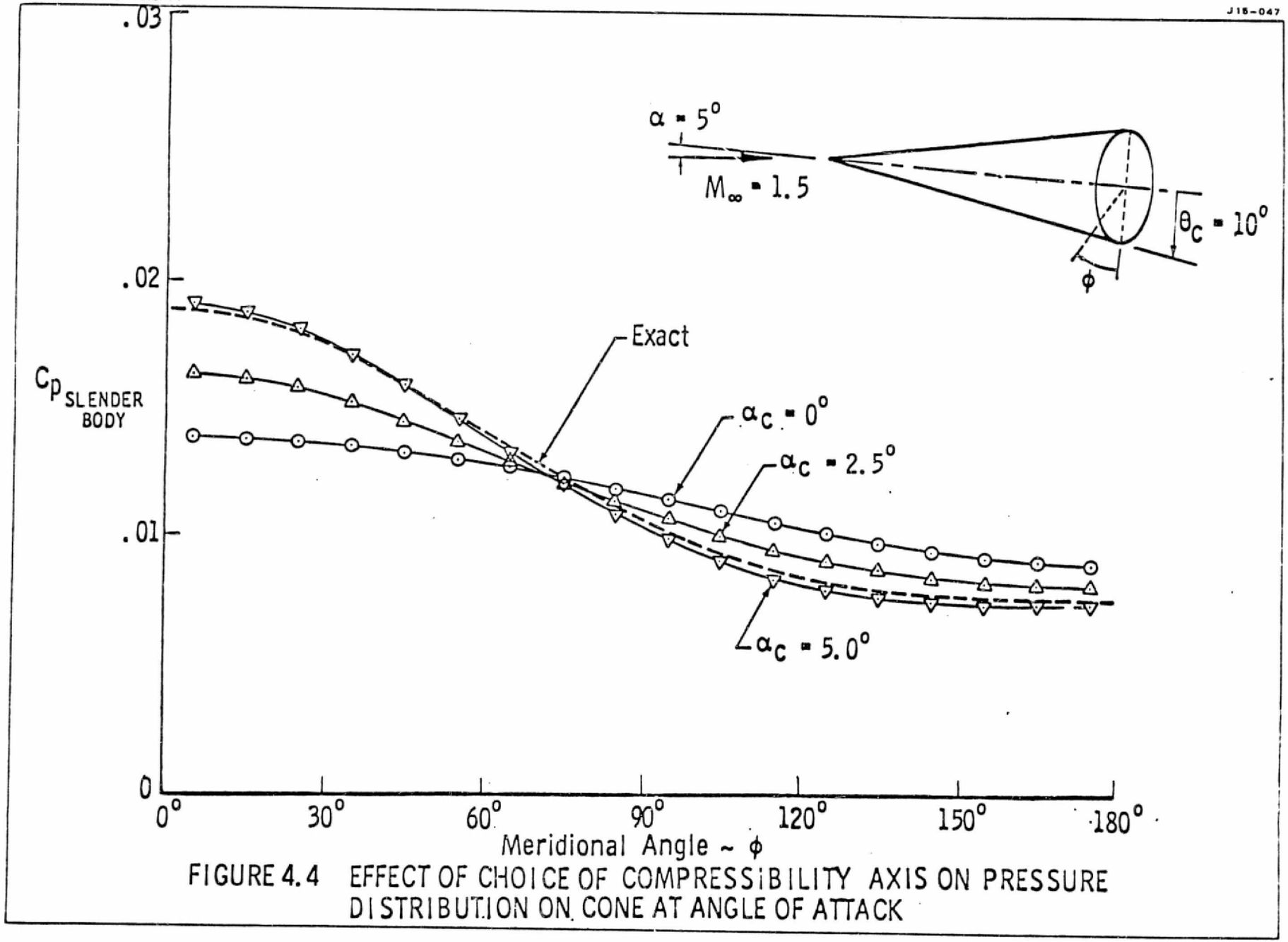

FIGURE 4.4 EFFECT OF CHOICE OF COMPRESSIBILITY AXIS ON PRESSURE DISTRIBUTION ON CONE AT ANGLE OF ATTACK

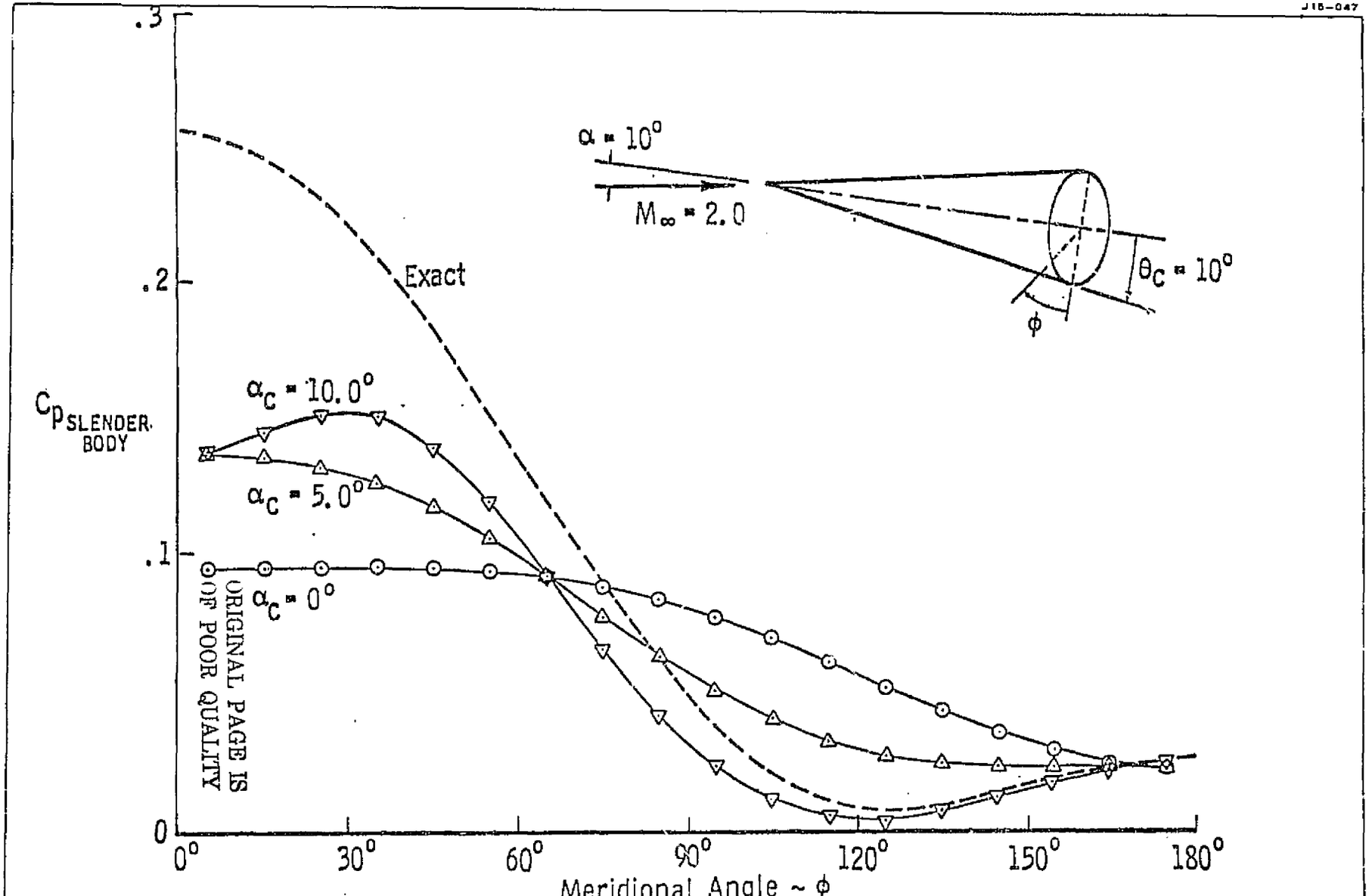

FIGURE 4.5 EFFECT OF CHOICE OF COMPRESSIBILITY AXIS ON PRESSURE DISTIBUTION ON CONE AT ANGLE OF ATTACK

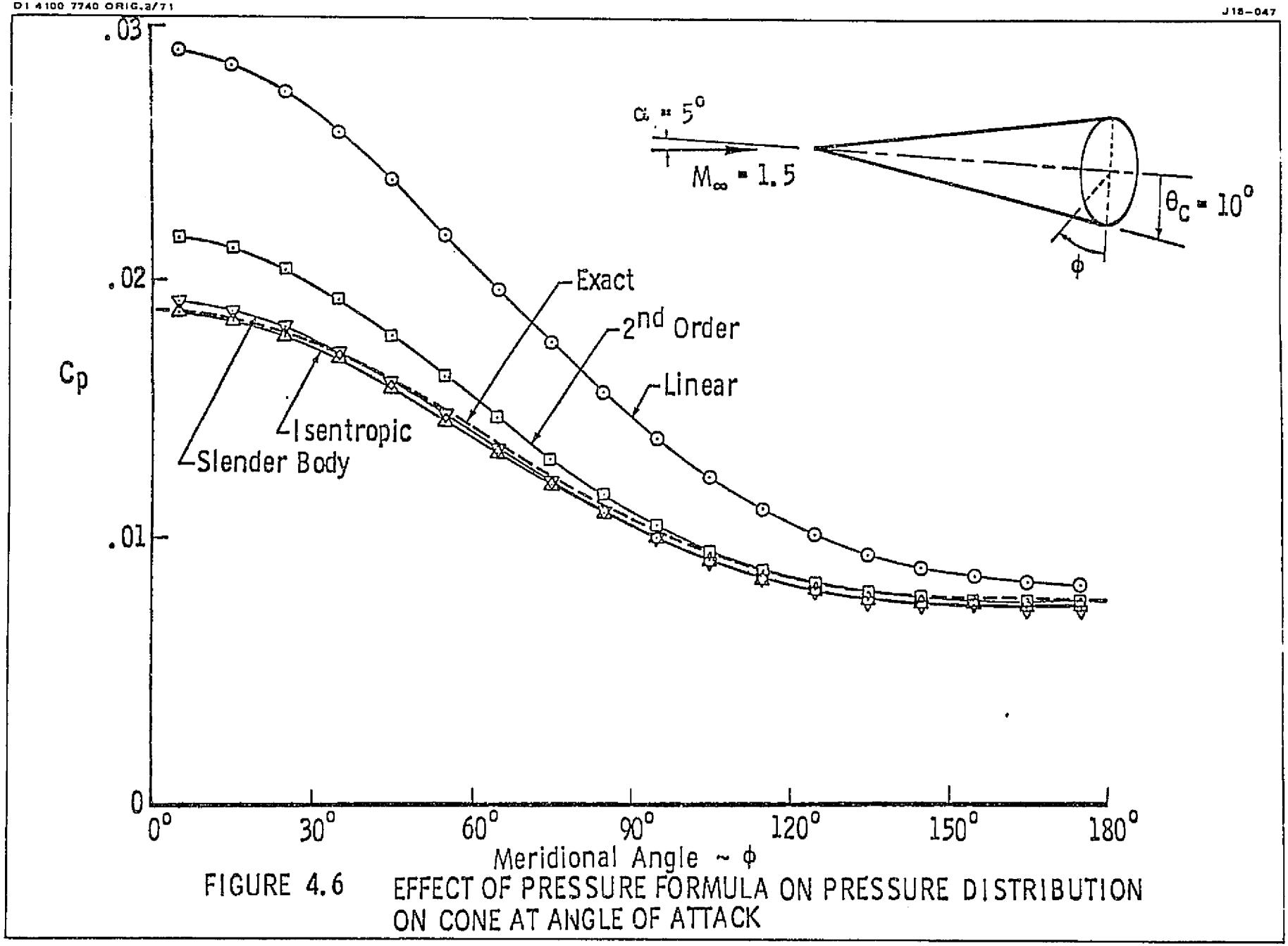

FIGURE 4.6 EFFECT OF PRESSURE FORMULA ON PRESSURE DISTRIBUTION ON CONE AT ANGLE OF ATTACK

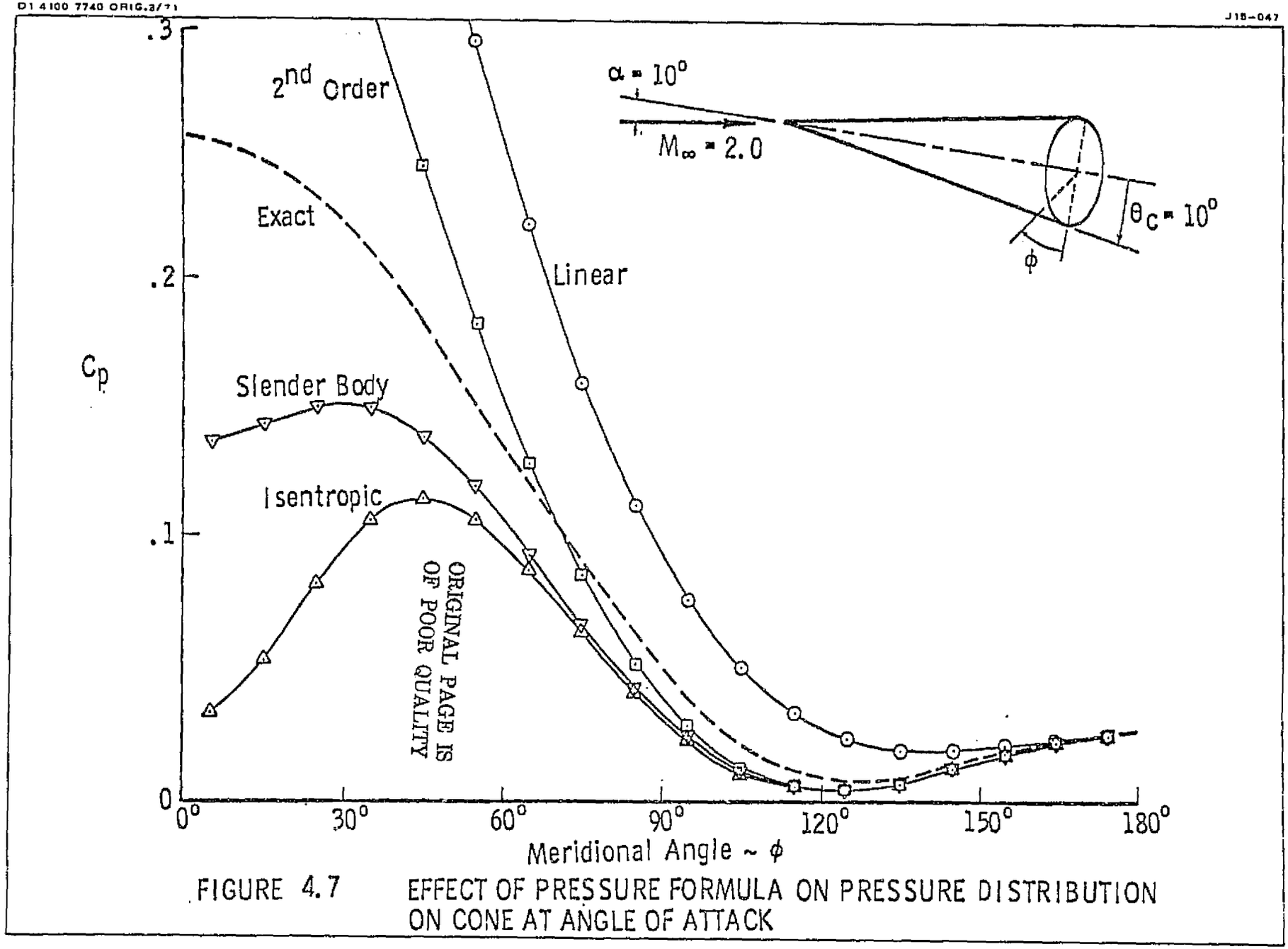

FIGURE 4.7 EFFECT OF PRESSURE FORMULA ON PRESSURE DISTRIBUTION ON CONE AT ANGLE OF ATTACK

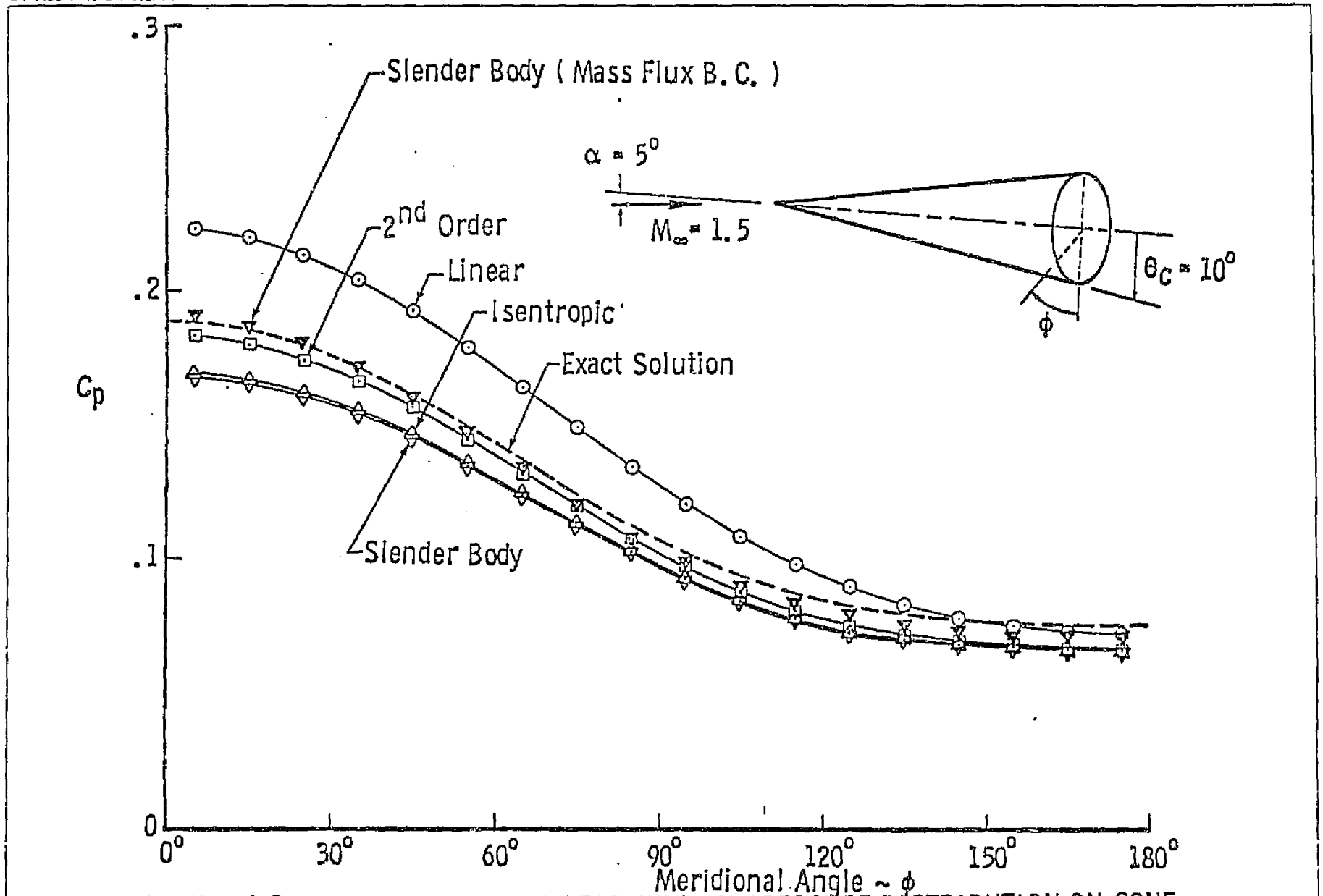

FIGURE 4.8 EFFECT OF PRESSURE FORMULA ON PRESSURE DISTRIBUTION ON CONE AT ANGLE OF ATTACK - VELOCITY BOUNDARY CONDITION

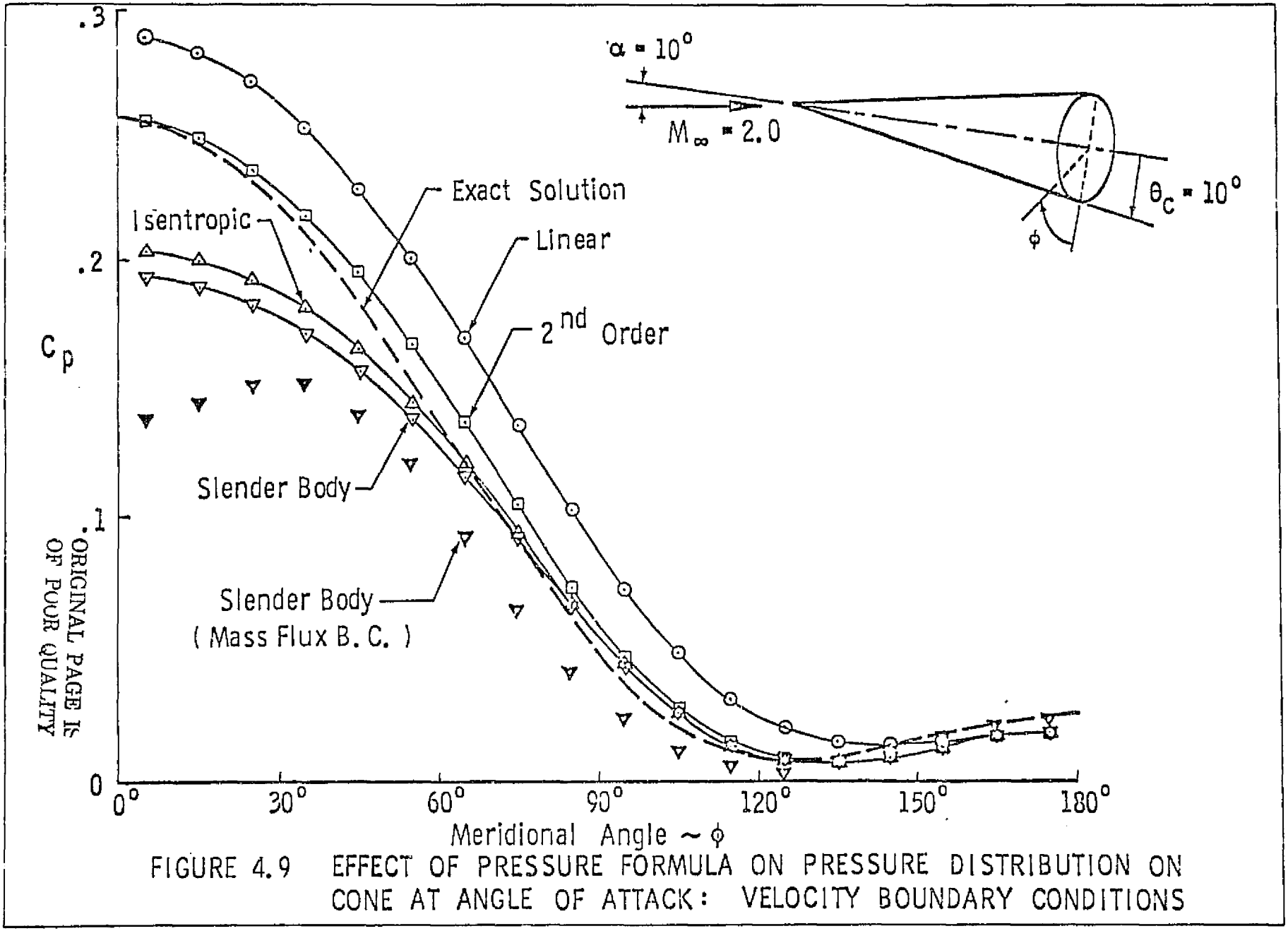

FIGURE 4.9 EFFECT OF PRESSURE FORMULA ON PRESSURE DISTRIBUTION ON CONE AT ANGLE OF ATTACK: VELOCITY BOUNDARY CONDITIONS

4.3 FLAT DELTA WINGS

As indicated in Section 1.1, it is impossible to panel a triangular wing with exclusively quadrilateral panels, and one must choose the vertex in whose vicinity the panels will be triangular. Fig. 4.10 shows the effect of paneling on the velocity ratio V_y/V_x on the surface of a flat delta wing with straight trailing edge at angle of attack. According to linear theory reference 4, this ratio ought to be linear in y/x. Fig. 4.10 shows that the conical paneling "A" gives results in excellent agreement with linear theory, as would be hoped, since this paneling best accommodates the nature of the solution. However, paneling "C", in which the triangular panels are located near the midpoint of the trailing edge, works just as well, which makes the failure of paneling "B", in which the tips are treated with triangular panels, all the more surprising. This effect of paneling needs further study.

4.4 DELTA WINGS WITH THICKNESS

The flow about thick delta wings was also calculated. Here the upper and lower wing surfaces were modeled by separate composite panel networks. The boundary conditions employed to obtain these results were the usual impermeable surface conditions described in Section 1.3 and 2.5.1.

Results for a case with a supersonic leading edge are shown in Fig. 4.11. These results are in good agreement with the conical flow linear theory. The computed results do show a slight pressure oscillation near the Mach cone from the leading edge. This is quite typical in that the panel method assumes a degree of continuity which is often absent in supersonic flow. Fig. 4.12 shows the pressure distribution on a delta wing with a subsonic leading edge. Results are in excellent agreement with linearized theory.

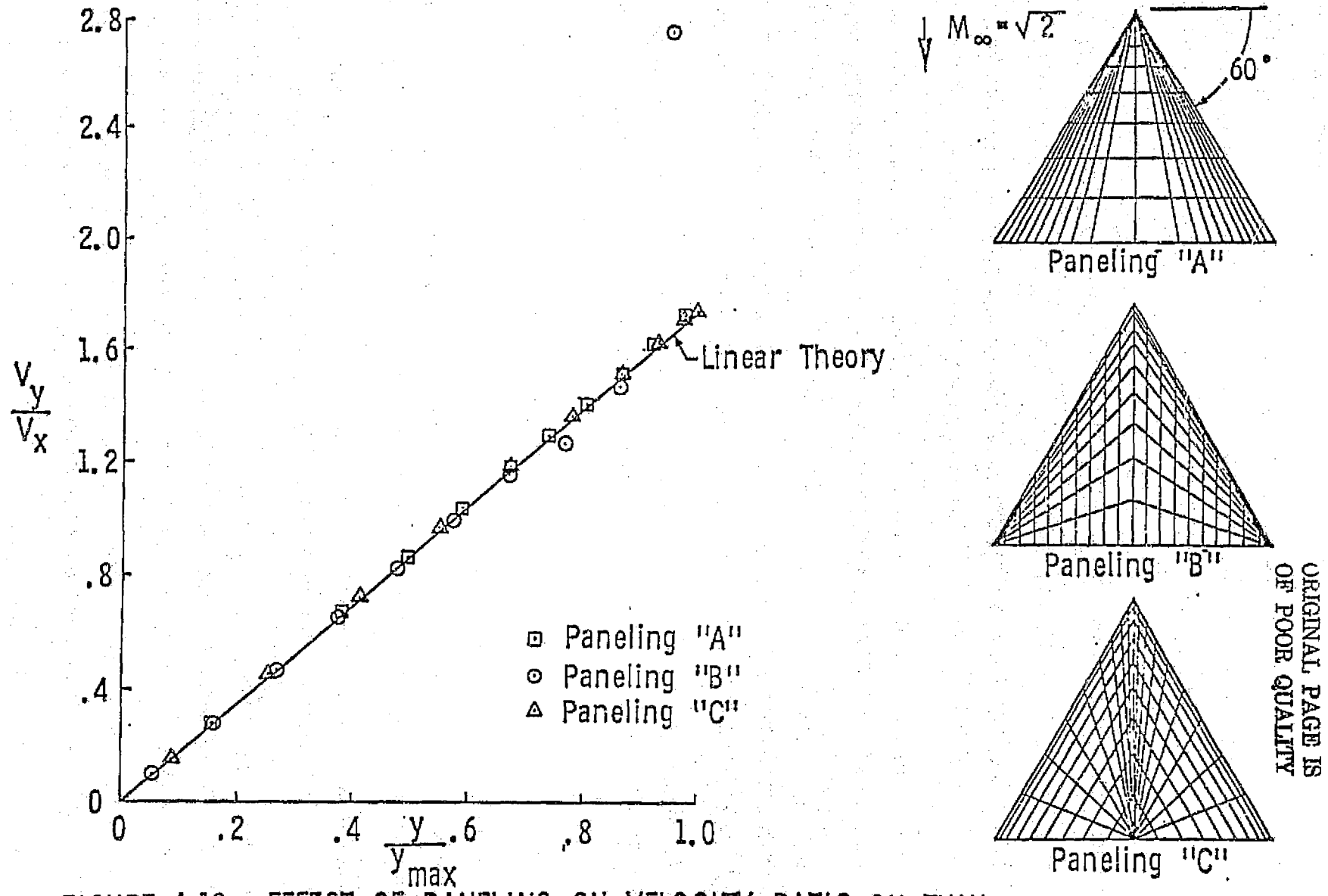

FIGURE 4.10 EFFECT OF PANELING ON VELOCITY RATIO ON THIN DELTA WINGS AT ANGLE OF ATTACK

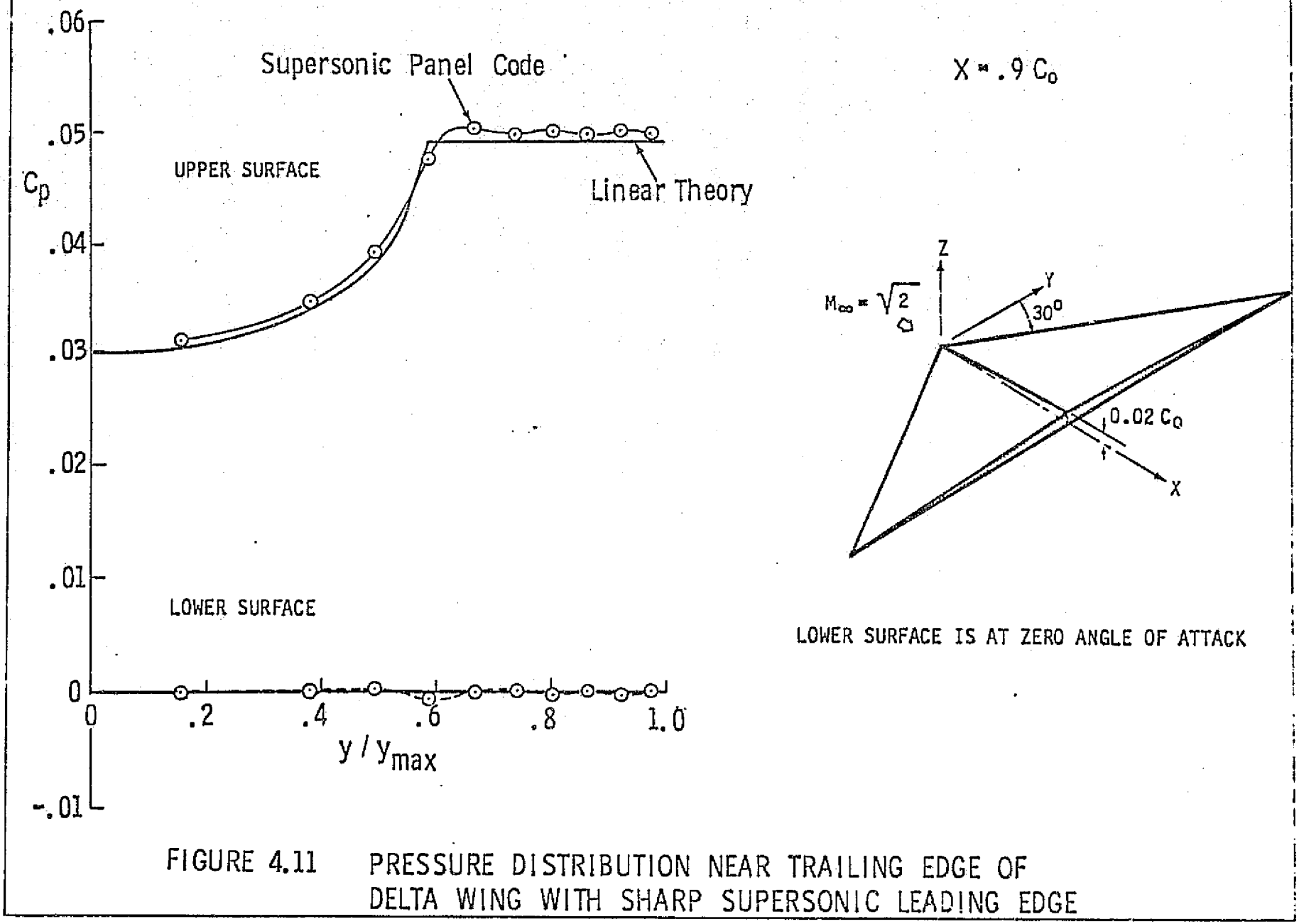

FIGURE 4.11 PRESSURE DISTRIBUTION NEAR TRAILING EDGE OF DELTA WING WITH SHARP SUPERSONIC LEADING EDGE

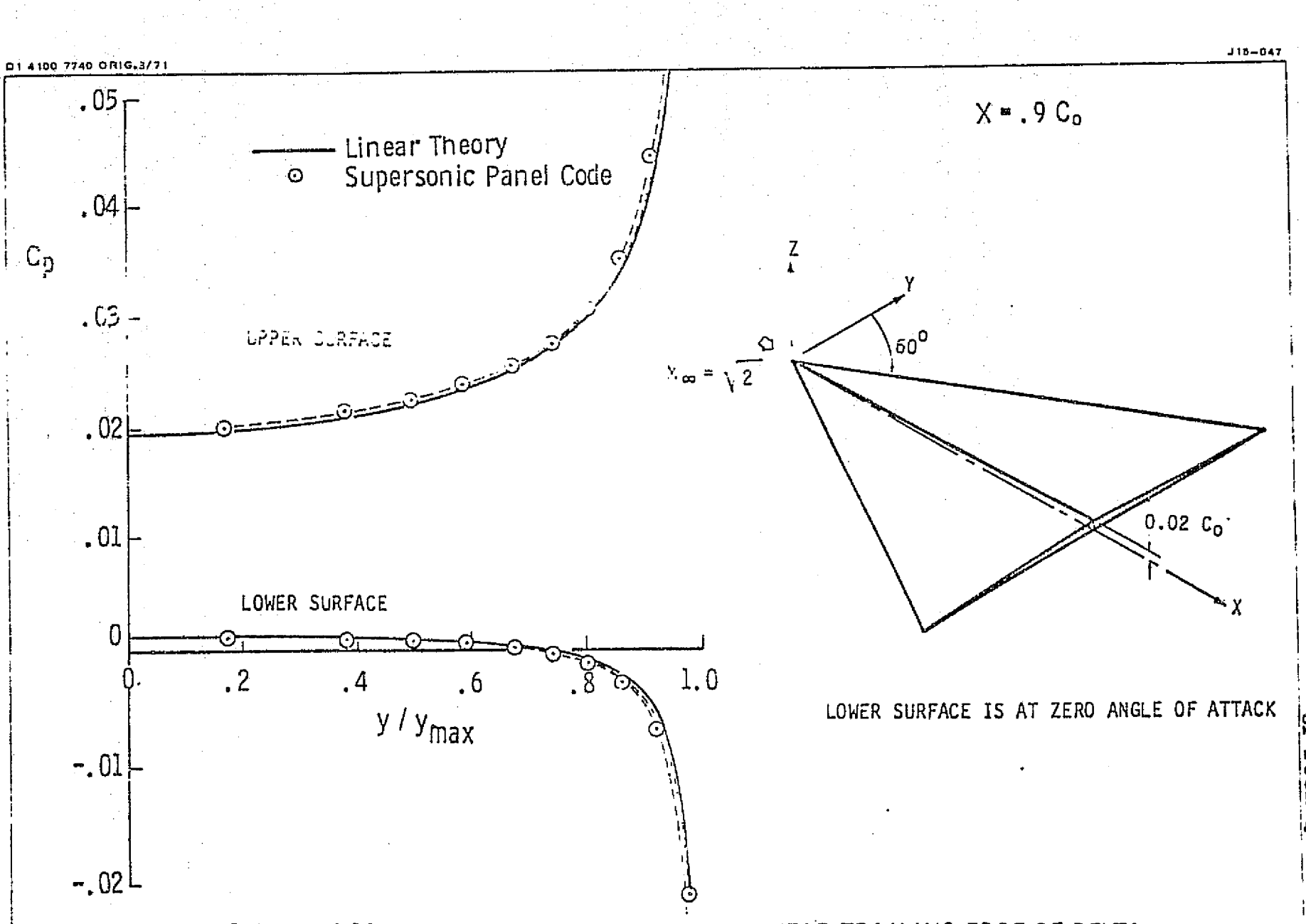

FIGURE 4.12 PRESSURE DISTRIBUTION NEAR TRAILING EDGE OF DELTA WING WITH SHARP SUBSONIC LEADING EDGE

The results plotted in Fig. 4.11 and 4.12 were obtained with a conical paneling like that called "A" in Fig. 4.10. Similar results were obtained when the triangular panels were situated near the midpoint of the trailing edge, as in paneling "C" of Fig. 4.10.

4.5 FLOW INDUCED ON A PLANE BY A CONE ABOVE THE PLANE

In order to assess the utility of the panel code to study interference effects, we considered the problem illustrated in Fig. 4.13, in which a cone at zero angle of attack is positioned above a plane, also at zero angle of attack. An exact solution can be constructed by the method of images, i.e., by taking the x-y plane to be a plane of symmetry.

Quite good results were obtained for the pressure distribution on the plane when it was taken to be a source network with just one row of panels in front of the trace of the Mach cone on the plane. When doublets were used to meet the flow tangency condition on the plane, the results were much poorer, with noticeable "leakage" of the pressure distribution ahead of the Mach cone trace. This is due to the larger data base used to generate the doublet spline. As described in Appendix A, the doublet distribution over a panel is related to the doublet strength at 20 surrounding panels, while the source strength spline relates the source strength at just 8 contigious panels.

The errors shown in Fig. 4.13 for the pure-doublet network were noticeably reduced (but still worse than for the pure-source network) both when more panels were put in ahead of the Mach cone trace and when, by refining the mesh spacing, more control points in the second row of panels (just aft of x=1.0, the most forward position of the Mach cone trace) were behind the Mach cone. These results are also consistent with the dependence of the doublet spline on the doublet strength on a fairly large number of contigious panels.

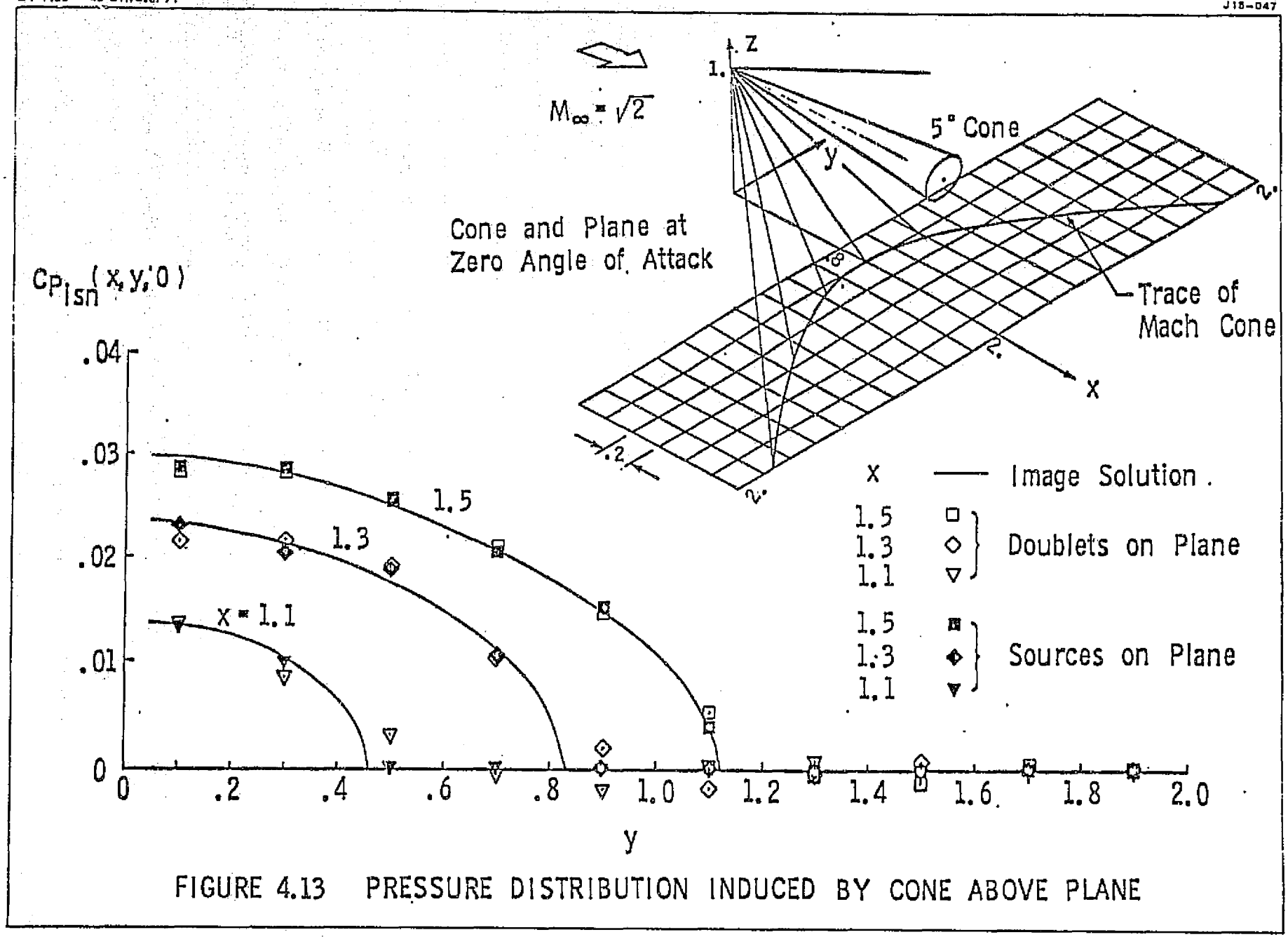

FIGURE 4.13 PRESSURE DISTRIBUTION INDUCED BY CONE ABOVE PLANE

4.6 FLOW PAST A CAMBERED, TWISTED WING

Extensive experimental data are available for the Carlson wing 2T reference 6, an arrow wing with sharp leading and trailing edges, twist, and camber. Results of the panel code are compared in Fig. 4.14 and 4.15 with data taken at Mach 2.05, at which the leading edge is subsonic but the trailing edge supersonic. The theoretical results compare well with the experimental data except at the wing tip, where the theory tends to over predict the experimental results. This may be due to the paneling in this region, which left an open gap between upper and lower surfaces of the wing at the tip. The boundary condition imposed that $\phi_\ell = 0$ requires a closed surface. With the tip open, flow through the tip would cause erroneous results in this region and this was verified by the existence of significantly non-zero values of WNU (as computed from the velocity influence coefficients) at control points on the upper and lower panel columns adjacent to the tip.

4.7 FLOW PAST ON ARROW WING-BODY CONFIGURATION

An analysis was also performed on the arrow wing-body configuration shown in Fig. 2.5. This configuration has been the subject of an extensive series of wind tunnel tests ranging in Mach numbers from 0.40 to 2.50 including supersonic Mach numbers as low as 1.05, reference 7 and 8. The configuration for which the comparisons are made featured a flat (no twist) wing with a rounded leading edge. The paneling representation is illustrated in Fig. 4.16 and 4.17. Details of the wing body intersection are shown in Fig. 4.18 and 4.19. Composite source-doublet singularities are used to represent the configuration. The boundary condition imposed specify the source strength so as to cancel the normal component of the freestream mass flux $(\vec{W}_u + \vec{V}_\infty) \cdot \vec{n} = 0$ and the doublet distribution to cause the perturbation potential to vanish inside the configuration, $\phi_\ell = 0$. Details of the boundary condition specifications were given in Section 2.5.4.

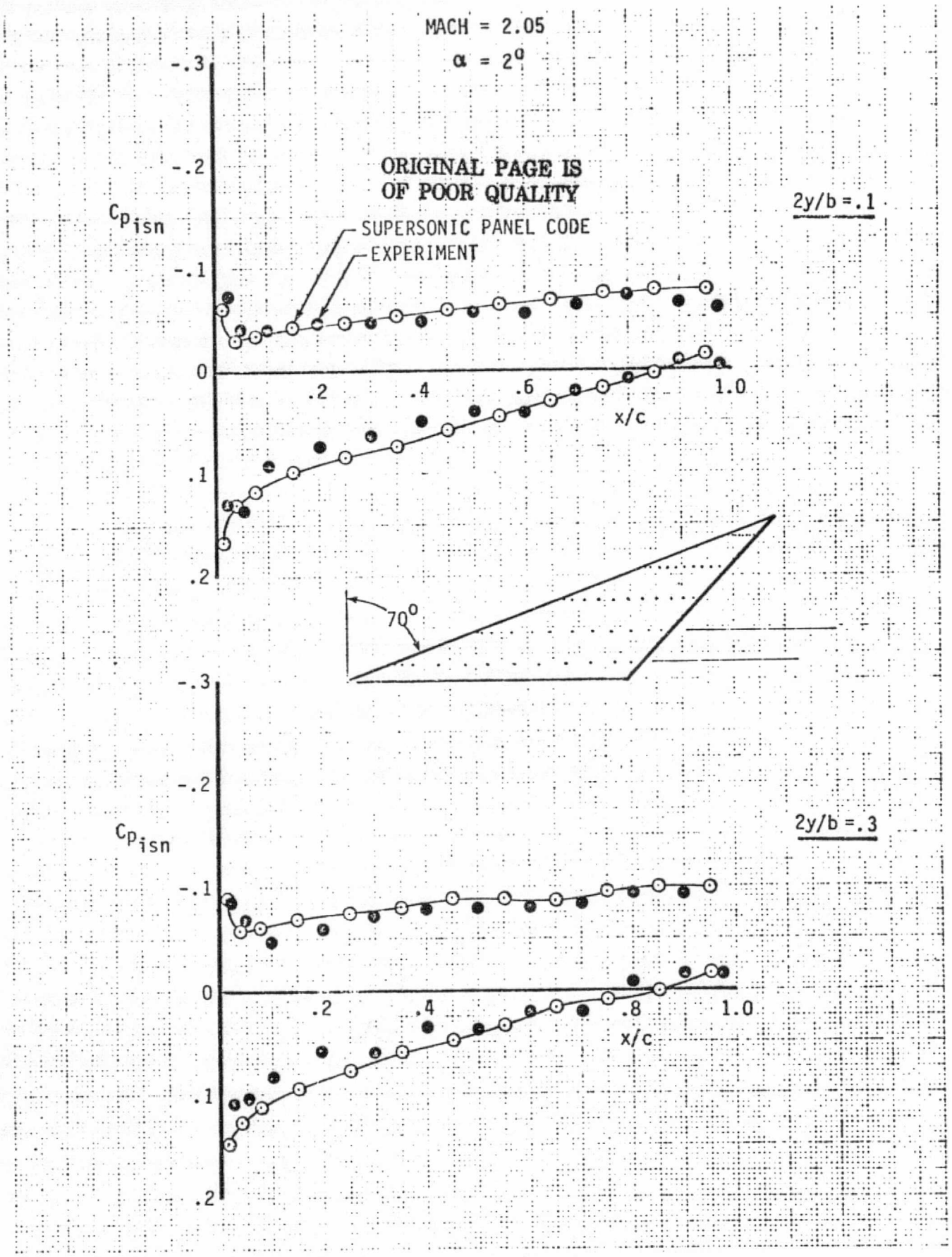

Figure 4.14 Test-Theory Comparison Wing Pressure Distribution Carlson Wing 2

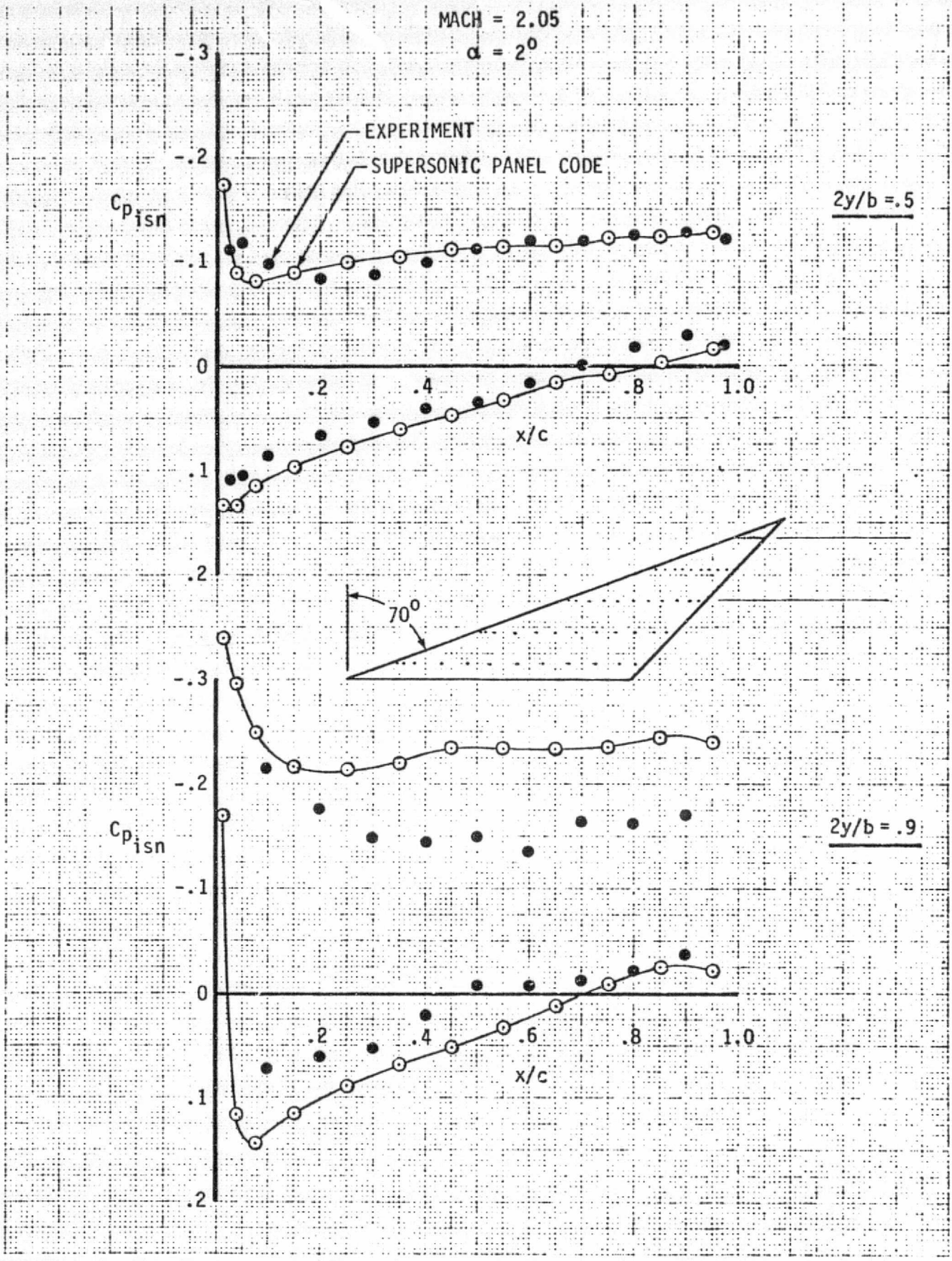

Figure 4.15 Test-Theory Comparison Wing Pressure Distribution Carlson Wing 2 (Cont'd.)

A comparison of wing surface pressure distributions is shown in Fig. 4.20 and 4.22, for a Mach number 1.70 and 2^{0} angle of attack. Experimental data are compared to calculate results from the supersonic panel code and to linearlized supersonic results calculated by the FLEXSTAB programs, References 9 and 10. Note that the supersonic panel code results are taken to lie along the panel centerlines and do not necessarily correspond to the wing buttline at which the pressure measurements were made. The FLEXSTAB results, however, have been interpolated to the same buttlines as the experimental data. The comparisons show general good agreement between the two theories and the experimental data. The lack of better test-theory agreement near the upper surface leading edge on the outboard portion of the wing is due to flow separation and the beginning of the formation of a leading edge vortex. Experimental isobar plots shown in Fig. 4.23 illustrate the presence of the leading edge vortex at this low angle of attack. This configuration is characterized by a very slender body and a thin highly swept wing which lends itself very well to the linearized approximation of the FLEXSTAB code. At first glance, both theories seem to yield very comparable results, but upon close examination it is clear the supersonic advanced panel pilot code is in better agreement with experiment near the leading edge where the linearized approximation tends to breakdown. The predicted results from the supersonic panel code at the leading edge of the two inboard wing stations have been degraded by poor edge matching at the wing body intersection.

Fig. 4.24 compares surface pressure distributions along the body. Again, the location of the supersonic panel results do not exactly correspond to location of the experimental measurements. Very good agreement is seen between the two theories and the experimental data except for the supersonic panel results near the leading edge of the wing body intersection. As previously stated, this descrepancy is due to a problem in the network edge matching in this area.

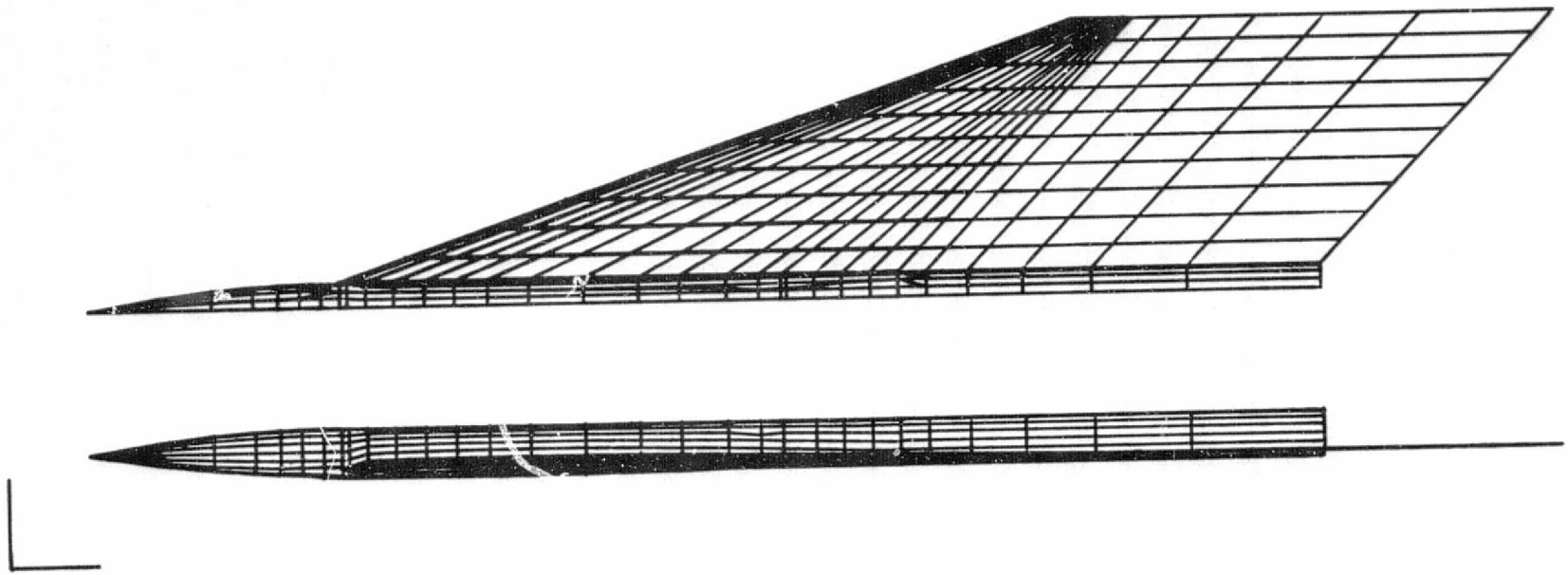

FIGURE 4.16 ARROW WING / BODY PANELING

ORIGINAL PAGE IS
OF POOR QUALITY

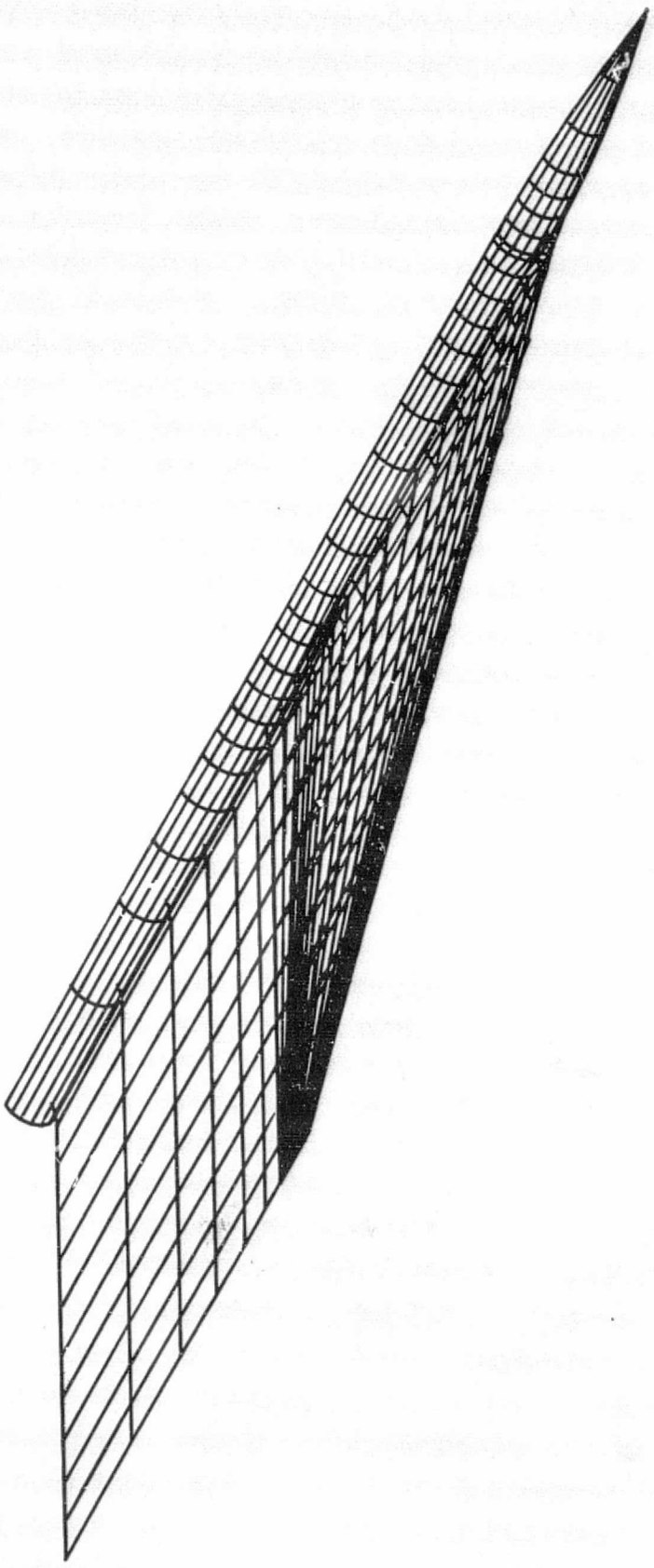

FIGURE 4.17 ARROW WING / BODY PANELING

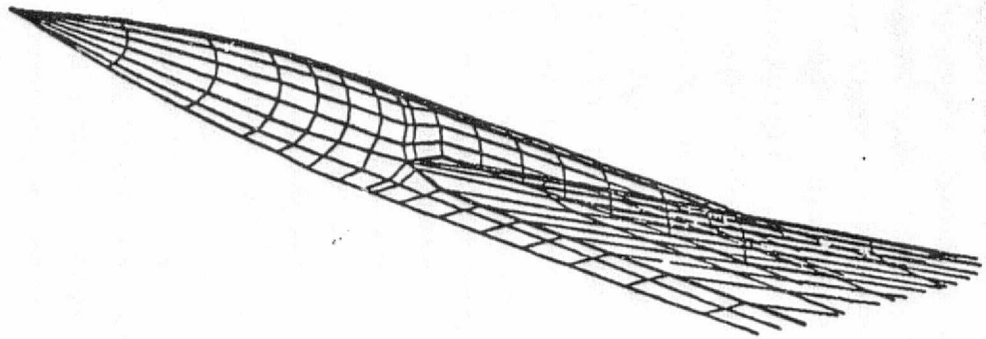

FIGURE 4.18 WING-BODY INTERSECTION DETAIL - L.E.

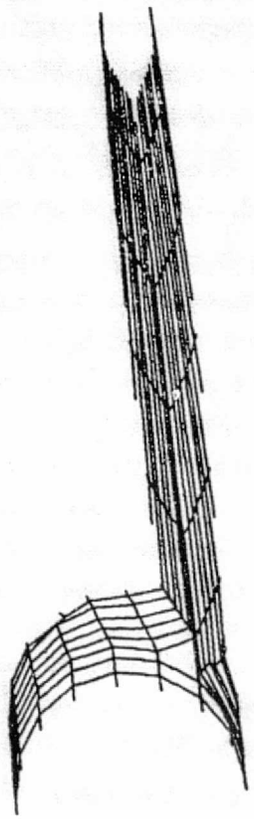

FIGURE 4.19 WING BODY INTERSECTION DETAIL T.E.

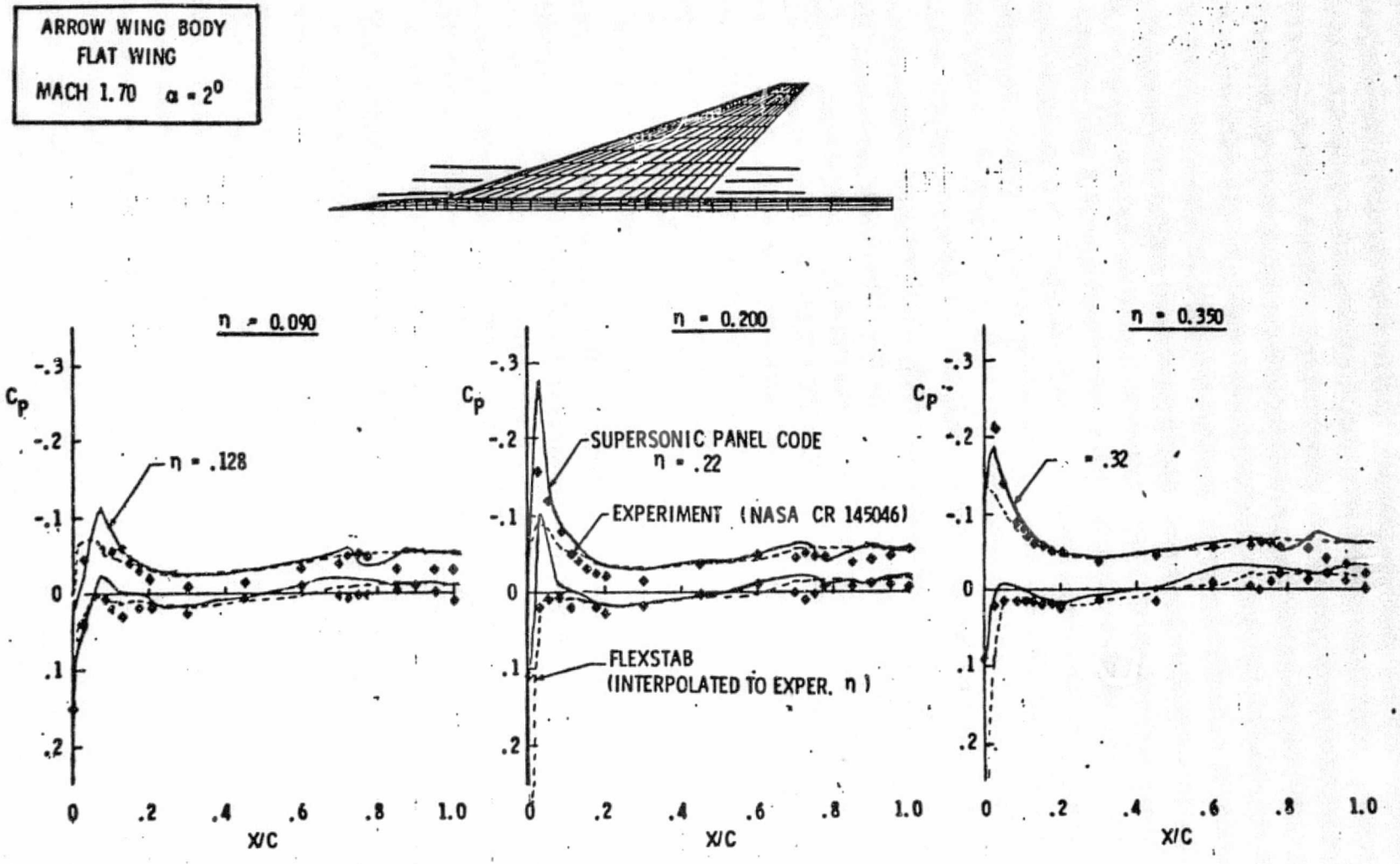

FIGURE 4.20 WING SURFACE PRESSURE DISTRIBUTION

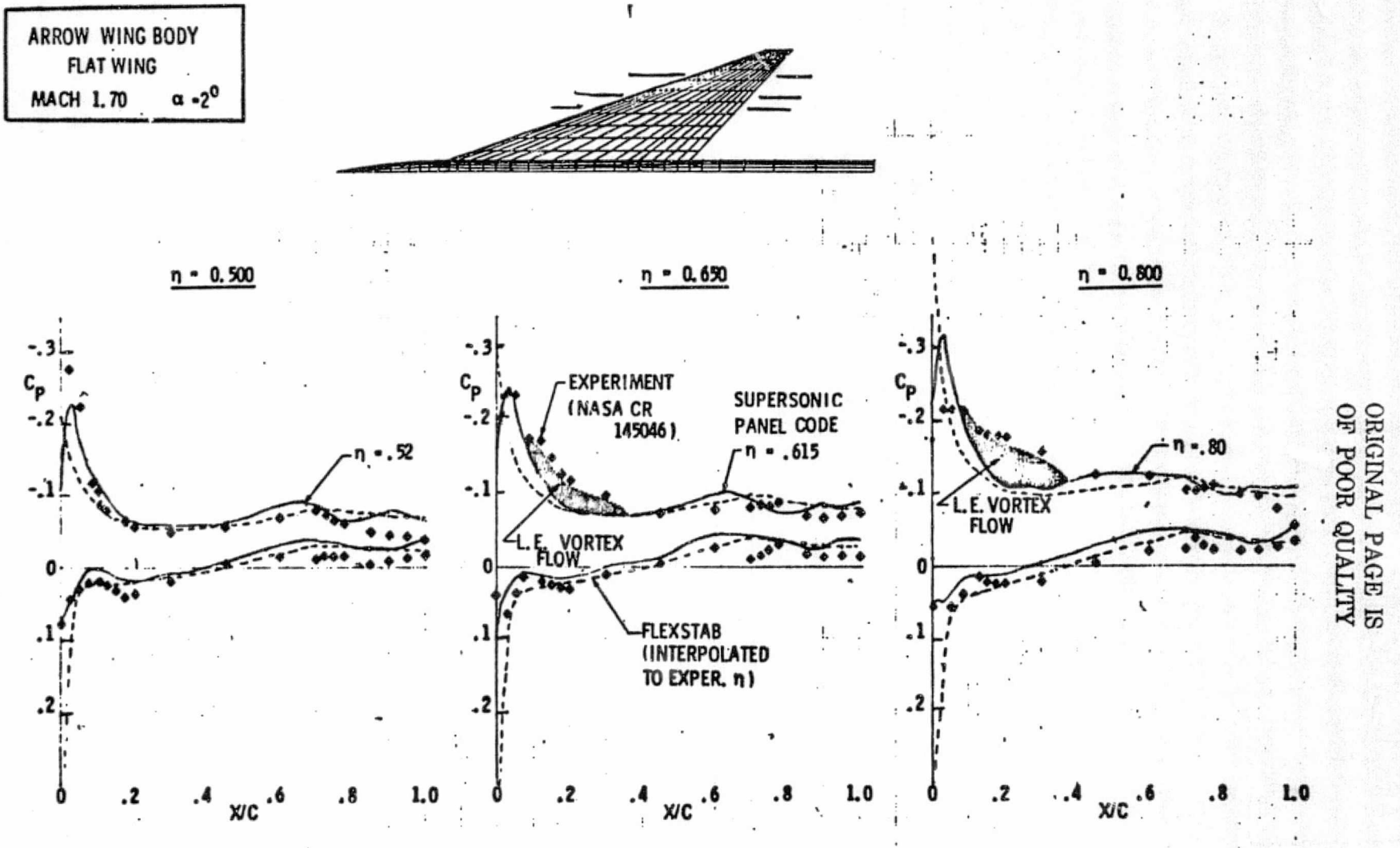

FIGURE 4.21 WING SURFACE PRESSURE DISTRIBUTION

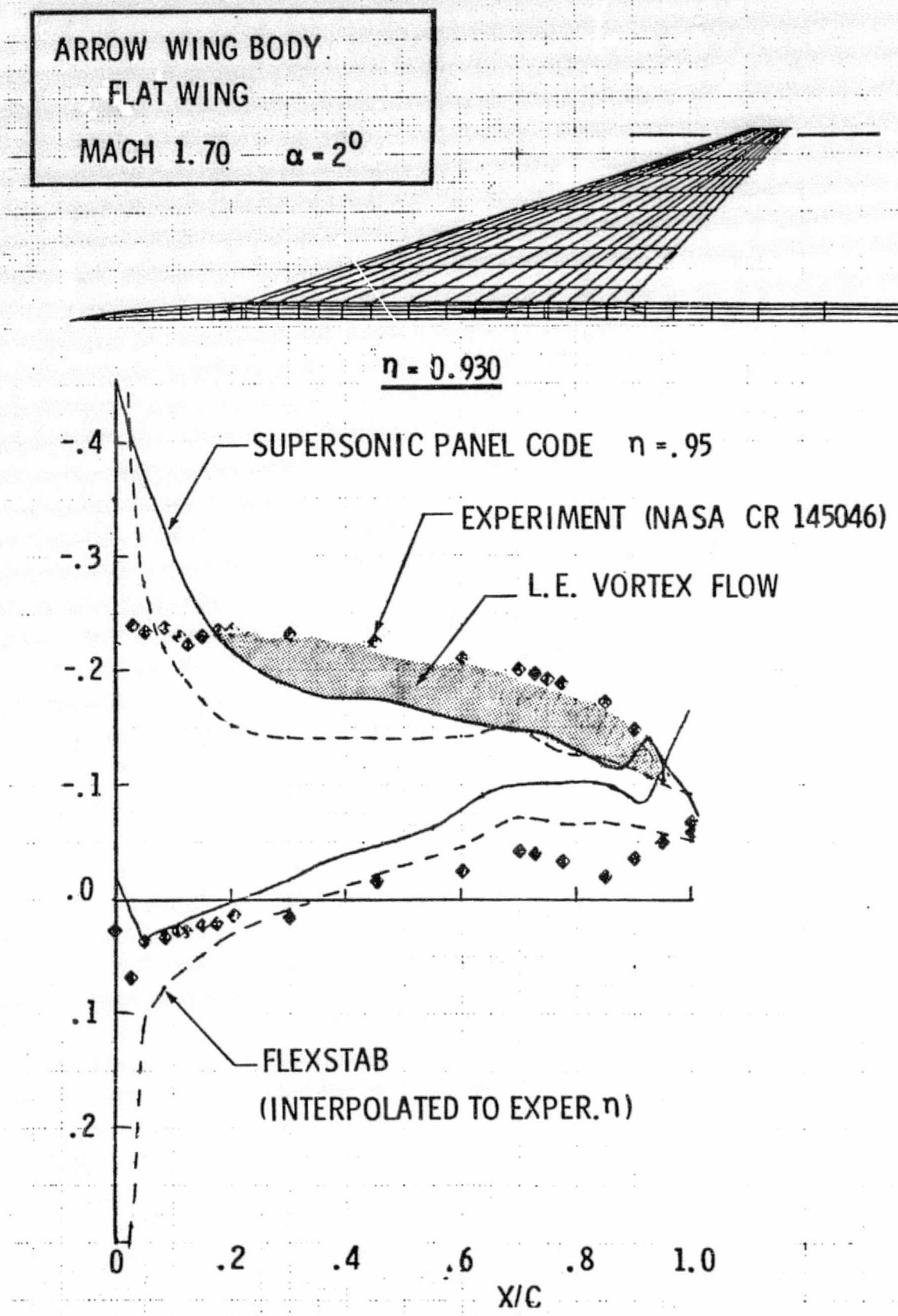

FIGURE 4.22 WING PRESSURE DISTRIBUTION

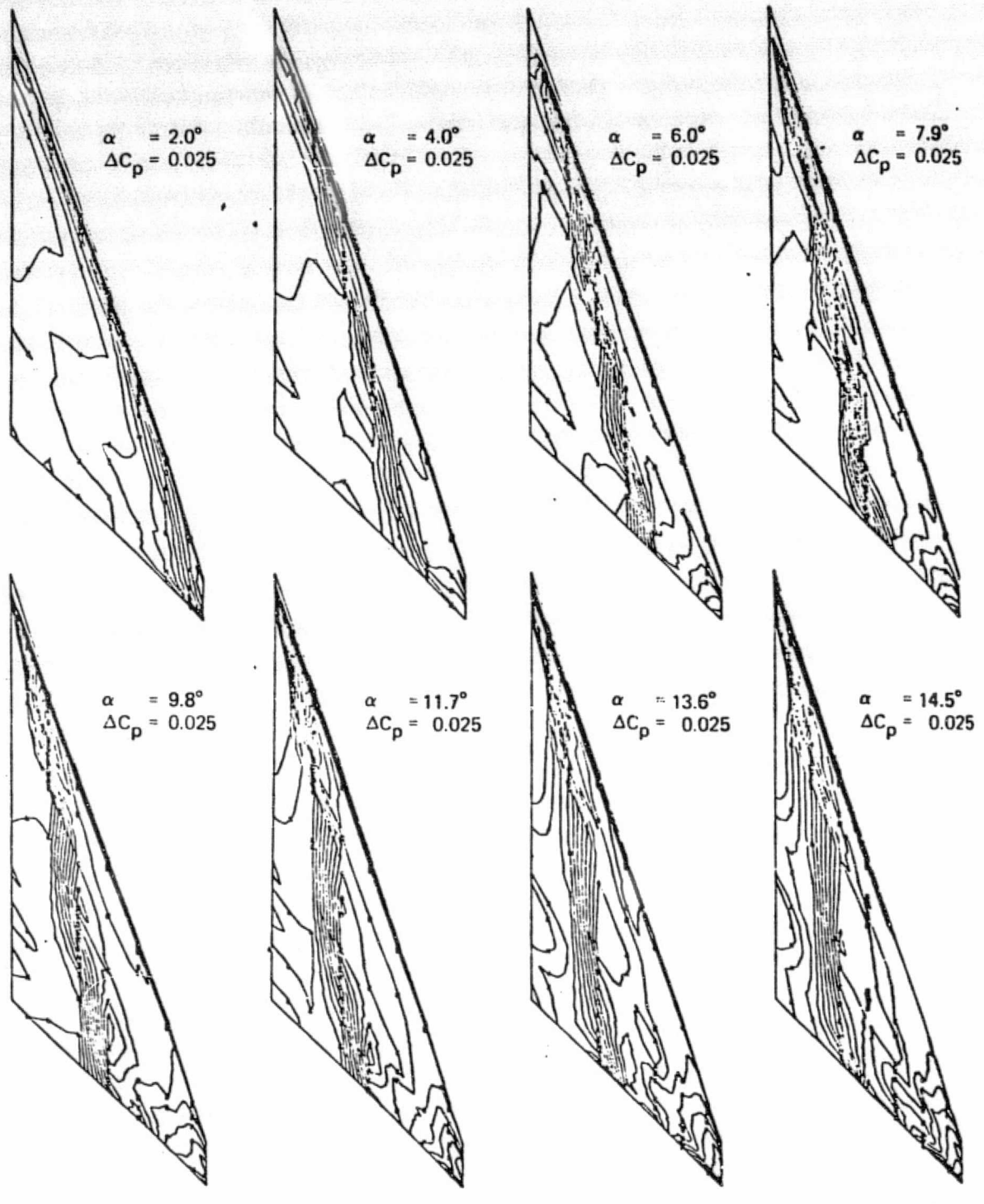

FIGURE 4.23 EXPERIMENTAL WING UPPER SURFACE ISOBARS, FLAT WING, M = 1.70

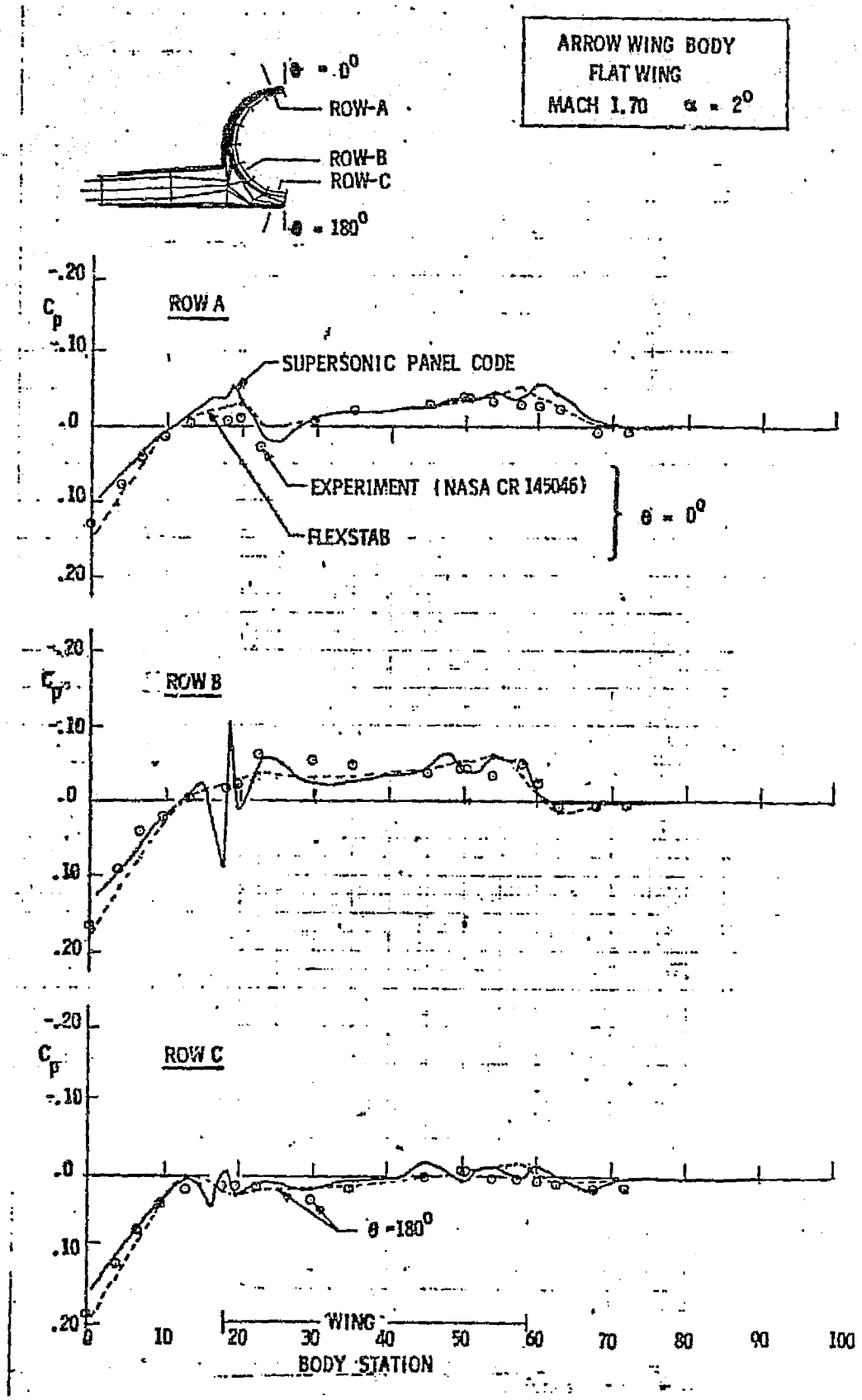

FIGURE 4.24 BODY SURFACE BRESSURE DISTRIBUTION

4.8 FLOW PAST A CONFIGURATION FEATURING SUPERINCLINED PANELS

An example of the use of superinclined panels is shown by the configuration in Fig. 4.25. Here an axisymmetric nacelle is modeled. A plane superinclined network was placed inside a nacelle at axial position 2.25 as shown in the figure. This was done as a test case to cancel the disturbance due to the upstream portion of the nacelle. In practice the superinclined network could be placed at the face of the nacelle and would be necessary to cancel disturbance from the upstream portion of the remainder of the configuration. On the portion of the nacelle ahead of the superinclined network, zero normal mass flux boundary conditions, $\overline{w}_u \cdot \overline{n} = 0$, were prescribed on the upper (or outer) surface of the source network. Potential boundary conditions (Morino-type) were prescribed on the remaining surfaces. Fig. 4.25 shows the exterior surface pressure distribution on the nacelle as a function of axial position for two different panelings. The 48 panel network is seen to be too coarse to absorb adequately the interior reflections. Doubling the panels by increasing the number of radial divisions to form 96 panels smooths out the pressure distribution. The pressure is seen to be in good agreement with Lighthill's theory.

The results shown in this section have shown very reasonable comparisons between advanced panel pilot code and other theories and experimental data. The limited number of cases studied could in no way cover the spectrum of problems one may wish to analyze in the future. Nor, have any configurations of complex geometry which would better illustrate the advantages of the advanced panel pilot code over existing linearized theories been attempted. Never-the-less, the results seen to date have been very encouraging as to the success of this new aerodynamic analysis method.

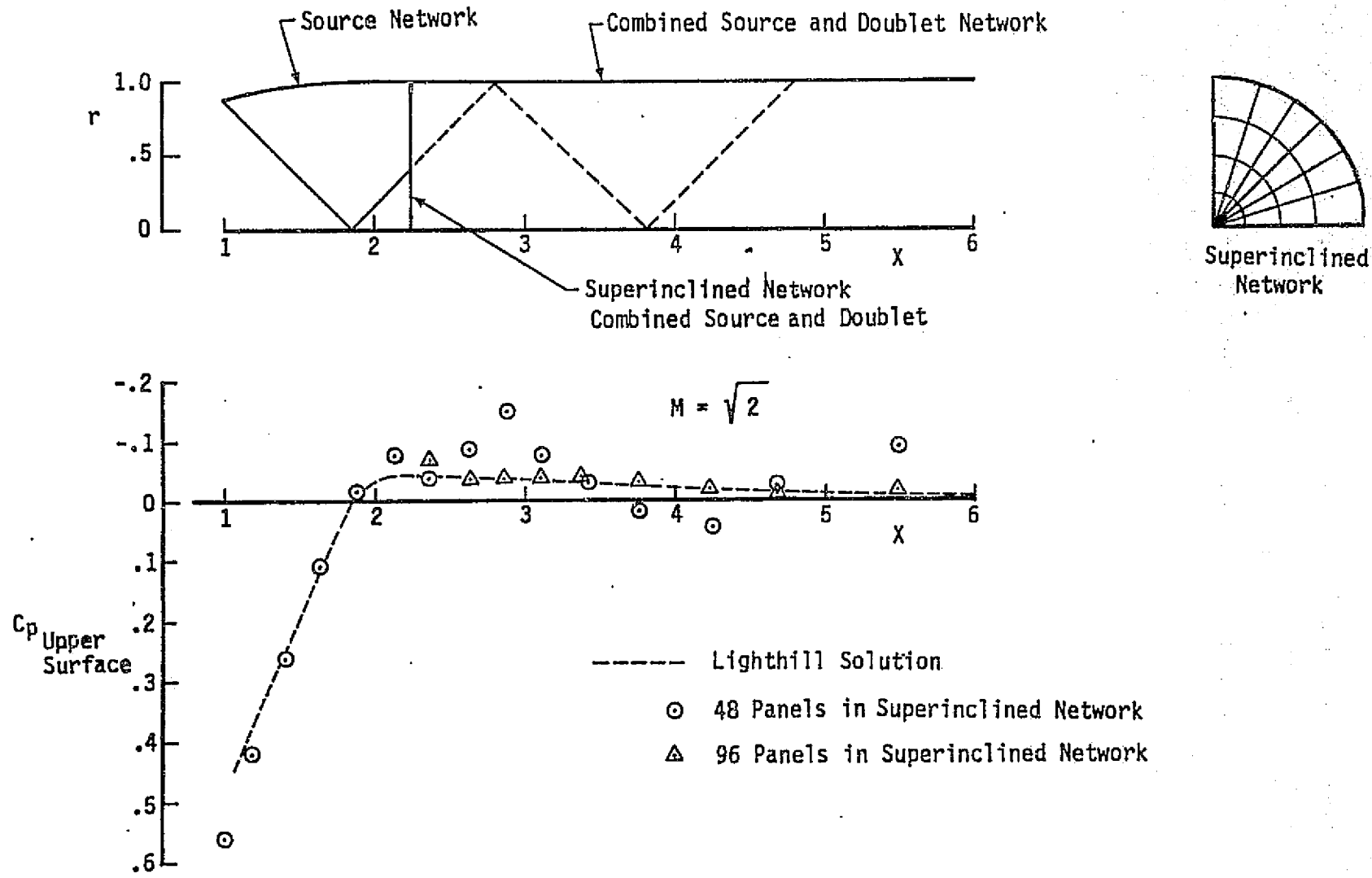

Figure 4.25 Solution of Supersonic Flow Over Nacelle with Interior Superinclined Netw...

5.0 References

1. Ehlers, R. E.; Johnson, F. T.; and Rubbert, P. E., "A Higher Order Panel Method for Linearized Supersonic Flow". AIAA Paper 76-381 July 1976.

2. Morino, L.; Chen, L. T.; and Suciu, E. O., "Steady and Oscillatory Subsonic and Supersonic Aerodynamics Around Complex Configurations". AIAA Journal Vol. 13, No. 3, 1975.

3. Jones, D. J., "Tables of Inviscid Supersonic Flow About Circular Cones at Incidence", 1.4 AGARDOGRAPH137 (19).

4. Puckett, H. J., "Supersonic Wave Drag of Thin Airfoils" Journal of Aeronautical Science, Vol. 13, p. 475-489, September 1946.

5. Stewart, H. J., "Lift of a Delta Wing at Supersonic Speeds" Quarterly of Applied Math, Vol. 4, No. 3, p. 246-254, October 1946.

6. Carlson, H. W., "Pressure Distributions at Mach Number 2.05 On a Series of Highly Swept Arrow Wings Employing Various Degrees of Twist and Camber", NASA Tech. Note D - 1264 (1962).

7. Manro, M. E.; Manning, K. J. R.; Hallstaff, T. H.; and Rogert, J. T., "Transonic Pressure Measurements and Comparison of Theory to Experiment for an Arrow-Wing Configuration", NASA CR-2610, August 1976.

8. Manro, M. E., "Supersonic Pressure Measurements and Comparison of Theory to Experiment for an Arrow-Wing Configuration", NASA CR-145046, November 1976.

9. Tinoco, E. N.; and Mercer, J.E., "FLEXSTAB-A Summary of the Functions and Capabilities of the NASA Flexible Airplane Analysis Computer System". NASA CR-2564, October 1974.

10. Dusto, A. R., et al, "A Method for Predicting the Stability Characteristics of an Elastic Airplane". Volume 1, FLEXSTAB Theoretical Manual, NASA CR-114712, 1974.

Appendix A - Singularity Splines

SOURCE DISTRIBUTION

On each panel, a plane may be defined which passes through the panel center and the panel edge midpoints. The source strength on a panel is taken to be linear in the coordinates of this plane:

$$\sigma = \sigma_o + \sigma_x X + \sigma_y Y \qquad (1A)$$

The three parameters σ_o , σ_x , and σ_y which are needed to specify the source strength on each panel are not, per se, basic unknowns of the problem. Rather, they are calculated as needed in terms of the source strengths at the centers of the panels, which in turn are determined so as to meet the specified boundary conditions.

Specifically, the parameters of Eq. (1A) are determined by a weighted least-squares fit to the source strength at the centers* of the eight surrounding panels. That is, if the source strength at the center of the ith of the 9 panels involved is called σ_i , and the coordinates of the ith panel center are x_i, y_i, z_i the quantity

$$\sum_{i=1}^{a} w_i(\delta_i - \sigma_o - \sigma_x X_i - \sigma_y Y_i)^2$$

is made stationery with respect to variations in σ_o , σ_x , and σ_y . The weight $w = 10^4$ if i is the label of the center of the panel under study, and $w = 1$ otherwise.

If the panel is at the edge of the network, there are fewer surrounding panels, but always enough to make this system determinate. Even when the

*By "center" of a panel we mean just the average position of the four corner points. If two points are coincident, no special action is taken in locating the panel center, which thus weights the collapsed point twice as heavily as the other two.

panel is at a corner of the network, there are three neighboring panels, so the only effect is to reduce the number of terms in the sum which is minimized. See Fig. A.1.

Two points are worth noting about this representation of the source strength. First, there is no reason for the source strength to be continuous from one panel to the next, since there is no special consideration given to the source strength at interpanel boundaries. Of course, in the limit as the grid is refined, we expcet the discontinuities in the source strength to vanish, so that these discontinuities furnish a measure of whether the mesh is sufficiently fine. Secondly, since the source distribution within the panels is determined in terms of the source strength at the centers of nearby panels, the number of parameters governing the source strength is exactly equal to the number of panels.

DOUBLET STRENGTH

The jump in normal mass flux (conormal velocity) across a surface singularity distribution is directly equal to the source strength. However, the jump in tangential velocity across a singularity distribution is equal to the gradient of the doublet strength. Hence it is necessary to use a higher-order representation of the doublet strength than of the source strength to assure the same level of representation of their velocity fields. Thus the doublet strength is represented by a quadratic:

$$\mu = \mu_o + \mu_x X + \mu_y Y + \mu_{xx} \frac{X^2}{2} + \mu_{xy} XY + \mu_{yy} \frac{Y^2}{2} \qquad (2A)$$

where (x,y) are now the coordinates of points in a subpanel, a different quadratic being used for each subpanel.

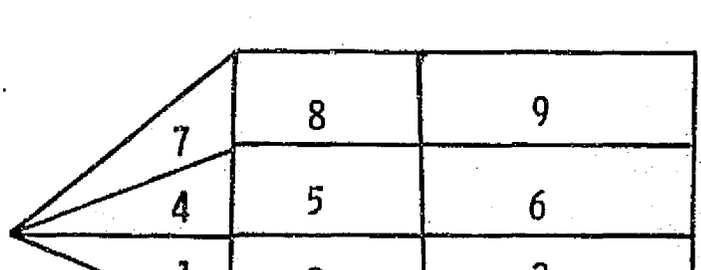

PANEL	OTHER PANELS USED IN DETERMINING SOURCE STRENGTH IN GIVEN PANEL
1	2, 4, 5
2	1, 3, 4, 5, 6
3	1, 2, 3, 4, 6, 7, 8, 9

FIGURE A.1 PANEL USED IN DETERMINING SOURCE STRENGTH

The determination of the doublet strength is complicated both by the necessity to use six parameters to specify the quadratic distribution and by the nesessity to avoid discontinuities in the doublet strength at either panel or subpanel boundaries. The determination is accomplished in stages, as follows:

1. For each panel, nine "doublet-strength parameters" are defined, which may be associated with the doublet strength at the nine vertices of the eight triangular subpanels. As will be seen below in Fig. A.2,

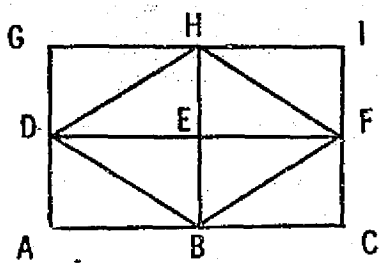

FIGURE A.2 SUBPANELS OF A DOUBLET PANEL

these definitions are such that the doublet-strength parameters associated with points on the boundary between two adjacent panels are exactly the same, regardless of which panel is under study. This helps to achieve the desired continuity of doublet-strength across panel boundaries.

2. Six of the ten straight lines which bound subpanels contain three subpanel vertices. In Fig. A.2, these are the lines ABC, DEF, GHI, ADG, BEH, and CFI. The doublet-strength parameters associated with the vertices may therefore be fitted with quadratics along each of these six lines. Quadratics may also be used to describe the doublet-strength variation along the other four lines (BD, DH, HF, FB in Fig. A.2), as follows. At point D, for example, the derivatives of the doublet-strength in the directions of the straight lines ADG and DEF may be computed by differentiating the quadratics already fitted to the doublet-strength parameters along those lines. These data determine the derivatives of the doublet-strength at D along the lines DH and BD. Similar operations supply directional derivatives of the

doublet-strength at the other three midpoints of panel edges. A quadratic is then fitted to the doublet-strength variation along DH, using the values of the doublet-strength parameters at D and H and, in a least-square fashion, the derivatives of the doublet-strength at those points.

3. We now have quadratic representations for the doublet-strength along each subpanel boundary in terms of the doublet-strength at the nine vertices of the subpanels. These quadratics may be used to estimate

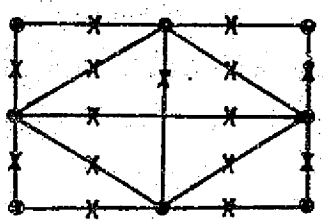

FIGURE A.3 SUBPANEL CONTROL POINTS

the doublet-strength at the midpoints of the subpanel edges (X's in Fig. A.3) in terms of the same nine parameters. Then, for each subpanel, we have six bits of information on the doublet-strength; its values at the three vertices of the subpanel and at the midpoints of its three sides. These six bits of data are just enough to determine the six coefficients of a quadratic representation of the doublet-strength within the subpanel.

4. Thus, within each panel, we have a piecewise-quadratic representation of the doublet-strength in terms of nine doublet-strength parameters. The representation can be seen to be continuous across subpanel boundaries, as follows. The quadratics in the neighboring subpanels BCF and BEF (see Fig. A.4) are each determined, in part, by values of the doublet

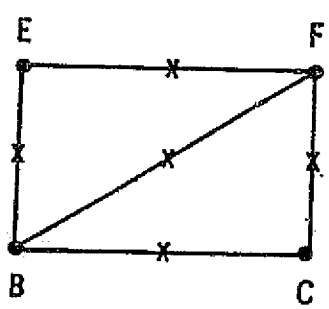

FIGURE A.4 SUBPANEL CONTROL POINTS

strength at B, F, and the midpoint of BF. Along FG, these quadratics become quadratic in the distance along BF. Since a quadratic in one variable is determined uniquely by three values, these quadratics must agree at every point along BF, not just at the three interpolation points. Similarly, since the singularity parameters associated with points along panel edges are the same for the panels on either side of the edge, the piecewise quadratic representation is continuous between panels. However, its normal derivative may be discontinuous both at panel and subpanel boundaries.

5. It remains to define the nine doublet-strength parameters. As in the case of the source distribution, it is convenient to regard as basic unknowns the doublet-strength at the panel centers. This helps to assure a close correspondence between the number of unknowns and the number of panels. For panels well within the network interior, the doublet-strength parameter at a corner of a panel is determined by least-squares fitting of a quadratic to the doublet-strength at the centers of 12 nearby panels, as shown in Fig. A.5a. Again, the squared errors at the four panel midpoints closest to the corner point in question are weighted 10^8 times as much as the squared errors at the outer six panel midpoints. Similarly, the doublet-strength parameters at the midpoint of a panel edge is found by least-squares fitting a quadratic to the doublet strength at the center of eight nearby panels, the squared errors at the centers of the two panels bordering the edge being weighted 10^8 more heavily than the other errors. Finally, the doublet-strength parameter at the center of a panel is simply set equal to the doublet-strength at that point. These arrangements are illustrated in Fig. A 5b and A. 5c. When a panel corner point or edge midpoint is near the network boundary, the fixing of the doublet-strength parameter at that point can be made similar to the procedure employed in the interior by introducing, as additional basic unknowns, quantities related to the doublet-strength at the midpoints of the panel edges which border the network. Fig. A 6a through A. 6e illustrate the utility of this arrangement. We also add to our list of basic unknowns the doublet-strength at the corner of the network, which then becomes the doublet strength parameter for the corresponding corner of the corner panel; see Fig. A. 6f.

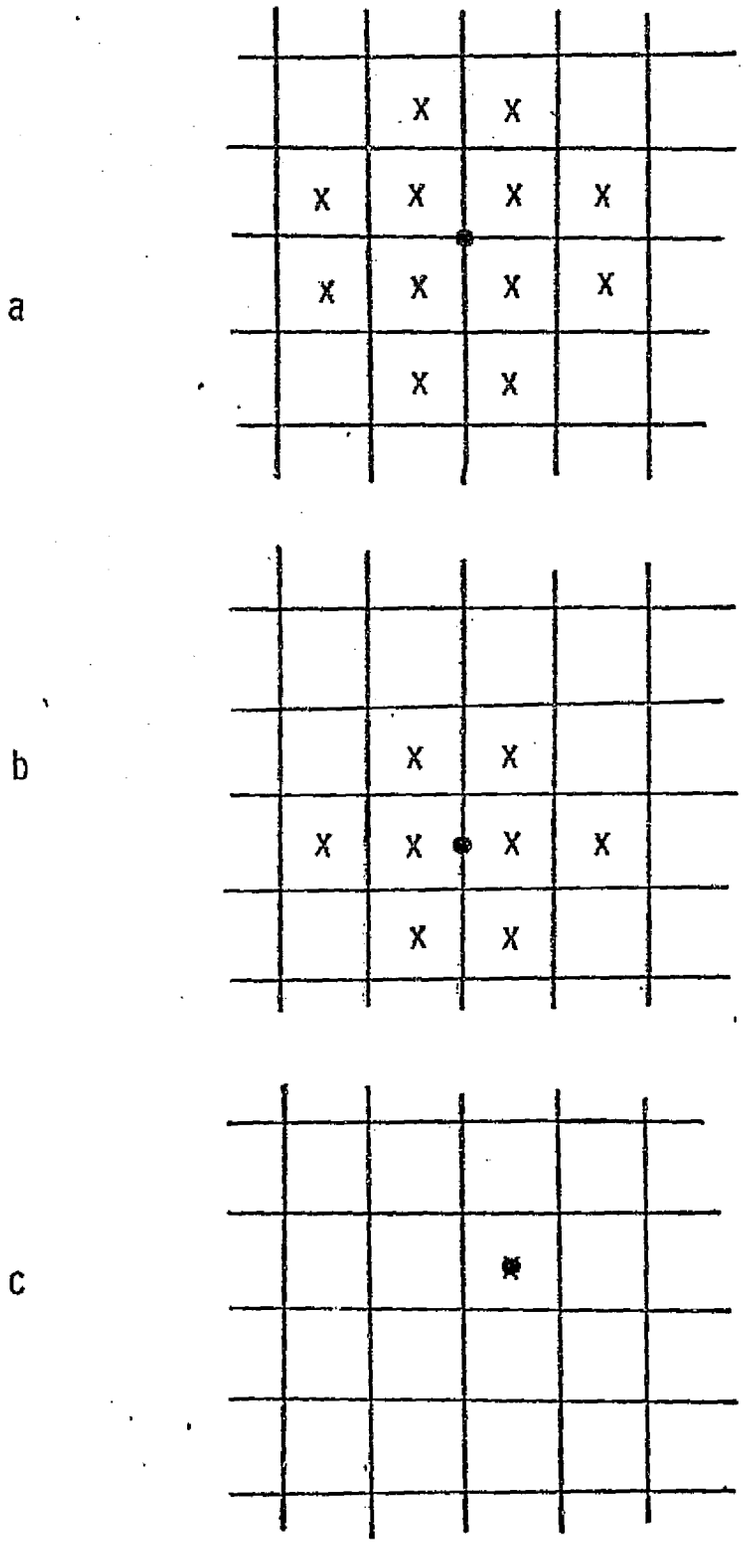

FIGURE A.5 FIXING DOUBLET STRENGTH PARAMETERS FOR PANELS NOT CLOSE TO NETWORK EDGE

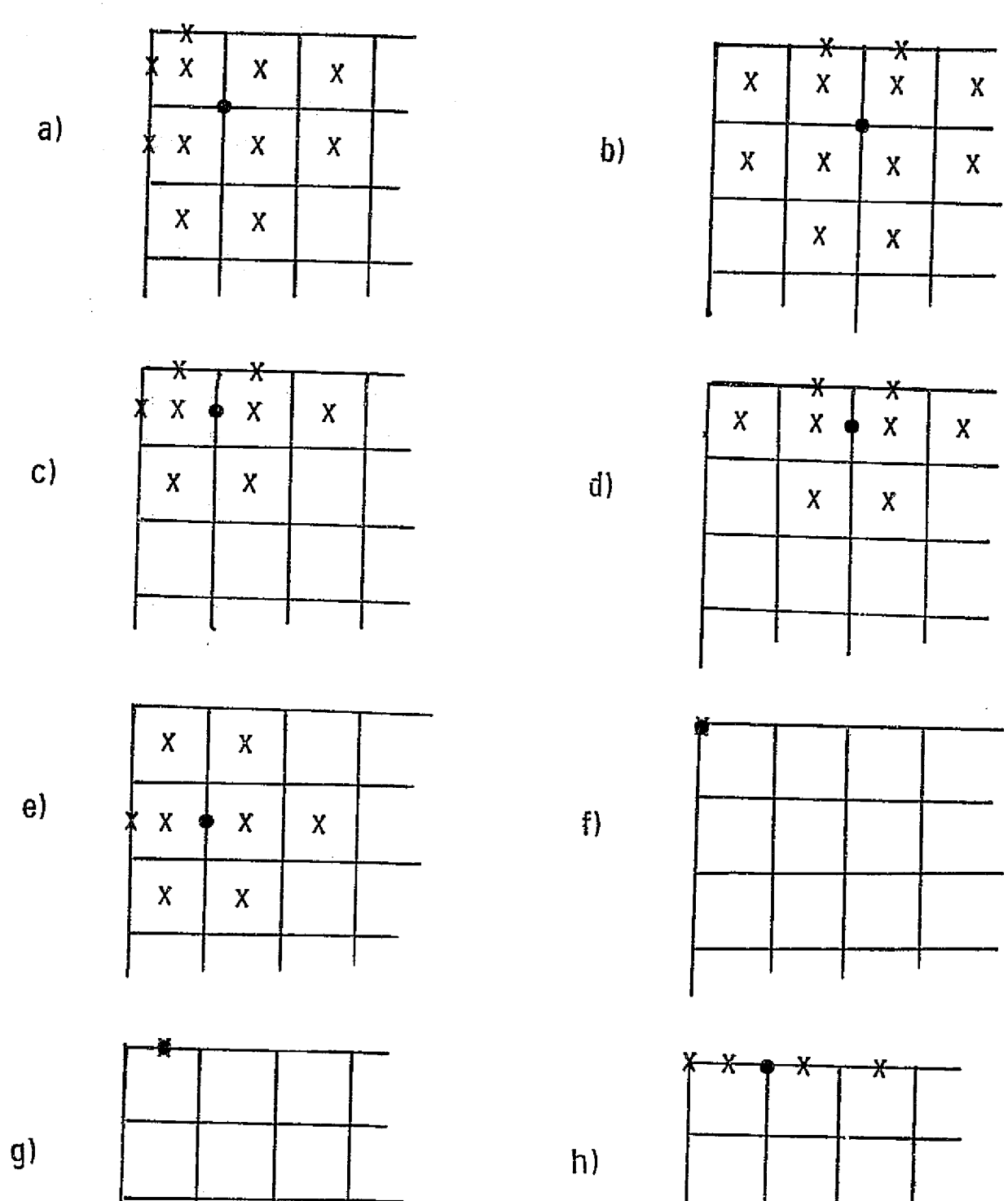

FIGURE A.6 FIXING DOUBLET STRENGTH PARAMETERS FOR PANELS ON EDGE OF NETWORK

Then the doublet-strength parameters at the network corner and at the midpoint of a panel edge which lies on the network edge are determined directly in terms of the corresponding unknown; see Fig. A.6f and A.6g. Finally, the parameter at a panel corner point which lies on the network edge is determined by least-squares fitting a quadratic to the doublet-strength at the four neighboring point shown in Fig. A.6h.

The upshot is that the number of unknowns which govern the doublet-strength equals the number of panels, plus the number of panel edges which border the network, plus the number of network corner points.

Naturally, special attention must be given in cases for which the panels, as illustrated in Fig. A.7, are triangular rather than quadrilateral, if only because it is impossible to fit a quadratic to three values at a common point! However, the same basic selection of unknowns serves to define enough doublet-strength parameters to fix piecewise continuous quadratics in each of the six subpanels of any triangular panel.

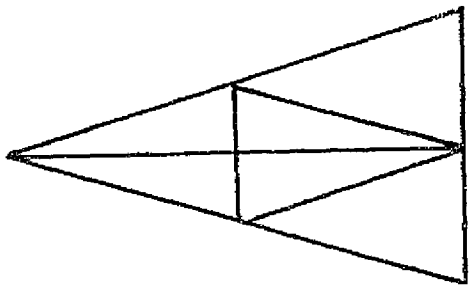

FIGURE A. 7 SUBPANELS OF TRIANGULAR PANEL